Chapter 1

The integer quantum Hall effect I

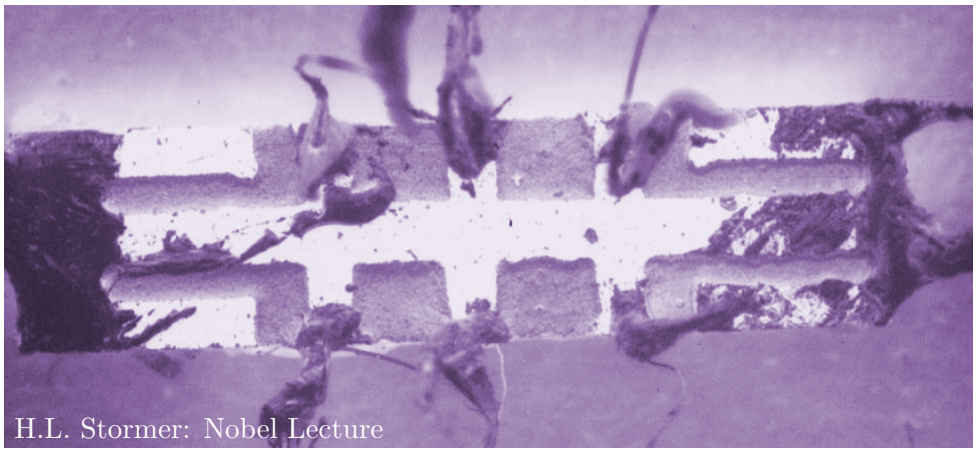

Learning goals

- We know the basic phenomenology of the quantum Hall effect (QHE)
- We know the structure of the lowest Landau level (LLL)
- We understand the role of disorder for the QHE.

- K. von Klitzing, G. Dorda, and M. Pepper, Phys. Rev. Lett. **45**, 494 (1980)

In large parts of this chapter we follow reference [2].

1.1 Preliminaries

The Lorentz force acting on charged particles moving in a two-dimensional plane leads to a build-up of charges perpendicular to the direction of motion. This is the classical Hall effect first discussed by Edwin Hall in 1879 [3]. To understand this, let us consider a two-dimensional system which is translationally invariant. We move to a frame moving with $-\mathbf{v}$ where we therefore see a current

$$\mathbf{J} = ne\mathbf{v}, \tag{1.1}$$

where n is the particle density and e the electron charge. In the laboratory frame we have $\mathbf{E} = \mathbf{0}$ and $\mathbf{B} = B\hat{\mathbf{z}}$. Hence, in the moving frame we obtain

$$\mathbf{E} = \mathbf{v} \wedge \mathbf{B} \qquad \text{and} \qquad \mathbf{B} = B\hat{\mathbf{z}}. \tag{1.2}$$

We can express the electric field as

$$\mathbf{E} = \frac{B}{ne}\mathbf{J} \wedge \hat{\mathbf{z}}. \tag{1.3}$$

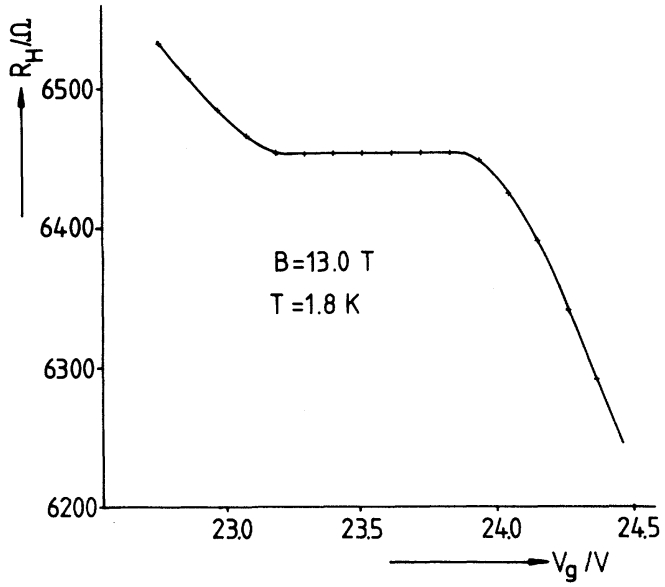

Figure 1.1: Measured Hall resistivity as a function of an applied back-gate which leads to a change in the particle density n. The pronounced plateau is the hallmark of the quantum Hall effect. Figure taken from Ref [1].

The resistivity ρ is defined as the relation between the current and the electric field $E^\mu = \rho_{\mu\nu} J^\nu$. We thus find

$$\rho = \frac{B}{ne}\begin{pmatrix} 0 & 1 \\ -1 & 0 \end{pmatrix} \qquad \Rightarrow \qquad \sigma = \frac{ne}{B}\begin{pmatrix} 0 & -1 \\ 1 & 0 \end{pmatrix}. \tag{1.4}$$

We see that owing to the non-zero σ_{xy} the longitudinal resisitivity $\rho_{xx} = \sigma_{xx} = 0$ is equal to the longitudinal conductivity. Moreover, the Hall resistivity is proportional to the magnetic field

$$\rho_{xy} = \frac{B}{ne}. \tag{1.5}$$

This is in striking contrast to the seminal discovery of von Klitzing and his co-workers in 1980 [1], see Fig. 1.1. The only ingredient in our theoretical model so far, however, was translational symmetry. In the following, we first take steps towards a quantum mechanical understanding of electrons in a magnetic field before we come back to the issue of translational symmetry breaking via disorder.

1.2 Classical Lagrangian

To motivate how the magnetic field enters our quantum mechanical description, we recall that the classical equations of motions are reproduced by the following Lagrangian $\mathcal{L} = \frac{m}{2}\dot{x}^\mu \dot{x}^\mu - e\dot{x}^\mu A^\mu$.

$$-\frac{\partial}{\partial t}\frac{\partial \mathcal{L}}{\partial \dot{x}^\mu} + \frac{\partial \mathcal{L}}{\partial x^\mu} = 0 \qquad \Rightarrow \qquad m\ddot{x} = -eB\dot{y} \quad \text{and} \quad m\ddot{y} = eB\dot{x}. \tag{1.6}$$

The canonical momentum is given by $p^\mu = \frac{\partial \mathcal{L}}{\dot{x}^\mu} = m\dot{x}^\mu - eA^\mu$ and therefore the Hamiltonian reads

$$H(x^\mu, p^\mu) = \dot{x}^\mu p^\mu - \mathcal{L}(x^\mu, \dot{x}^\mu) = \frac{1}{2m}\left(p^\mu + eA^\mu\right)\left(p^\mu + eA^\mu\right). \tag{1.7}$$

With this small detour into classical mechanics we are now in the position to tackle the quantum mechanical problem of a particle in a magnetic field.

1.3 Landau levels

We have to solve for the eigenstates of the following Hamiltonian

$$H = \frac{1}{2m}(\mathbf{p} + e\mathbf{A})^2. \tag{1.8}$$

As only the vector potential $\mathbf{A}$ enters the Hamiltonian we have to chose an appropriate gauge. For now we choose the Landau gauge where $A = xB\hat{\mathbf{y}}$. We check that $\nabla \wedge \mathbf{A} \equiv \mathbf{B} = (\partial_x A_y - \partial_y A_x)\hat{\mathbf{z}} = B\hat{\mathbf{z}}$. Inserted into the above Hamiltonian we obtain

$$H = \frac{1}{2m}\left[p_x^2 + (p_y + exB)^2\right]. \tag{1.9}$$

We immediately observe that this Hamiltonian has a translational symmetry in y direction. We therefore choose the following ansatz for the wave function $\psi(x, y) = e^{iky} f_k(x)$. With this ansatz we obtain a family of one-dimensional problems (one per momentum k in y-direction)

$$h_k = -\frac{\hbar^2 \partial_x^2}{2m} + \frac{1}{2}m\omega_c^2 \left(x + kl^2\right)^2 \qquad \text{with} \qquad \omega_c = \frac{eB}{m} \qquad \text{and} \qquad l = \sqrt{\frac{\hbar}{eB}}. \tag{1.10}$$

We see that we are dealing with a (displaced) one-dimensional harmonic oscillator. The characteristic frequency is known as the the cyclotron frequency ω_c. The displacement is proportional to the y-momentum and measured in the natural length scale, the magnetic length l. Solving the harmonic oscillator we find that

1. $\epsilon_k = \hbar\omega_c \left(s + \frac{1}{2}\right)$ with $s \in \mathbb{N}$.

2. For $s = 0$, i.e., the LLL the wave function is a Gaussian centered at $X_k = -kl^2$

$$\psi(x, y) = \frac{1}{\sqrt{\pi^{1/2} L_y l}} e^{iky} e^{-\frac{1}{2l^2}(x+kl^2)^2} = \frac{1}{\sqrt{\pi^{1/2} L_y l}} e^{iky} e^{-\frac{1}{2l^2}(x-X_k)^2}, \tag{1.11}$$

   where L_y is the extent in y-direction as shown in Fig. 1.2.

3. We have a vastly degenerate system. The number of degenerate states in each LL is given by

$$N = \frac{L_y}{2\pi}\int_0^{L_x/l^2} dk = \frac{L_x L_y}{2\pi l^2} = \frac{L_x L_y B}{\Phi_0}, \tag{1.12}$$

   where $\Phi_0 = h/e$ is the magnetic flux quantum. In other words, per magnetic flux quantum that penetrates the sample we have one state per Landau level.

Before we continue we should remind ourselves that in the case of huge degeneracies any perturbation might have dramatic effect. Moreover, the choice of basis can facilitate the description of these effects. For the case of a magnetic field, the choice of gauge determined the shape of the basis wave-functions. We will come back to this point later.

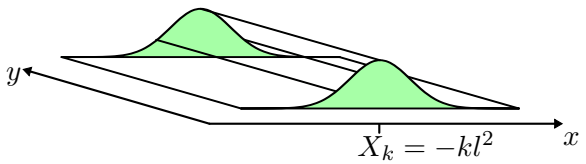

Figure 1.2: Eigenfunctions of the LLL in the Landau gauge.

1.4 Currents

We set out to understand the Hall conductivity. To make further progress, we need to calculate currents. We evaluate the current operator in y direction, $J_y = -\frac{e}{m}(\mathbf{p_y} + eA_y)$, in the LLL eigenfunctions

$$\langle\psi|J_y|\psi\rangle = -\frac{e}{m\pi^{1/2}l}\int dx\, e^{-\frac{(x-X_k)^2}{2l^2}}(\hbar k + eBx)e^{-\frac{(x-X_k)^2}{2l^2}} \tag{1.13}$$

$$= -\frac{e\omega_c}{\pi^{1/2}l}\int dx\, e^{-\frac{(x-X_k)^2}{l^2}}(x + kl^2) = -\frac{e\omega_c}{\pi^{1/2}l}\int d\alpha\, e^{-\frac{\alpha^2}{l^2}}\alpha = 0. \tag{1.14}$$

The last equality holds as the integrand is odd under $\alpha \to -\alpha$. In other words, no net current is flowing as shown in Fig. 1.3.

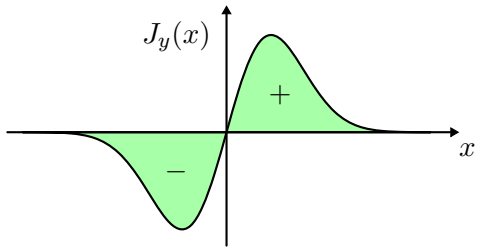

Figure 1.3: Current distribution in the lowest Landau level.

For a current to flow, we need to add an electric field in x-direction $V(x) = eEx$. We still are translationally invariant in y-direction and the one-dimensional problem is changed to

$$h_k = -\frac{\hbar^2\partial_x^2}{2m} + \frac{1}{2}m\omega_c^2\left(x + kl^2\right)^2 + eEx \tag{1.15}$$

$$= -\frac{\hbar^2\partial_x^2}{2m} + \frac{1}{2}m\omega_c^2\left(x + kl^2 + \frac{eE}{m\omega_c^2}\right)^2 - eEX_k' + \frac{1}{2}m\bar{v}, \tag{1.16}$$

where the center of the Gaussians is shifted

$$X_k' = -kl^2 - eE/m\omega_c^2 \tag{1.17}$$

and an additional energy $\frac{1}{2}m\bar{v}^2$ with $\bar{v} = -E/B$ is arises from the drift of the electrons. The immediate conclusion is that the new energy depends on k, i.e., the huge degeneracy is lifted

$$\epsilon_k = \frac{1}{2}\hbar\omega_c + eEX_k' + \frac{1}{2}m\bar{v}^2. \tag{1.18}$$

With an energy that depends on k we can also calculate a non-zero group velocity

$$v_{\text{group}} = \frac{1}{\hbar}\frac{\partial\epsilon_k}{\partial k} = \frac{eE}{\hbar}\frac{\partial X_k'}{\partial k} = -\frac{eE}{\hbar}l^2 = -\frac{E}{B} = \bar{v}. \tag{1.19}$$

We this we reach the classical result

$$\langle J_y\rangle = -e\bar{v} \qquad \Rightarrow \qquad \sigma_{xy} = -\frac{ne}{B}. \tag{1.20}$$

We this result we reach the same conclusion as with the classical manipulations based entirely on translational symmetry in the beginning of this chapter. In order to make further progress we should take a closer look at the finite extent of a realistic sample as well as on disorder effects to understand the quantization of σ_{xy}.

1.5 Edge states

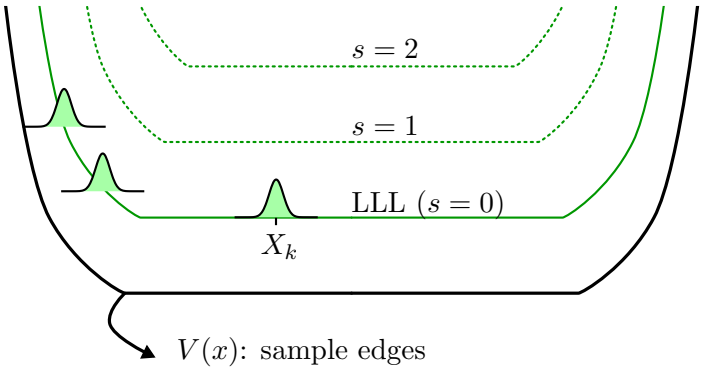

Figure 1.4: Edge states from curved Landau levels.

We try to build an understanding of the influence of the edges of a two dimensional sample by considering a strip which is finite in x-direction and infinite (or periodic) in y-direction. The basis wave functions of the LLL, or equivalently the gauge choice for $\mathbf{A}$, which we used above is optimally tailored to this geometry. Remember that the wave functions are localized in x-direction with a typical extent l. If we now consider a potential $V(x)$ that confines the electrons to a finite region which is smooth over the length-scale l, we can expect the wave function to remain approximately Gaussian. However, the wave functions centered in the vicinity of the edges will be lifted in energy. As the position of the wave function is linked to the momentum k in y-direction we obtain dispersive edge channels.

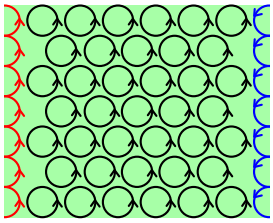
Figure 1.5: Classical skipping orbits.

In order to determine how the current is distributed we again calculate the group velocity.

$$v_{\text{group}} = \frac{1}{\hbar}\frac{\partial \epsilon_k}{\partial k} = \frac{1}{\hbar}\frac{\partial \epsilon_k}{\partial X_k}\frac{\partial X_k}{\partial k} = -\frac{l^2}{\hbar}\frac{\partial \epsilon_k}{\partial X_k} = \begin{cases} < 0 & \text{right edge} \\ > 0 & \text{left edge} \end{cases}. \tag{1.21}$$

These simple manipulations reveal that the two opposite edges carry opposite current. This can also be understood from the classical "skipping orbits" picture as shown on the left.

In order to calculate σ_{xy} we now apply a voltage V_H between the two edges (in x-direction) and calculate the resulting current along the sample (in y-direction). Moreover, we assume that the Fermi energy E_{F} lies in between two Landau levels.

The obtain the total current I_y we sum over the contribution ev_k of all occupied states

$$I_y = -e\int_{-\infty}^{\infty}\frac{dk}{2\pi}\frac{1}{\hbar}\frac{\partial \epsilon_k}{\partial k}n_k, \tag{1.22}$$

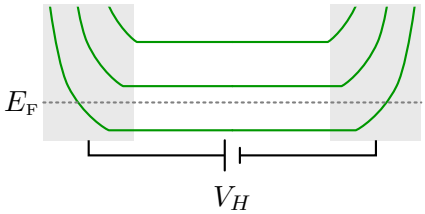

Figure 1.6: Voltage bias.

where n_k is the occupation probability of the k'th mode. Under the assumption that we only fill the LLL and that we are at zero temperature the occupation numbers only take the values $n_k = \{1, 0\}$. Under these assumptions we arrive at

$$I_y = -\frac{e}{h}\int_{\mu_L}^{\mu_R} d\epsilon = -\frac{e}{h}(\mu_R - \mu_L), \tag{1.23}$$

where $\mu_{R/L}$ are the respective chemical potentials on the two sides. As we can write $eV_H = \mu_R - \mu_L$ we arrive at

$$I_y = -\frac{e^2}{h}V_H \qquad \Rightarrow \qquad \sigma_{xy} = -\frac{e^2}{h}. \tag{1.24}$$

Let us move now the Fermi energy in between any two LL and we immediately conclude that

$$\sigma_{xy} = -\nu\frac{e^2}{h}, \tag{1.25}$$

where the integer ν counts the number of filled LL's.

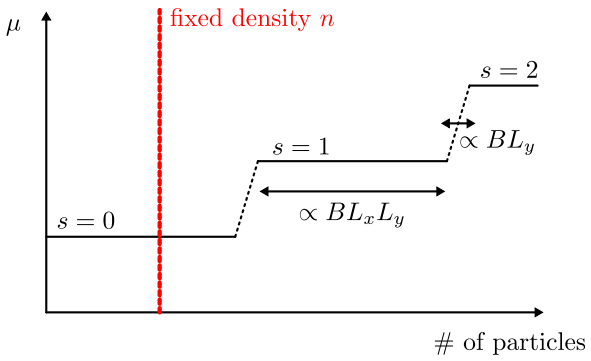

Figure 1.7: Chemical potential stuck to Landau levels.

1.5.1 The effect of disorder

The above result is strongly suggestive that one dimensional edge channels are responsible for the transport in the quantum Hall effect. Generically the current carried by a one-dimensional channel is given by

$$I = \frac{e^2}{h}|T|^2, \tag{1.26}$$

where $|T|^2$ denotes the probability for an electron to be transmitted through a disordered region. However, our edge channels are *chiral* where the electrons have no way to be back-scattered and therefore $|T|^2 = 1$. These arguments explain why even in the case of a disordered sample σ_{xy} can be quantized. However, we did not yet reconcile a quantized σ_{xy} with the general result $\sigma_{xy} = ne/B$ for a clean system.

We assumed the Fermi energy to lie between two Landau levels. Let us see under which conditions this can be the case. We assume the sample to be L_x wide and the edge region which is curved up to extend over the length $W \ll L_x$. From the finite size (or periodic) quantization in y-direction we know that the momentum can take the values $k_i = \frac{2\pi}{L_y} i$ with $i \in \mathbb{Z}$. Hence, we find for the centers of the Localized wave functions $X_i = \frac{2\pi}{L_y} l^2 i$. We now count how many wave functions fit into the bulk and how many into the edge:

$$\text{edge} \quad : \quad \frac{W}{X_i - X_{i-1}} \propto L_y, \qquad \text{bulk} \quad : \quad \frac{L_x}{X_i - X_{i-1}} \propto L_x L_y. \tag{1.27}$$

We see that there are extensively many bulk states but only a sub-extensive number of edge states as shown in Fig. 1.7.

Translated to a fixed density but varying magnetic field B we find that for almost all values of B the Fermi energy will lie in the bulk, not the edge! Meaning, our assumption that the we have a completely filled LL and the relevant physics is happening only on the edge was not justified. Hence we need to get a better understanding of disorder effects.

References

1. V. Klitzing, K., Dorda, G. & Pepper, M. "New Method for High-Accuracy Determination of the Fine-Structure Constant Based on Quantized Hall Resistance". *Phys. Rev. Lett.* **45,** 494 (1980).

2. *Topological aspects of low dimensional systems* (eds Comtet, A., Jolicoeur, T., Ouvry, S. & David, F.) (Springer-Verlag, Berlin, 1999).

3. Hall, E. "On a New Action of the Magnet on Electric Currents". *Amer. J. Math.* **2,** 287 (1879).

Chapter 2

Scaling theory of localization

Learning goals

- We appreciate the role of the dimensions for the localization of electrons.
- We can reproduce the gang-of-four scaling plot.

- M. A. Paalanen G. A. Thomas, Helv. Phys. Acta **56**, 27 (1983)

2.1 Conductance versus conductivity

We want to study the influence of disorder on the electrical resistance R relating the applied voltage U to the electrical current I

$$U = RI. \tag{2.1}$$

R connects two macroscopic observables and therefore characterizes a macroscopic sample. The conductance g is defined as the inverse of the resistance

$$g = \frac{1}{R}. \tag{2.2}$$

These quantities have to be contrasted with the microscopic quantities such as the conductivity σ

$$j = \sigma E, \tag{2.3}$$

where E is the electric field and j the microscopic current density. In this chapter we want to understand if there is a simple bridge between the microscopic quantity σ (which we might be able to calculate from first principles in simple model situations) and the macroscopic conductance g. We try to do so by starting from a relatively small system where we are in principle up to the task of calculating g exactly. We then want to successively increase the system size and see what we can deduce.

2.2 One parameter scaling

The key step in the program of successively increasing the system size dates back to the very influential paper by what we now call the the "gang of four": Abrahams, Anderson, Licciardello, and Ramakrishnan [1]. Their key insight was that the conductance $g(2L)$of a block of size $2L$ only depends on one parameter, namely the conductance $g(L)$ of the block of size L out of which the larger was formed, cf. Fig. 2.1. In other words

$$g(2L) = f[g(L)] \qquad \text{and not} \qquad g(2L) = h[g(L), L, \dots]. \tag{2.4}$$

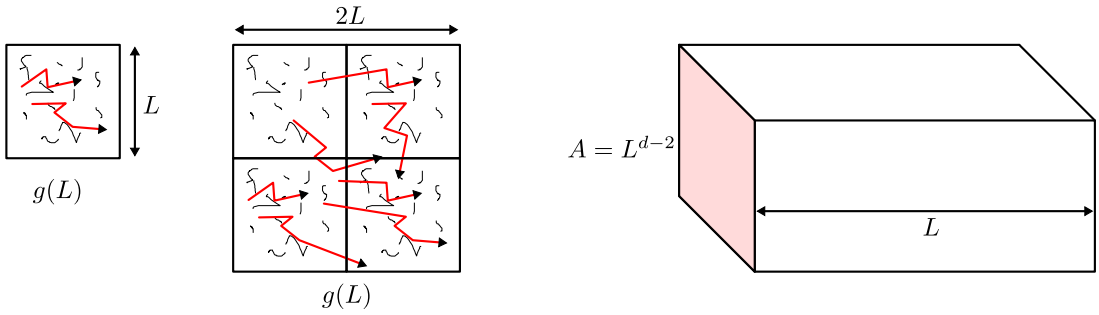

Figure 2.1: Setup for the renormalization of the conductance.

This statement is not easy to motivate in a systematic way. Instead of attempting to legitimate (2.4), we want to analyze its consequences in the following. To make further progress we write (2.4) in a form that contains no scales

$$\frac{L}{g}\frac{dg(L)}{dL} = \frac{d\log(g)}{d\log(L)} = \beta(g). \tag{2.5}$$

Let us have a look at simple limiting cases.

For a good conductor $g \gg 1$ we know that the "one parameter scaling" holds in the form of Ohm's law

$$R = \rho\frac{L}{A} = \rho\frac{L}{L^{d-1}} \qquad \Rightarrow \qquad g = \sigma_0 L^{2-d}. \tag{2.6}$$

From this we immediately obtain

$$\frac{d\log(g)}{d\log(L)} = d-2 \qquad \Rightarrow \qquad \lim_{g\to\infty}\beta(g) = d-2. \tag{2.7}$$

In the other limit of very strong disorder, all wave-function will be exponentially localized. Therefore, we expect the conductance to behave as

$$g(L) \propto e^{-L/\xi} \qquad \Rightarrow \qquad \frac{d\log(g)}{d\log(L)} = -\frac{L}{\xi} = \log(g). \tag{2.8}$$

Hence in the limit of vanishingly small conductance, the β function reads

$$\lim_{g\to 0}\beta(g) = \log(g). \tag{2.9}$$

We summarize these results in Fig. 2.2. Due to the dependence of the β-function on the dimension d, disorder seems to have very different effects depending on the spatial dimension. Let us discuss the consequences of Fig. 2.2 for one, two, and three dimensions separately.

2.2.1 One dimension

In one dimension, $\beta(g) < 0$ is always negative. In other words, by increasing the system size, the conductance g always flows to zero, irrespective of the conductance of a short section of the wire.

Let us define a localization length ξ, where $g(L=\xi) = 1$. We find

$$\frac{d\log(g)}{d\log(L)} = -1 \qquad \Rightarrow \qquad g(L) = \frac{g_0}{L} \qquad \Rightarrow \qquad \xi \sim g_0, \tag{2.10}$$

where g_0 is the conductance calculated for a small segment.

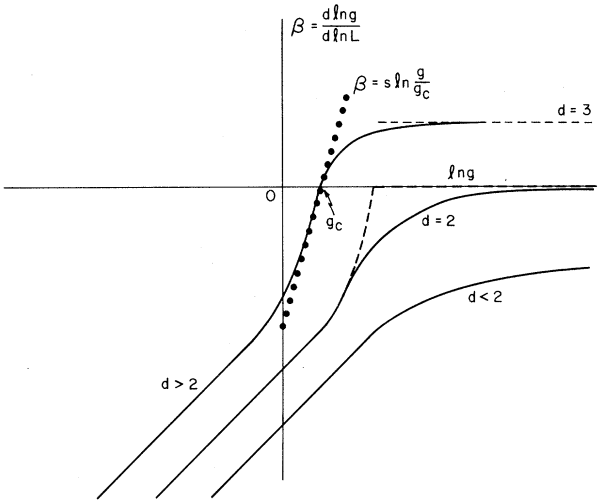

Figure 2.2: Plot of $\beta(g)$ as a function of $\log(g)$ for various dimensions. Figure take from Ref. [1] (Copyright (1979) by The American Physical Society).

2.2.2 Two dimensions

In two dimensions we encounter a somewhat more intriguing situation. For large values of g the β-function is zero. In other words, to first order in $1/g$, the conductance does not change under a change in L. Such a situation is called marginal. As we have identified the limit $g \gg 1$ as the classical regime where Ohm's law holds, this means quantum corrections will play a crucial role in how $\beta(g)$ behaves away from $g \gg 1$. These quantum corrections are called "weak (anti-) localization". Their detailed calculation is beyond the scope of this course. However, we can estimate them using a simple trick. Let us just calculate the probability for a particle to return to the point where we inject it into the system

$$P = |\langle \psi^\dagger(x)\psi(x)\rangle|^2. \tag{2.11}$$

When we calculate $\langle \psi^\dagger(x)\psi(x)\rangle$, we have to sum over all path the particle can take from x, back to the same point x. In quantum mechanics, each path is associated with an amplitude and a phase. Due to the disorder (which we try to study, after all), all paths sum up incoherently. If we have a time-reversal invariant system, however, there are paths who's amplitude and phase are correlated as shown in Fig. 2.3. Owing to the time-reversal symmetry the blue and the red path have a well defined phase relation. If we now calculate P the sum contains the following contributions shown in Fig. 2.4.

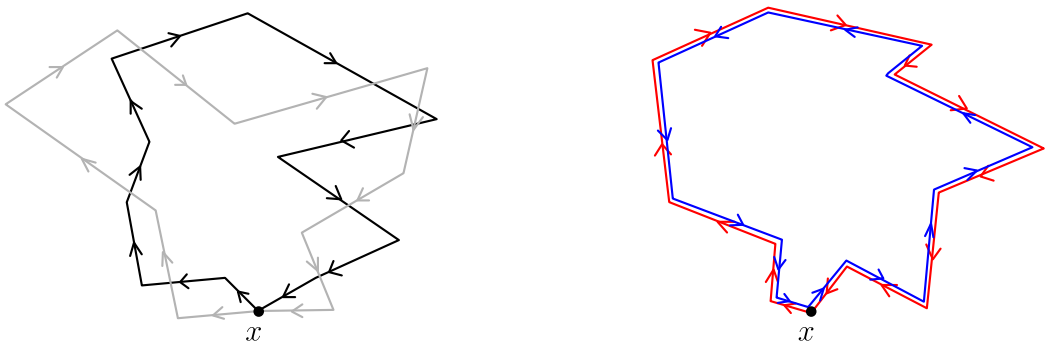

Figure 2.3: Return probability.

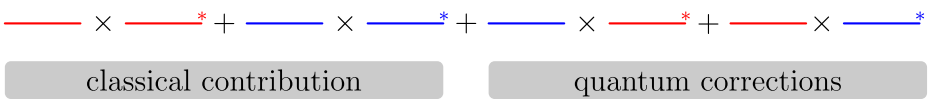

The endpoints of any segment are related to some state $|\phi\rangle$. In order to invert the arrow of time we use the time reversal operator $\mathcal{T}$ on these states:

Figure 2.4: Interference in the return probability.

From this we conclude that we can have two distinctly different situations

1. $\mathcal{T}^2 = -\mathbb{1}$ $\Rightarrow$ the return probability P is reduced, hence quantum mechanical effects lead to more extended states and we deal with weak *anti-localzation*.
2. $\mathcal{T}^2 = \mathbb{1}$ $\Rightarrow$ the return probability P is enhanced, i.e., the states are more localization: weak *localization*.

However, a word of caution is in order here! When applying this argument for spin-1/2 fermions we generically have $\mathcal{T}^2 = -\mathbb{1}$. But if the Hamiltonian does not mix the spin degrees of freedom, we can go to the individual spin sectors and describe the physics as two spin-0 problems. In this case however, $\mathcal{T}^2 = \mathbb{1}$. The situation changes if we deal with *spin-orbit* coupling. In this case we have to stick with the spin-1/2 description and therefore we generically expect *anti-localization* in this case.

Let us now analyze the case of no spin-orbit interactions, i.e., weak localization. We solve the equation

$$\frac{d\log(g)}{d\log(L)} = -\frac{C}{g} \qquad \text{or} \qquad \frac{dg}{d\log(L)} = -C < 0. \tag{2.12}$$

We find

$$g = g_0 - C\log(L/l), \tag{2.13}$$

where l is the small length at which we managed to solve the problem exactly and found $g(l) = g_0$. We can now again determine the localization length by equating $g(\xi) = 1$ to find

$$\xi \sim l e^{g_0/C}. \tag{2.14}$$

Indeed, all states are localized. However, $g \gg g_0$ and the localization length is astronomical.

2.2.3 Three dimensions

Three dimensions (or two with spin-orbit) are the most interesting cases. Depending on the initial value g_0, $\beta(g)$ is either positive or negative, i.e., a macroscopic sample can either be conducting or insulating. In other words, there is a metal-insulator transition as a function of g_0. For the time being three dimensions are not in the scope of the course and we will come back to it (and spin-orbit in two dimensions) later.

References

1. Abrahams, E., Anderson, P. W., Licciardello, D. C. & Ramakrishnan, T. V. "Scaling Theory of Localization: Absence of Quantum Diffusion in Two Dimensions". *Phys. Rev. Lett.* **42,** 673 (1979).

Chapter 3

The integer quantum Hall effect II

Learning goals

- We know the pumping argument of Laughlin and the concept of spectral flow.
- We know that there is always a delocalized state in each LL.
- We know that σ_{xy} is given by the Chern number.
- We understand why the Chern number is an integer.

- K. von Klitzing, G. Dorda, and M. Pepper, Phys. Rev. Lett. **45**, 494 (1980)

3.1 Laughlin's argument for the quantization of σ_{xy}

In the following we try to understand the pumping argument presented by R. Laughlin [1].

3.1.1 Spectral flow

The idea of *spectral flow* is central to the pumping argument of Laughlin. We try to understand this idea on the example of a particle on a ring threaded by a flux Φ

$$H = \frac{1}{2}\left(-\partial_\phi - eA\right)^2 \qquad \Rightarrow \qquad \psi_n(\phi) = \frac{1}{\sqrt{2}} e^{in\phi} \qquad \text{with} \qquad \epsilon_n = \frac{1}{2}\left(n - \frac{\Phi}{\Phi_0}\right)^2 . \tag{3.1}$$

After the insertion of a full flux quantum Φ_0, the Hamiltonian returns to itself. However, if we follow each state adiabatically, we see that the first excited and the ground state exchanged their positions. This situation is called spectral flow: While the spectrum has to be the same for $\Phi = 0$ and $\Phi = \Phi_0$, the adiabatic evolution does not need to return the ground state to itself! This is illustrated in Fig. 3.1. While the example of a particle on a ring is particularly simple, the same situation can occur for a general setup where after the insertion of a flux ϕ_0 the original ground state is adiabatically transferred to an excited state. Let us now see how this spectral flow effect applies to the quantum Hall problem.

3.1.2 The ribbon geometry

Laughlin proposed that if σ_{xy} is quantized, it should not depend on the details of the geometry. One is therefore allow to smoothly deform a rectangular sample in the following way: where in the last step we replaced the applied voltage $V \to \partial_t \Phi$ with the electromotive force of a time-dependent flux through the opening of the "Corbino" disk.

Let us see what happens when we inset this flux. We make use of the eigenfunctions in the radial gauge[1] $\psi \sim z^m \exp(-z^* z/4)$, where $z = (x + iy)/l$ which we can also write as

[1] See exercise 9.2.

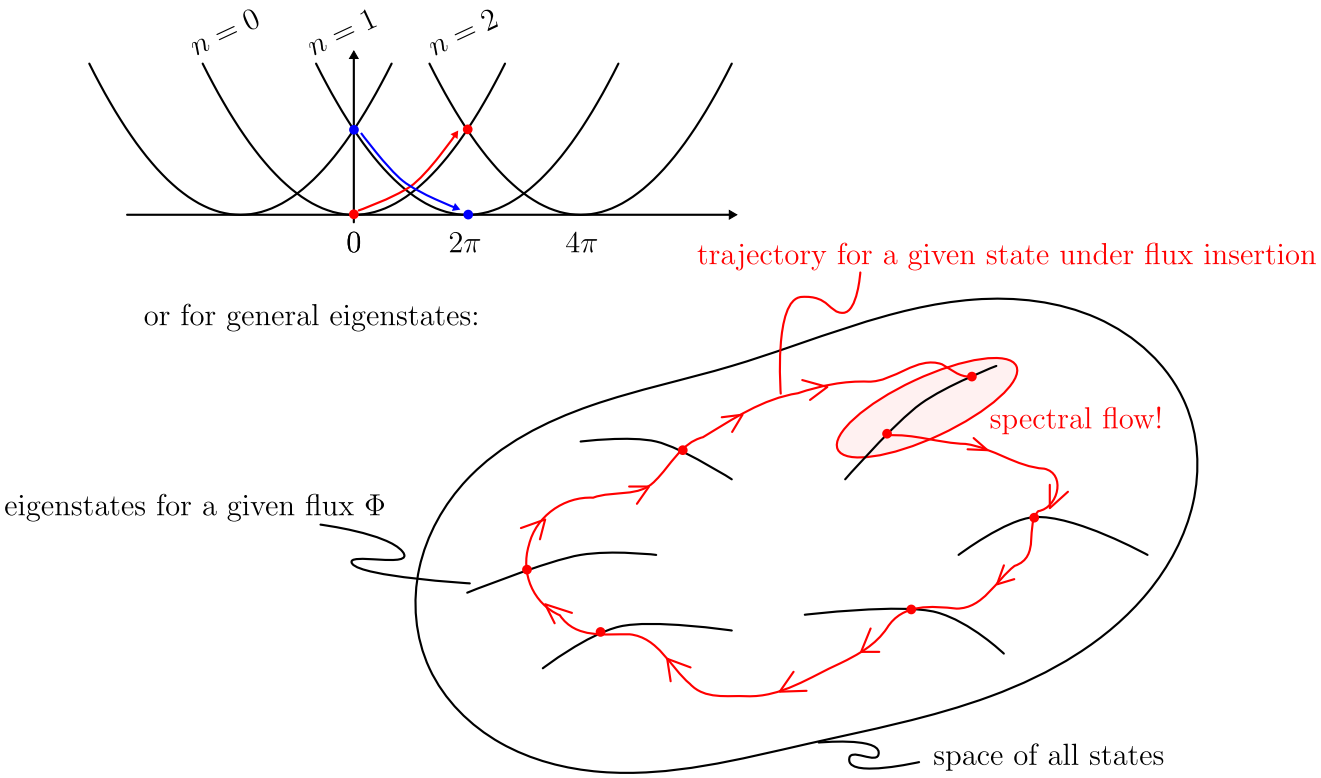

Figure 3.1: Spectral flow.

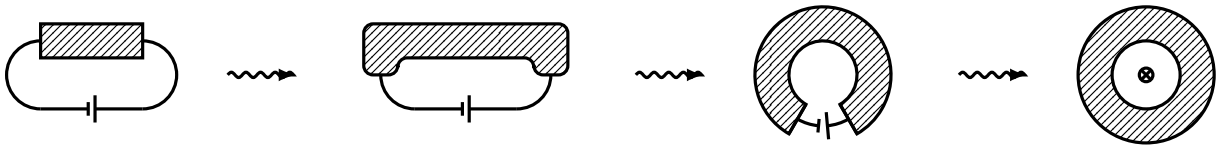

Figure 3.2: Change of geometry for Laughlin's pumping argument.

$e^{im\phi}r^m \exp(-r^2/4l^2)$. Again, we see that these are Gaussians in one of the coordinate, however, shifted in radial direction depending on m. By calculating $\partial_r\psi = 0$ we find that they are localized around $r_m = \sqrt{2m}l$. Therefore the flux enclosed by the m'th wave function is given by

$$\pi r_m^2 B = 2\pi m \frac{\hbar}{eB} B = m\Phi_0. \tag{3.2}$$

We now add slowly another flux Φ_0 into the opening of the Corbino disk. Slowly means on a time-scale $t_0 \gg 1\omega_c$, such that we do not excited any particles into the next LL. From the above considerations we conclude that

$$r_m(\Phi) \to r_m(\Phi + \Phi_0) = r_{m+1}(\Phi). \tag{3.3}$$

In other words, by inserting a flux quantum we transferred one state from the inner edge of the disk to the outer perimeter. To reach equilibrium, the system will let the charge relax again and we obtain

$$V_{\hat{\phi}} = -\frac{\partial\Phi}{\partial t} = \frac{h}{et_0}; \qquad I_{\hat{r}} = \frac{e}{t_0} \qquad \Rightarrow \qquad \sigma_{xy} = \frac{I_{\hat{r}}}{V_{\hat{\phi}}} = -\frac{e^2}{h}. \tag{3.4}$$

This closes the argument of R. Laughlin [1]: The insertion of one flux quantum transfers a quantized charge across the ribbon and hence leads to the quantized Hall conductance measured in the experiment. At this point it is in place to review the assumptions that went into this argument

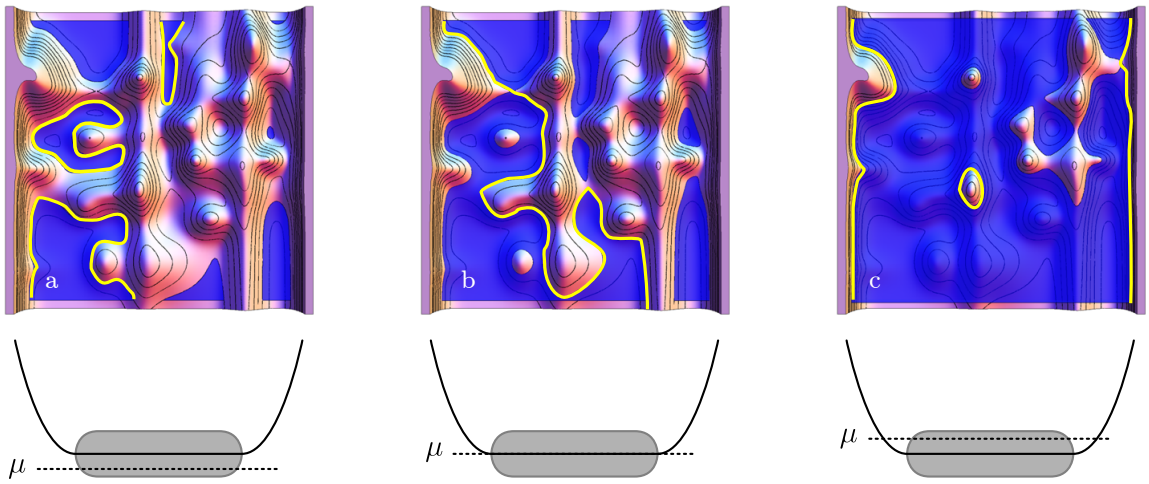

Figure 3.3: (a) Chemical potential below the center of the LL: All states are localized in the form of orbits around lakes. (b) At the percolation threshold there is one shoreline connecting the two sides of the sample. (c) Above the middle of the LL all but the two edge states are localized around islands.

1. $\hbar/t_0 \ll \hbar\omega_c$, i.e., we adiabatically inserted the flux. This is well justified as σ_{xy} describes *linear response*.

2. Spectral flow lead us to an excited state, i.e., the system was sensitive to the flux insertion!

How does this compare to the fact that we argued in the last chapter that in two dimensions all eigenstates are localized? After all a localized state in the vicinity of the outer edge should not feel anything of the flux inserted in the middle!

3.2 The percolation transition

In the last lecture we have seen that for spinless fermions and for a time-reversal invariant system all states are localized in two spatial dimensions. How can we reconcile this with the above argument for the quantization of σ_{xy}. The answer is, that for the case of a magnetic field, where time reversal symmetry is broken, the gang-of-four argument does not hold.

There is, however, a relatively simple picture in terms of percolating clusters. We know that eigenstates in a disordered LL level are given by orbits along equipotential lines.[2] The question is, if there is always an orbit in each LL that connects the two edges of our Corbino disk. If this is the case, this state mediates the sensitivity to the flux insertion and Laughlin's argument goes through also in the disordered case. Luckily the answer to this question is an affirmative yes!

In Fig. 3.3 energy landscape for a disordered LLL with a confinig potential is shown. Eigenstates are given by equipotential orbits. At low chemical potential μ as shown here, all orbits are "lakes" and hence all states are localized.

When filling in more water (raising μ) we switch at some point from "lakes" to "island". Right at the point where this happens, the shoreline has to connect through the whole sample. This is the sought after extended state in the middle of the sample. Above the center of the LL we are left with "islands" where all states in the bulk are localized. However, we get one edge state on either side of the sample as discussed for the case of no disorder.

We can now summarize our discussion of disorder effects: (i) We found the extended state in the LL needed for Laughlin's pumping argument to hold. (ii) The disorder allows the chemical

[2] See exercise number one.

potential to smoothly change also between the LL's. Therefore, there is an extensive window where the chemical potential lies in the range of the (mobility) gap and hence we find

$$\sigma_{xy} = -\frac{e^2}{h}\nu \qquad \nu \in \mathbb{Z}. \tag{3.5}$$

3.3 The TKNN integer

We have now seen that the Hall conductivity has to be quantized in two independent ways. Once, we saw that the edge states of the QHE are chiral one dimensional channels which carry a conductivity of e^2/h. On the other hand, we saw that the pumping argument requires σ_{xy} to be quantized. In both cases the effect was not only stable to disorder but actually required a certain amount of dirt the lift the huge degeneracy of the LL's which made the chemical potential to cling to the bulk states. The obvious question is now if there is a deeper, "topological" reason that links these two arguments given above. The answer was given in another seminal paper by Thouless, Kohmoto, Nightingale, and den Nijs (TKNN) in 1982 [2].

3.3.1 Landau levels on the torus

The original paper [2] considered electrons in a periodic potential. Here we want to follow a different route inspired by Avron and Seiler [3] (See also lecture notes by A. Kitaev).

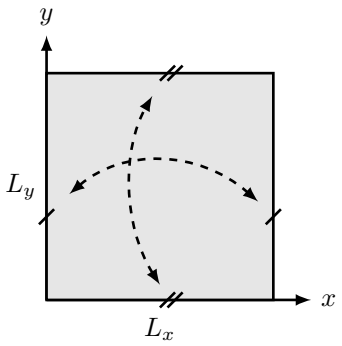

Figure 3.4: Real space torus.

We consider the problem of a magnetic field on a torus. We use the gauge field

$$A_x = \frac{\Phi_x}{L_x}, \quad A_y = \frac{\Phi_y}{L_y} + Bx, \tag{3.6}$$

where we added fluxes $\Phi_{x/y}$ through the openings of the torus. The boundary conditions on the torus in the presence of a magnetic field are somewhat non-trivial. Let us define them with respect to the magnetic translation operators which are defined via the canonical momentum operator $(i\hbar\nabla - e\mathbf{A})$

$$T^A_{\mathbf{u}} = e^{\frac{i}{\hbar}\mathbf{u}\cdot\mathbf{p}} = e^{\frac{i}{\hbar}\mathbf{u}\cdot(i\hbar\nabla - e\mathbf{A})} = e^{\frac{ie}{\hbar}u_y Bx} T^{A=0}_{\mathbf{u}}. \tag{3.7}$$

Note that these operators depend on the choice of gauge. To derive the boundary conditions, we now consider $\mathbf{u}_1 = (L_x, 0)$ and $\mathbf{u}_2 = (0, L_y)$.

$$T^A_{\mathbf{u}_1}\psi(x,y) = \psi(x + L_x, y) \stackrel{!}{=} \psi(x,y), \tag{3.8}$$

$$T^A_{\mathbf{u}_2}\psi(x,y) = e^{\frac{ie}{\hbar}BxL_y}\psi(x, y + L_y) \stackrel{!}{=} \psi(x,y). \tag{3.9}$$

These two conditions are only compatible if

$$T^A_{\mathbf{u}_1} T^A_{\mathbf{u}_2} = T^A_{\mathbf{u}_2} T^A_{\mathbf{u}_1}. \tag{3.10}$$

This is only the case for

$$\frac{eB}{\hbar} L_x L_y = \frac{L_x L_y}{l^2} = 2\pi n \tag{3.11}$$

with $n \in \mathbb{Z}$. In other words, an integer number flux quanta has to pierce the surface of the torus (we can only put quantized magntic monopoles inside the torus). One can also see that the boundary conditions contain a "gluing phase"

$$\psi(0,y) = \psi(L_x, y), \tag{3.12}$$

$$\psi(x,0) = e^{-\frac{ie}{\hbar}BxL_y}\psi(x, L_y). \tag{3.13}$$

In order to appreciate the role of (Φ_x, Φ_y) we calculate the Wilson loops

$$W_x(y) = \oint dx \tilde{A}_x(x,y) = BL_x y + \Phi_x, \tag{3.14}$$

$$W_y(x) = \oint dy \tilde{A}_y(x,y) = BL_y x + \Phi_y, \tag{3.15}$$

where we absorbed the gluing phase in the vector potential $\tilde{\mathbf{A}}$. $\mathbf{W} = (W_x(y), W_y(x))$ is a gauge invariant vector and shows that on a torus a magnetic field breaks all translational symmetries. Moreover, we see, that we can view (Φ_x, Φ_y) as a shift in (x, y). Equipped with these details about the problem of a magnetic field on a torus we now want to embark on the calculation of the Hall conductivity.

3.3.2 Kubo formula

For a microscopic calculation of the conductivity we need a bit of linear response theory. We are interested in the (linear) response of a system to a (small) applied perturbation. In our case the response of interest is the current density $\mathbf{j}(r) = \frac{e}{2m}\sum_i [\mathbf{p}_i \delta(\mathbf{r} - \mathbf{r}_i) + \delta(\mathbf{r} - \mathbf{r}_i)\mathbf{p}_i)]$. The perturbation is given by an applied electric field $\mathbf{E} = -\partial_t \mathbf{A}$. The perturbing Hamiltonian can therefore be written as

$$H' = -\int d\mathbf{r}\, \mathbf{j}(\mathbf{r}) \cdot \mathbf{A}(\mathbf{r}), \tag{3.16}$$

We are interested in the expectation value of the current density operator

$$\bar{\mathbf{j}}(\mathbf{r}, t) = \langle \psi | U^\dagger(t) \mathbf{j}(\mathbf{r}, t) U(t) | \psi \rangle \qquad \text{with} \qquad U(t) = T_t e^{-\frac{i}{\hbar}\int_{-\infty}^{t} dt' H'(t')}, \tag{3.17}$$

and

$$\mathbf{j}(\mathbf{r}, t) = e^{\frac{i}{\hbar}\int_{-\infty}^{t} dt'\, H_0(t')} \mathbf{j}(\mathbf{r}) e^{-\frac{i}{\hbar}\int_{-\infty}^{t} dt'\, H_0(t')} \quad \text{and} \quad H'(t) = e^{\frac{i}{\hbar}\int_{-\infty}^{t} dt'\, H_0(t')} H' e^{-\frac{i}{\hbar}\int_{-\infty}^{t} dt'\, H_0(t')} \tag{3.18}$$

Here, T_t is the time-ordering operator and $|\psi\rangle$ is the unperturbed ground state of the original Hamiltonian H_0. As usual for perturbation theory, we switched to the interaction representation.

We assume the vector potential in H' to be given by $\mathbf{A} = (\Phi_x/L_x, \Phi_y/L_y)e^{t/\tau}$, which corresponds to slowly turning on the fluxes through the opening of the torus. Moreover, we only drive with a spatially constant field. Note, that $\mathbf{A}_0 = Bx\hat{\mathbf{y}}$ is not included in H' as this is not considered to be small but part of the unperturbed Hamiltonian H_0. In linear response we can expand the exponent in $U(t)$ to obtain

$$\bar{j}_\alpha(\mathbf{r}, t) = \frac{i}{\hbar}\sum_\beta \int_{-\infty}^{t} dt'\, A_\beta(t') \langle [j_\alpha(\mathbf{r}, t), \int d\mathbf{r}' j_\beta(\mathbf{r}', t')] \rangle \tag{3.19}$$

$$= \frac{i}{\hbar}\sum_\beta \int_{-\infty}^{t} dt'\, A_\beta(t') \langle [j_\alpha(\mathbf{r}, t), J_\beta(t')] \rangle. \tag{3.20}$$

We write $J_\beta(t')$ for the $\mathbf{q} = 0$ Fourier-component of the current as it represent the *total* current. Moreover, as we only drive with $\mathbf{q} = 0$, we only get response at this wave vector. To make this clearer we take the Fourier transform on both side with respect to $\mathbf{r}$

$$\bar{J}_\alpha(t) = \frac{i}{\hbar}\sum_\beta \int_{\infty}^{t} dt' \underbrace{\frac{\Phi_\beta}{L_\beta} e^{\frac{t'}{\tau}}}_{=\tau E^0_\beta e^{t'/\tau}} \langle [J_\alpha(t), J_\beta(t')] \rangle. \tag{3.21}$$

We can now relate the current density[3] to the final driving field E_y^0 to obtain an expression for the Hall conductance

$$\sigma_{xy}(t) = \frac{i\tau}{\hbar v}\int_{-\infty}^{t} dt'\, e^{\frac{t'}{\tau}}\langle[J_\alpha(t), J_\beta(t')]\rangle \tag{3.22}$$

The result (3.22) is known as the *Kubo formula*. Let us review this result again: The first current operator arises as we measure a current. The second one because the perturbing Hamiltonian H' is also proportional to the current. The commutator originates from the perturbation theory where $U(t)$ is once acting from the left and once from the right. The multiplication by τ accounts for the time derivative linking the electric field $\mathbf{E}$ and the vector potential $\mathbf{A}$. Finally, in our derivation we made the explicit assumption that we turn on the fluxes Φ_α adiabatically. Certainly the Kubo formula is more general and can be derived for an arbitrary time and space dependence of the perturbation.

To make progress we manipulate (3.22) further

$$\sigma_{xy} = \sigma_{xy}(t=0) = \frac{i\tau}{\hbar v}\int_{-\infty}^{0} dt'\,\tau e^{t'/\tau}\langle[J_\alpha(0), J_\beta(t')]\rangle \tag{3.23}$$

$$= \frac{i}{\hbar v}\int_0^\infty dt_1 \int_{-\infty}^{0} dt_2 \langle[J_x(t_1), J_y(t_2)]\rangle e^{-\frac{t_1-t_2}{\tau}} \tag{3.24}$$

$$= \frac{i}{\hbar}\langle[Q_x^+, Q_y^-]\rangle, \tag{3.25}$$

where the operators $Q_\alpha^\pm$ are defined as

$$Q_\alpha^+ = \frac{1}{L_\alpha}\int_0^\infty dt\, e^{-t/\tau} J_\alpha(t), \qquad \text{and} \qquad Q_\alpha^- = \frac{1}{L_\alpha}\int_{-\infty}^{0} dt\, e^{t/\tau} J_\alpha(t). \tag{3.26}$$

To evaluate the above formula for σ_{xy} we apply the *adiabatic approximation*: We try to exchange the current operators in (3.22) with something that explicitly only depends on the *ground state wave-function* $|\psi_t\rangle$ at a given time during the turn-on process. At this point it is convenient to introduce the (dimensionless) phases

$$\varphi_\alpha = \Phi_\alpha/\Phi_0 = \frac{e}{\hbar}\Phi_\alpha. \tag{3.27}$$

Inserted into (3.16) we have

$$H' = -\int d\mathbf{r}\,\mathbf{j}(\mathbf{r})\cdot\mathbf{A}(\mathbf{r}) = -\sum_\alpha J_\alpha \frac{\Phi_\alpha}{L_\alpha} e^{t/\tau} = -\sum_\alpha J_\alpha \frac{\hbar}{e}\frac{\varphi_\alpha}{L_\alpha} e^{t/\tau}. \tag{3.28}$$

Let us write the ground state wave function at $t=0$ by evolving the $t=-\infty$ wave function assuming φ_α to be small

$$|\psi_0\rangle = \hat{T}_t e^{-\frac{i}{\hbar}\int_\infty^0 dt'\, H'(t')}|\psi_{-\infty}\rangle \approx |\psi_{-\infty}\rangle - \sum_\alpha \frac{i}{e}\varphi_\alpha Q_\alpha^-|\psi_{-\infty}\rangle. \tag{3.29}$$

We now make use of the adiabatic approximation: We assume that we do not induce any transitions to states above *a postulated energy gap*. Moreover, the state at $t=-\infty$ does not depend on φ_α. When taking the derivative $\partial/\partial\varphi_\alpha$ on both sides of Eq. (3.29) we obtain

$$Q_\alpha^-|\psi_0\rangle = ie\left|\frac{\partial\psi_0}{\partial\varphi_\alpha}\right\rangle. \tag{3.30}$$

[3]Note that by taking the Fourier-transform

$$\bar{J}(\mathbf{q}) = \int d\mathbf{r} e^{i\mathbf{q}\cdot\mathbf{r}}\bar{j}(\mathbf{r})$$

we switched from current *density* to the total current. However, σ_{xy} relates the driving field $\mathbf{E}$ to the *current density* in $\bar{J}_x/v = \bar{J}_x/L_xL_y$. We account for that by dividing by the volume $v = L_xL_y$.

We achieved our goal to replace the unwanted current operators! For clarity and to make connection to more mathematical literature [4] we introduce the Berry connection

$$\mathcal{A}_\alpha = i\langle\psi_0|\partial_\alpha\psi_0\rangle, \qquad \text{or} \qquad \boldsymbol{\mathcal{A}} = i\langle\psi_0|\nabla\psi_0\rangle \tag{3.31}$$

and the corresponding Berry curvature

$$\mathcal{F}_{\alpha\beta} = \partial_\alpha\mathcal{A}_\beta - \partial_\beta\mathcal{A}_\alpha \qquad \text{or} \qquad \boldsymbol{\mathcal{F}} = \nabla \wedge \boldsymbol{\mathcal{A}}. \tag{3.32}$$

We can now write for σ_{xy}

$$\sigma_{xy} = \frac{e^2}{\hbar}\mathcal{F}_{xy}, \tag{3.33}$$

Let us take the step from the adiabatic turning-on of the field to a dc-field. In that case the field $\mathbf{A}$ grows linearly in time, or in other words, the phase φ_x winds as a function of time. We therefore average the above result over $\int d\varphi_x/2\pi$. To make matters more symmetric, we also average over φ_y. This leads us to the formula

$$\sigma_{xy} = \frac{e^2}{\hbar}\int\frac{d\varphi_x d\varphi_y}{(2\pi)^2}\mathcal{F}_{xy} = \frac{e^2}{h}\int\frac{d\varphi_x d\varphi_y}{2\pi}\mathcal{F}_{xy} = \frac{e^2}{h}\frac{\mathcal{C}}{2\pi}, \tag{3.34}$$

where we identified the Chern number $\mathcal{C}$ [4]. In order to get a better understanding of Eq. (3.34) we related it to the Berry phase of a spin-1/2 in a magnetic field before we motivate it to be quantized to an integer number times the quantum of conductance e^2/h.

3.4 The Berry phase

We would like to establish the link between the well known Berry phase [5] and the expression for the Hall conductance derived above. Let us assume that we have a Hamiltonian $H[\mathbf{R}(t)]$ that depends on time dependent parameters $\mathbf{R}(t)$. These parameters are supposed to evolve slowly

$$\hbar\frac{\partial R_i(t)}{\partial t} \ll \Delta, \tag{3.35}$$

where Δ is the minimal gap between the instantaneous ground state and the first excited state at any given time t. If we start at $t = 0$ in the ground state, we will always stay in the instantaneous ground state. However, along the way we will pick up a phase

$$e^{i\varphi(t)}|\psi_0(\mathbf{R})\rangle : \qquad i\hbar\partial_t e^{i\varphi(t)}|\psi_0(\mathbf{R})\rangle = H[\mathbf{R}(t)]e^{i\varphi(t)}|\psi_0(\mathbf{R})\rangle. \tag{3.36}$$

Multiplying this expression from the left with $\langle\psi_0(\mathbf{R})|e^{-i\varphi(t)}$ we obtain

$$\partial_t\varphi(t) = i\langle\psi_0(\mathbf{R})|\nabla_{\mathbf{R}}|\psi_0(\mathbf{R})\rangle\cdot\frac{\partial\mathbf{R}}{\partial t} - \frac{1}{\hbar}E_0(\mathbf{R}). \tag{3.37}$$

Integrating this equation leads to

$$\varphi(t) - \varphi(0) = \underbrace{\int_{\mathbf{R}(0)}^{\mathbf{R}(t)}\langle\psi_0(\mathbf{R})|i\nabla_{\mathbf{R}}|\psi_0(\mathbf{R})\rangle\cdot d\mathbf{R}}_{\text{geometrical phase}} - \underbrace{\frac{1}{\hbar}\int_0^t dt' E_0(t')}_{\text{dynamical phase}}. \tag{3.38}$$

If we now consider a path along a closed contour γ, the dynamical phase drops out and we find

$$\varphi_\gamma = \oint_\gamma d\mathbf{l}\, i\langle\psi_0|\nabla_{\mathbf{R}}\psi_0\rangle = \oint_\gamma d\mathbf{l}\,\boldsymbol{\mathcal{A}} = \int_\Gamma d\mathbf{S}\,\boldsymbol{\mathcal{F}}, \tag{3.39}$$

where Γ is the area enclosed by the contour γ. With this we see, that σ_{xy} is given by the Berry phase[4] of the ground state when we move the system once around the torus $[0, 2\pi] \times [0, 2\pi]$. Let us gain a deeper understanding of the Berry phase by recalling the example of a spin-1/2 in a magnetic field.

3.4.1 Spin-1/2 in a magnetic field

The Hamiltonian of a spin-1/2 in a magnetic field is given by

$$H = -\mathbf{h} \cdot \boldsymbol{\sigma} = -\sum_{\alpha=x,y,z} h_\alpha \sigma_\alpha. \tag{3.40}$$

If we write the magnetic field in spherical coordinates

$$h_x = h \sin(\vartheta) \cos(\varphi), \tag{3.41}$$
$$h_y = h \sin(\vartheta) \sin(\varphi), \tag{3.42}$$
$$h_z = h \cos(\vartheta), \tag{3.43}$$

the ground state can be written as

$$|\xi_1\rangle = \begin{pmatrix} \cos(\vartheta/2) \\ e^{i\varphi} \sin(\vartheta/2) \end{pmatrix} \qquad \text{or} \qquad |\xi_2\rangle = \begin{pmatrix} e^{-i\varphi} \cos(\vartheta/2) \\ \sin(\vartheta/2) \end{pmatrix}. \tag{3.44}$$

Both states $|\xi_1\rangle$ and $|\xi_2\rangle$ describe the ground state. However, $|\xi_1\rangle$ is singular at $\vartheta = \pi$ (or at the south-pole), while $|\xi_2\rangle$ is singular at the north-pole. In other words, we had to introduce two patches on the sphere to obtain a smooth parameterization of the instantaneous eigenstates, see Fig. 3.5. However, we can glue these two patches together via a gluing phase

$$|\xi_1\rangle = e^{i\zeta(\varphi)} |\xi_2\rangle \qquad \text{with} \qquad \zeta(\varphi) = \varphi \tag{3.45}$$

along the equator. Let us calculate the Berry connection for the two states. Recall that in spherical coordinates the differential operators take the forms

$$\nabla f = \frac{\partial}{\partial r} f \, \hat{\mathbf{r}} + \frac{1}{r} \frac{\partial}{\partial \vartheta} f \, \hat{\boldsymbol{\vartheta}} + \frac{1}{r \sin(\vartheta)} \frac{\partial}{\partial \varphi} f \, \hat{\boldsymbol{\varphi}}, \tag{3.46}$$

and

$$\nabla \wedge \mathbf{A} = \frac{1}{r \sin(\vartheta)} \left\{ \frac{\partial}{\partial \vartheta} \left[A_\varphi \sin(\vartheta) \right] - \frac{\partial A_\vartheta}{\partial \varphi} \right\} \hat{\mathbf{r}} + \frac{1}{r} \left\{ \frac{1}{\sin(\vartheta)} \frac{\partial A_r}{\partial \varphi} - \frac{\partial}{\partial r} \left(r A_\varphi \right) \right\} \hat{\boldsymbol{\vartheta}} + \frac{1}{r} \left\{ \frac{\partial}{\partial r} \left(r A_\vartheta \right) - \frac{\partial A_r}{\partial \vartheta} \right\} \hat{\boldsymbol{\varphi}}. \tag{3.47}$$

With this we immediately find

$$\boldsymbol{\mathcal{A}} = \frac{1}{2r} \hat{\boldsymbol{\varphi}} \cdot \begin{cases} -\tan(\vartheta/2) & |\xi_1\rangle \\ \cot(\vartheta/2) & |\xi_2\rangle \end{cases} \qquad \text{and} \qquad \boldsymbol{\mathcal{F}} = -\frac{\alpha}{2r^2} \hat{\mathbf{r}}. \tag{3.48}$$

Here, we introduced $\alpha = 1$ for later purposes. A few remarks are in order: (i) The "**B**"-field $\mathcal{F}_{\varphi\vartheta}$ corresponds to a monopole field of a monopole of strength $-\alpha$ at the origin. This can be seen by integrating $\mathcal{F}_{\varphi\vartheta}$ over the whole sphere S^2

$$\int_{S^2} d\boldsymbol{\Omega} \, \boldsymbol{\mathcal{F}} = -\alpha. \tag{3.49}$$

[4] Why to we call this a phase? Note that

$$0 = \partial_\eta 1 = \partial_\eta \langle \psi | \psi \rangle = \langle \partial_\eta \psi | \psi \rangle + \langle \psi | \partial_\eta \psi \rangle = \langle \partial_\eta \psi | \psi \rangle + \langle \partial_\eta \psi | \psi \rangle^* = a + a^*.$$

Therefore $a = -a^*$ and hence, $\mathrm{Re}[a] = 0$.

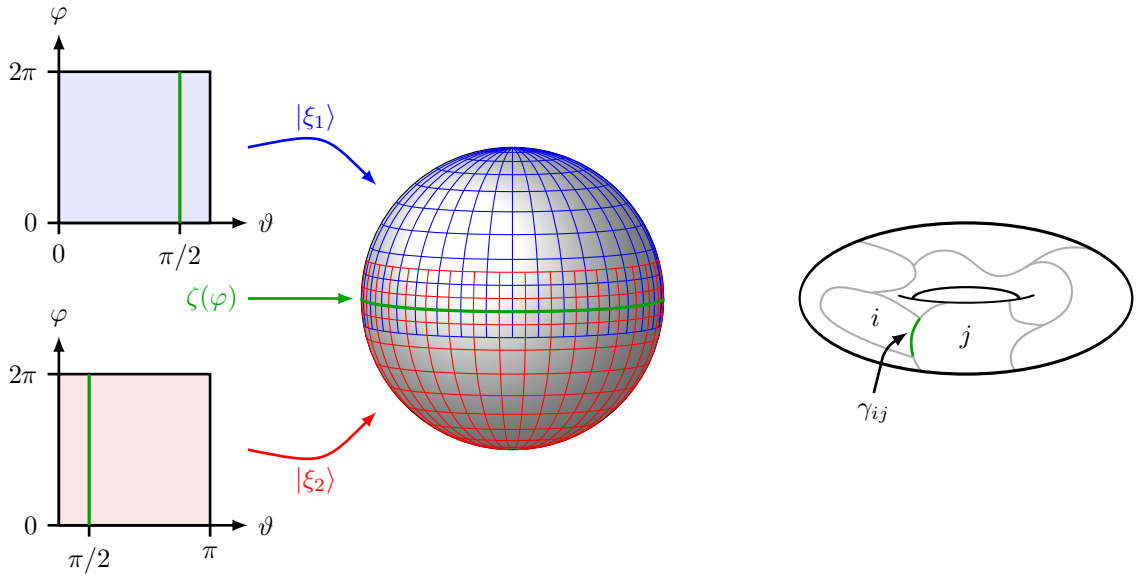

Figure 3.5: Left: Two patches introduced by the gauge choice for the ground state of a spin-1/2 in a magnetic field. No single patch can describe all eigenstate. However, the two patches can be glued together via $\zeta(\varphi)$. Right: Triangulation of the torus where the gluing phase between two individual patches i and j is indicated.

(ii) Integrated over the solid angle $d\boldsymbol{\Omega}$ we obtain a Berry phase $\varphi = -\frac{\alpha}{2} d\Omega$. (iii) The field $\boldsymbol{\mathcal{A}}$ corresponds to a monopole at $\mathbf{h} = 0$. At $\mathbf{h} = 0$ the Hamiltonian is zero, i.e., the system is *doubly degenerate*. To appreciate this further, we write (see Ref. [5] for details)

$$\boldsymbol{\mathcal{F}} = \mathbf{B} = \nabla \wedge \langle\psi|\nabla\psi\rangle = \langle\nabla\psi| \wedge |\nabla\psi\rangle = \sum_{m\neq 0} \langle\nabla\psi|m\rangle \wedge \langle m|\nabla\psi\rangle = \sum_{m\neq 0} \frac{\langle\psi|\nabla H|m\rangle \wedge \langle m|\nabla H|\psi\rangle}{(E_m - E_0)^2}.$$

It is easy to show that $\nabla \cdot \mathbf{B} = 0$ if $E_m - E_0 \neq 0$.

To take another step towards understanding the quantization of the Chern number, let us show that α cannot take arbitrary values. We calculate the Berry phase along a path γ that does not contain the south pole. For simplicity, let us take the equator. We can therefore write

$$\varphi_\gamma = \oint_\gamma d\mathbf{l}\, \boldsymbol{\mathcal{A}} = \int_\Gamma d\boldsymbol{\Omega}\, \boldsymbol{\mathcal{F}} = -\alpha\Omega(\Gamma)/2 \mod 2\pi, \tag{3.50}$$

where $\Omega(\Gamma)$ is the solid angle of the surface Γ. We closed γ such that Γ contains the north pole. Alternatively we could have closed γ to $\Gamma' = S^2 - \Gamma$ and write

$$\varphi_\gamma = -\int_{\Gamma'} d\boldsymbol{\Omega}\, \boldsymbol{\mathcal{F}} = \alpha(4\pi - \Omega(\Gamma))/2 \mod 2\pi. \tag{3.51}$$

In order for (3.50) and (3.51) to yield the same result we require

$$\alpha \in \mathbb{Z}. \tag{3.52}$$

This observation leads us back to the definition of the Chern number

$$\mathcal{C} = \frac{1}{2\pi} \int_M d\boldsymbol{\Omega}\, \boldsymbol{\mathcal{F}} \quad \in \quad \mathbb{Z} \tag{3.53}$$

for any "well behaved", compact, two-dimensional manifold M without boundaries. It can be shown that $\mathcal{C}$ is a topological invariant of the *fiber bundle* looking locally like $M \times U(1)$, where $M = S^2$ is the base manifold defined by the parameters of the Hamiltonian (or more precisely,

the parameters defining the projectors $|\psi_0\rangle\langle\psi_0|$ onto the ground state) and $U(1)$ is called the fibre defined by the phase of the ground state a any given point on S^2. Note, however, that the fibre bundle we are dealing with only *locally* looks like $S^2 \times U(1)$. To get the full fibre bundle we need to stitch together the two patches defined by $|\xi_{1/2}\rangle$. The role of the gluing phases ζ_{ij} for patches i, j on the compact manifold M can be further highlighted through the formula

$$\mathcal{C} = \frac{1}{2\pi} \sum_{i<j} \int_{\gamma_{ik}} d\zeta_{ij} \quad \in \quad \mathbb{Z}. \tag{3.54}$$

In other words, a non-vanishing Chern number $\mathcal{C}$ is intrinsically linked to the inability to chose a smooth gauge, i.e., only if we have to chose several patches that we glue together with ζ_{ij} can $\mathcal{C}$ be non-zero, see Fig. 3.5. A concrete example of this is our example of the spin-1/2 for which we have

$$\mathcal{C} = \frac{1}{2\pi} \int_{S^2} d\boldsymbol{\Omega}\, \boldsymbol{\mathcal{F}} = -1 = \frac{1}{2\pi} \oint_{\text{equator}} d\varphi\, \zeta(\varphi). \tag{3.55}$$

For further details we refer to the book by Nakahara [4] for a detailed mathematical exposition or the book by Bohm et al. [6] for a more physical approach. We finish this section by stating the long-sought formula

$$\boxed{\sigma_{xy} = \frac{e^2}{h}\nu \qquad \text{with} \qquad \nu \in \mathbb{Z}.} \tag{3.56}$$

3.5 Translation invariant systems

Above we made an effort to formulate the derivation of σ_{xy} free of relations to momentum integrals. This allows our formalism to be applied to disordered or interacting systems [3]. However, much of what will follow in Chern insulators and eventually the so-called "topological insulators" will be formulated in translation-invariant systems.

Both for a systems in free space as well as on a lattice it is easy to see that the (quasi) momentum $\mathbf{k}$ is doing nothing but making the wave-function acquire a phase $\exp(i\mathbf{k}\cdot\mathbf{x})$ which is linearly growing in $\mathbf{x}$. Moreover k_α is the proportionality constant in α-direction. The fluxes (Φ_x, Φ_y) do exactly the same. This can easily be seen by performing a gauge transformation

$$\psi(x) = e^{ikx} \longrightarrow \psi'(x) = e^{i\frac{e}{\hbar}\int_0^x dx' A(x')} e^{ikx} = e^{i\frac{e}{\hbar}\Phi_x x} e^{ikx} = e^{i(k+\varphi)x} = e^{ik'x}. \tag{3.57}$$

We see that therefore the integrals over φ in (3.34) are nothing but momentum space integrals for periodic systems [2]. Show to yourself that for a ground state wave-function which is a Slater determinant of momentum eigenstates, the expression (3.34) is particularly simple.

3.6 Berry curvature as a magnetic field in momentum space

Before we move on to examples beyond Landau levels which carry a Chern number, we want to get another intuition of what a non-zero Berry curvature represents. We consider electrons in a periodic potential under a weak perturbation. Under the right circumstances one can describe the dynamics in a semiclassical model described by the equations of motion for a wave-packet

$$\dot{\mathbf{r}} = \mathbf{v}_n(\mathbf{k}) = \frac{1}{\hbar}\nabla_{\mathbf{k}}\epsilon_n(\mathbf{k}), \tag{3.58}$$

$$\hbar\dot{\mathbf{k}} = -e\left[\mathbf{E}(\mathbf{r},t) + \dot{\mathbf{r}} \wedge \mathbf{B}(\mathbf{r},t)\right], \tag{3.59}$$

where n labels the n'th Bloch band. A proper derivation of these equations is beyond the scope of this course. We refer the reader to Ashcroft & Mermin [7] for a basic introduction and to

the excellent review by Xiao, et al. [8]. When band properties are taken more properly into account, one finds the above equations have to be adjusted to read [8]

$$\dot{\mathbf{r}} = \mathbf{v}_n(\mathbf{k}) = \frac{1}{\hbar}\nabla_{\mathbf{k}}\epsilon_n(\mathbf{k}) - \dot{\mathbf{k}} \wedge \mathbf{\Omega}_n(\mathbf{k}), \tag{3.60}$$

$$\hbar\dot{\mathbf{k}} = -e\left[\mathbf{E}(\mathbf{r},t) + \dot{\mathbf{r}} \wedge \mathbf{B}(\mathbf{r},t)\right], \tag{3.61}$$

with

$$\mathbf{\Omega}_n(\mathbf{k}) = \langle \partial_{k_x}\varphi_n(\mathbf{k})| \wedge |\partial_{k_y}\varphi_n(\mathbf{k})\rangle = \boldsymbol{\mathcal{F}}_n(\mathbf{k}) \tag{3.62}$$

the Berry curvature of the n'th band and $\varphi_n(\mathbf{k})$ the corresponding Bloch eigenfunctions. From these equations we can conclude that the Barry curvature takes the role of a "magnetic field" in $\mathbf{k}$-space.

References

1. Laughlin, R. B. "Quantized Hall conductivity in two dimensions". *Phys. Rev. B* **23,** 5632 (1981).
2. Thouless, D. J., Kohmoto, M., Nightingale, M. & den Nijs, M. "Quantized Hall Conductance in a Two-Dimensional Periodic Potential". *Phys. Rev. Lett.* **49,** 405 (1982).
3. Avron, J. E. & Seiler, R. "Quantization of the Hall Conductance for General, Multiparticle Schrödinger Hamiltonians". *Phys. Rev. Lett.* **54,** 259 (1985).
4. Nakahara, M. *Geometry, Topology and Physics* (Taylor and Francis, New York and London, 2003).
5. Berry, M. V. "Quantal Phase Factors Accompanying Adiabatic Changes". *Proc. R. Soc. Lond. A* **392,** 45 (1984).
6. Bohm, A., Mostafazadeh, A., Koizumi, H., Niu, Q. & Zwanziger, J. *The Geometric Phase in Quantum Systems* (Springer-Verlag, Heidelberg, 2003).
7. Ashcroft, N. W. & Mermin, N. D. *Solid State Physics* (Harcourt, Orlando, 1987).
8. Xiao, D., Chang, M.-C. & Niu, Q. "Berry phase effects on electronic properties". *Rev. Mod. Phys.* **82,** 1959 (2010).

Chapter 4

Chern insulators

Learning goals

- We know Dirac fermions.
- We know what a Chern insulator is.
- We are acquainted with the Chern insulator of Haldane's '88 paper.

- G. Jotzu, M. Messer, R. Desbuquois, M. Lebrat, T. Uehlinger, D. Greif, and T. Esslinger, Nature **515**, 237 (2014)

So far we have been dealing with systems subject to a magnetic field $\mathbf{B}$. We could show how their ground state can be described with a topological invariant, the Chern number. In the present chapter we try to extend these ideas. The main question we are trying to answer is the following: Can there be lattice systems with Bloch bands that are characterized by a non-zero Chern number even in the absence of a net magnetic field? Such an insulator would be termed a *Chern insulator*. Before we embark on this question, we need to understand a simple continuum problem called the Dirac model.

4.1 Dirac fermions

Dirac fermions in two dimensions are described by the Hamiltonian

$$H(\mathbf{k}) = \sum_i d_i(\mathbf{k})\sigma_i \qquad \text{with} \qquad d_1(\mathbf{k}) = k_x, \;\; d_2(\mathbf{k}) = k_y, \;\; d_3(\mathbf{k}) = m. \tag{4.1}$$

The energies and eigenstates are given by

$$\epsilon(\mathbf{k})_\pm = d_\pm(\mathbf{k}) = \pm\sqrt{k^2+m^2} \qquad \text{and} \qquad \psi_\pm(\mathbf{k}) = \frac{1}{\sqrt{2d(\mathbf{k})[d(\mathbf{k})-d_3(\mathbf{k})]}}\begin{pmatrix} d_3(\mathbf{k}) \pm d(\mathbf{k}) \\ d_1(\mathbf{k}) - id_2(\mathbf{k}) \end{pmatrix}.$$

It is straight forward to show (exercise!) that the Berry connection of the lower band can be written as

$$\mathcal{A}_\mu(\mathbf{k}) = i\langle\psi_-(\mathbf{k})|\partial_{k_\mu}\psi_-(\mathbf{k})\rangle = -\frac{1}{2d(\mathbf{k})[d(\mathbf{k})+d_3(\mathbf{k})]}\left[d_2(\mathbf{k})\partial_{k_\mu}d_1(\mathbf{k}) - d_1(\mathbf{k})\partial_{k_\mu}d_2(\mathbf{k})\right] \tag{4.2}$$

And the corresponding Berry curvature is given by

$$F_{\mu\nu}(\mathbf{k}) = \frac{1}{2}\epsilon_{\alpha\beta\gamma}\hat{d}_\alpha(\mathbf{k})\partial_{k_\mu}\hat{d}_\beta(\mathbf{k})\partial_{k_\nu}\hat{d}_\gamma(\mathbf{k}) \qquad \text{with} \qquad \hat{\mathbf{d}}(\mathbf{k}) = \frac{\mathbf{d}(\mathbf{k})}{d(\mathbf{k})}. \tag{4.3}$$

Using our concrete d-vector we find

$$\mathcal{A}_x = \frac{-k_y}{2\sqrt{k^2+m^2}(\sqrt{k^2+m^2}+m)} \qquad \text{and} \qquad \mathcal{A}_y = \frac{k_x}{2\sqrt{k^2+m^2}(\sqrt{k^2+m^2}+m)}, \tag{4.4}$$

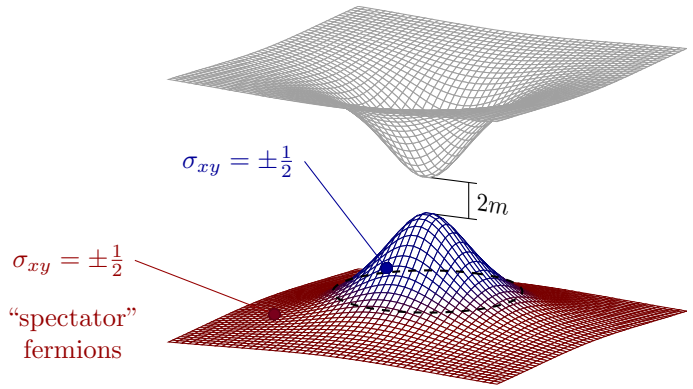

Figure 4.1: Regularization of the Dirac spectrum due to a lattice.

and therefore

$$\mathcal{F}_{\alpha\beta} = \frac{m}{2(k^2+m^2)^{3/2}}. \tag{4.5}$$

Let us plug that into the formula for the Hall conductance

$$\sigma_{xy} = \frac{e^2}{h}\frac{1}{2\pi}\int d\mathbf{k}\,\mathcal{F}_{\alpha\beta} = \frac{e^2}{h}\int_0^\infty dk k \frac{1}{2}\frac{m}{(k^2+m^2)^{3/2}} = \frac{e^2}{h}\frac{\text{sign}(m)}{2}. \tag{4.6}$$

We can draw several important insights from this results:

1. $\sigma_{xy} \neq 0 \;\Rightarrow$ we must have broken time-reversal invariance. How did this happen?
2. $\sigma_{xy} \neq \frac{e^2}{h}\nu$ with $\nu \in \mathbb{Z}$. How can this be?

Let us start with the first question. We have to make the distinction between two cases. (i) If the σ-matrices encode a real spin-1/2 degree of freedom the time reversal operator is given by

$$\mathcal{T} = i\sigma_y K,$$

where K denotes complex conjugation. Therefore

$$\mathcal{T}H(\mathbf{k})\mathcal{T}^{-1} = \sum_i -d_i(\mathbf{k})\sigma_i = -k_x\sigma_x - k_y\sigma_y - m\sigma_z.$$

If we want to above Hamiltonian to be time reversal invariant we need this to be

$$\mathcal{T}H(\mathbf{k})\mathcal{T}^{-1} \stackrel{!}{=} H(-\mathbf{k}) = -k_x\sigma_x - k_y\sigma_y + m\sigma_z.$$

From this we conclude that the Dirac fermions are only time reversal invariant for $d_3(\mathbf{k}) = m = 0$. However, in this case, there is no gap in the spectrum at $\mathbf{k} = 0$ and the calculation of σ_{xy} does

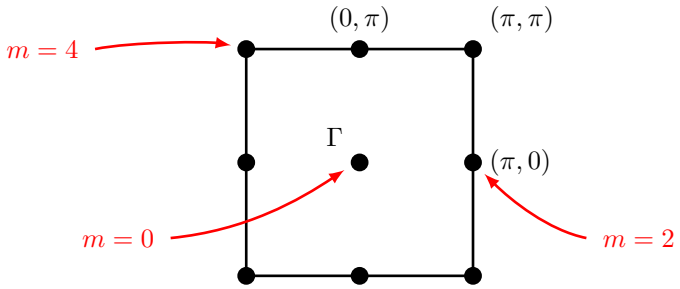

Figure 4.2: Band touching for a simple Chern insulator.

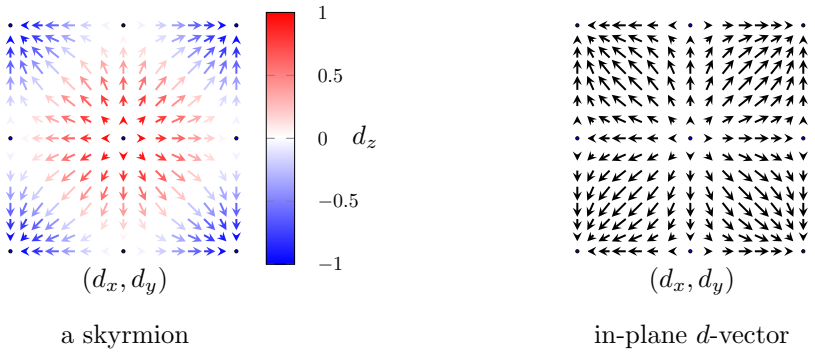

Figure 4.3: Left: spin-configuration of a skyrmion. Right: in-plane d-vector of H.

not make sense. (ii) For the case that the Pauli matrices describe some iso-spin where $\mathcal{T} = K$, we need to have $H(\mathbf{k}) = H(-\mathbf{k})$. Or in other words

$$d_1(\mathbf{k}) = d_1(-\mathbf{k}), \quad d_2(\mathbf{k}) = -d_2(-\mathbf{k}), \quad d_3(\mathbf{k}) = d_3(-\mathbf{k}).$$

From these considerations we conclude that our Hamiltonian breaks time reversal invariance in either case and we can indeed expect a non-vanishing Hall conductance.

Let us now address the non-quantized nature of σ_{xy}. The quantization of σ_{xy} arises from the quantized value of the Chern number. We have seen in our derivation, however, that it was crucial that the domain over which we integrated the Berry curvature was closed and orientable. Here we are in a continuum model where the integral over all momenta extends over the whole $\mathbb{R}^2$. We have therefore no reason to expect σ_{xy} to be quantized.

There is value to formula (4.6), however. Imagine that the Dirac Hamiltonian arises from some low-energy expansion ($\mathbf{k}\cdot\mathbf{p}$) around a special point in the Brillouin zone of a lattice model. For the full lattice, the $k \to \infty$ integral would be regularized due to the Brillouin zone boundary. The whole system has a quantized Hall conductivity. However, the region close to the "Dirac-point" contributes $\pm 1/2$ to the Chern number, see Fig. 4.1. Moreover, imagine a gap closing and re-opening transition described by the Dirac Hamiltonian where m changes its value. In such a situation the change in Chern number $\Delta\mathcal{C} = \pm 2\pi$. Therefore, the Dirac model is an excellent way to study *changes in the Chern number*.

Before we continue to the simplest possible Chern insulator we state the following formula without proof (exercise!)

$$H(\mathbf{k}) = \sum_{i,j=1}^{2} A_{ij} k_i \sigma_j + m\sigma_3 \qquad \Rightarrow \qquad \sigma_{xy} = \frac{e^2}{h} \frac{\operatorname{sign}(m)}{2} \operatorname{sign}(\det A). \tag{4.7}$$

4.2 The simplest Chern insulator

We obtain the simplest conceivable Chern insulator by elevating the Dirac model to a lattice problem

$$d_1 = k_x \to \sin(k_x), \quad d_2 = k_y \to \sin(k_y). \tag{4.8}$$

The σ matrices now act in a space of orbitals. The fact that the coupling between them is odd in $\mathbf{k}$ means that they need to differ by one quantum of angular momentum, e.g., an s-type and a p-type orbital. By symmetry, there can be an even in $\mathbf{k}$ term within each orbital, so we add it to our model

$$d_3 = m \to 2 - m - \cos(k_x) - \cos(k_y).$$

The Hamiltonian is gapped ($d(\mathbf{k}) \neq 0 \ \forall\, \mathbf{k}$) except at the special points in the Brillouin zone shown in Fig. 4.2.

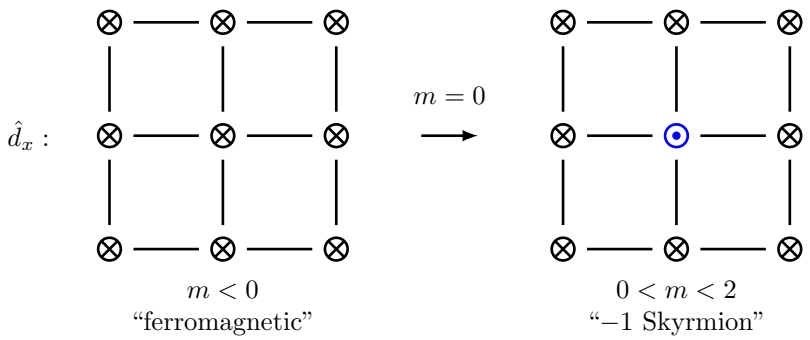

Figure 4.4: Change of the d_3 component at the first critical point.

We begin analyzing the Hamiltonian for $m \ll 0$ and $m \gg 4$. For $m = \pm\infty$, the eigenstates of the Hamiltonian are fully localized to single sites and the system certainly shows no Hall conductance. Another way to see this is to observe that

$$\frac{1}{2\pi}\int_{\mathrm{BZ}} d\mathbf{k}\, \epsilon_{\alpha\beta\gamma}\hat{d}_\alpha \partial_{k_x}\hat{d}_\beta \partial_{k_y}\hat{d}_\gamma$$

counts the winding of $\hat{\mathbf{d}}(\mathbf{k})$ throughout the Brillouin zone, i.e., it provides us what we know as the *skyrmion number*. In Fig. 4.3(a) we show a spin-configuration corresponding to a skyrmion. When we now look at the planar part of the d-vector, we see that we have all laid out for a skyrmion. The only addition we need is a sign change of d_3 at the right places in the Brillouin zone. This does not happen for $m < 0$ or $m > 4$. Note that exactly this sign change closes the gap in a fashion describable by Dirac fermions. Hence we appreciate the importance of the above discussion. It is now trivial to draw the phase diagram.

The case $0 \leq m < 2$: We start from $m = -\infty$ where $\sigma_{xy} = 0$ and go through the gap-closing at $\mathbf{k} = 0$ for $m = 0$. Around $\mathbf{k} = 0$ we find

$$H = k_x\sigma_x + k_y\sigma_y - m\sigma_x.$$

Therefore

$$\Delta\sigma_{xy} = \frac{e^2}{h}\left[\frac{1}{2}\mathrm{sign}(-m)\Big|_{m>0} - \frac{1}{2}\mathrm{sign}(-m)\Big|_{m<0}\right] = -\frac{e^2}{h} = \sigma_{xy}.$$

The correspoding change in $d_3(\mathbf{k})$ is shown in Fig. 4.4.

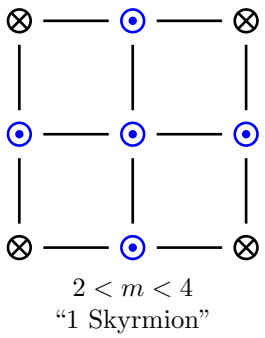

Figure 4.5: d_3 component after the second gap closing.

The case $2 \leq m < 4$: At $m = 2$ the gap closes at $(\pi, 0)$ and $(0, \pi)$. Let us expand the Hamiltonian around these points

$$H_{(\pi,0)} = \quad k_x\sigma_x - k_y\sigma_y + (2-m)\sigma_z, \tag{4.9}$$

$$H_{(0,\pi)} = -k_x\sigma_x + k_y\sigma_y + (2-m)\sigma_z. \tag{4.10}$$

From this we read out the change in σ_{xy}:

$$\Delta\sigma_{xy} = -2\frac{e^2}{h}\left[\frac{1}{2}\text{sign}(2-m)\Big|_{m>2} - \frac{1}{2}\text{sign}(2-m)\Big|_{m<2}\right] = 2\frac{e^2}{h}. \tag{4.11}$$

Note that the 2 in front stems from the two gap closings and the overall $-$ sign arises from the odd sign of the determinant A, cf. Eq. (4.7). Together with the value of σ_{xy} for $0 < m < 2$ we obtain

$$\sigma_{xy} = +\frac{e^2}{h}.$$

The corresponding $d_3(\mathbf{k})$ is shown in Fig. 4.5.

The case $4 \leq m$: The last gap-closing happens at (π, π) for $m = 4$. At this point

$$H_{(\pi,\pi)} = -k_x\sigma_x - k_y\sigma_y + (4-m)\sigma_z.$$

As before the change in σ_{xy} is given by

$$\Delta\sigma_{xy} = \frac{e^2}{h}\left[\frac{1}{2}\text{sign}(4-m)\Big|_{m>0} - \frac{1}{2}\text{sign}(4-m)\Big|_{m<0}\right] = -\frac{e^2}{h}.$$

And we arrive again at $\sigma_{xy} = 0$ as expected for a phase connected to the $m = \infty$ limit. Again, $d_3(\mathbf{k})$ is shown in Fig. 4.6.

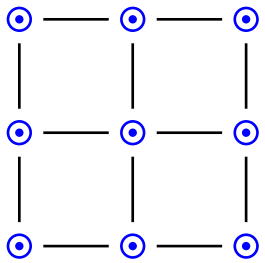

$4 < m$
"ferromagnetic"

Figure 4.6: Trivial insulator.

We can now summarize our analysis in Fig. 4.7.

We started from a Hamiltonian that breaks time-reversal invariance $\mathcal{T}$ and found a non-vanishing σ_{xy}. We did so not by calculating $\mathcal{F}_{\mu\nu}$ and performing complicated $\mathbf{k}$-space integrals but via a simple analysis of gap closings.

The Chern insulator presented here is the simplest one, but not the first discovered. We now discuss the first Chern insulator due to Haldane [1] as it motivated the first time-reversal invariant topological insulators which we will embark on next.

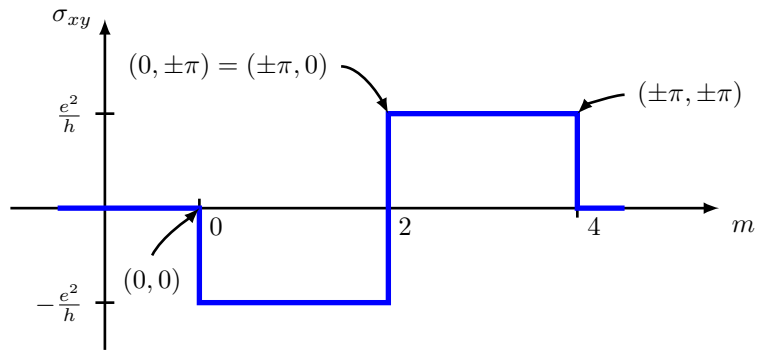

Figure 4.7: Evolution of the topological index as a function of m.

4.3 The Haldane Chern insulator

In his seminal paper [1], Haldane considered a honeycomb model with no net magnetic flux but with complex phases $e^{\pm i\varphi}$ on the next-to-nearest neighbor hoppings. A possible *staggered* flux pattern giving rise to such a situation is shown in Fig. 4.8. In Fig. 4.8 we also indicate the sign structure of the phases. The model can be written as

$$H = \sum_{\langle i,j\rangle} c_i^\dagger c_j + t \sum_{\langle\langle i,j\rangle\rangle} e^{\pm i\varphi} c_i^\dagger c_j + m \sum_i \epsilon_i c_i^\dagger c_i, \tag{4.12}$$

where $\epsilon_i = \pm 1$ for the two sub-lattices of the honeycomb lattice. Written in $\mathbf{k}$-space we find $H = \epsilon(\mathbf{k}) + \sum_i d_i(\mathbf{k})\sigma_i$ with

$$d_1(\mathbf{k}) = \cos(\mathbf{k}\cdot\mathbf{a}_1) + \cos(\mathbf{k}\cdot\mathbf{a}_2) + 1, \tag{4.13}$$
$$d_2(\mathbf{k}) = \sin(\mathbf{k}\cdot\mathbf{a}_1) + \sin(\mathbf{k}\cdot\mathbf{a}_2), \tag{4.14}$$
$$d_3(\mathbf{k}) = m + 2t\sin(\varphi)\left[\sin(\mathbf{k}\cdot\mathbf{a}_1) - \sin(\mathbf{k}\cdot\mathbf{a}_2) - \sin(\mathbf{k}\cdot(\mathbf{a}_1-\mathbf{a}_2))\right], \tag{4.15}$$

with $\mathbf{a}_1 = a(1,0)$ and $\mathbf{a}_2 = a(1/2,\sqrt{3}/2)$. We ignore the shift $\epsilon(\mathbf{k})$ in the following. What are the symmetries of this Hamiltonian? First, d_1 and d_2 are compatible with the time-reversal $\mathcal{T}$. However, $d_3(\mathbf{k}) = d_3(-\mathbf{k})$ holds only for $\varphi = 0, \pi$. We can therefore expect a non-vanishing Chern number for a general φ. The Hamiltonian has C_3 symmetry. Hence, the gap closings have to happen at the K or K' point, see Fig. 4.9 (Prove!),

$$K = \frac{2\pi}{a}\left(1, \frac{1}{\sqrt{3}}\right), \qquad K' = \frac{2\pi}{a}\left(1, -\frac{1}{\sqrt{3}}\right),$$

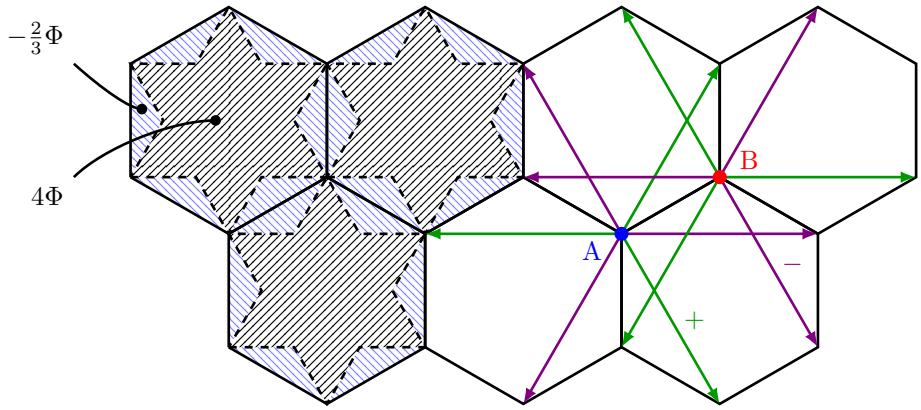

Figure 4.8: The Haldane Chern insulator model.

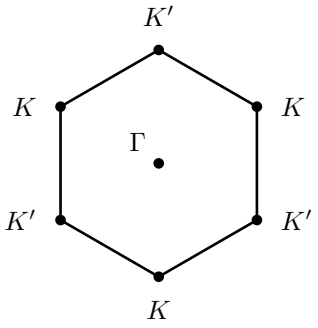

Figure 4.9: Gap closings for the Haldane Chern insulator.

where a denotes the lattice constant. To calculate the Chern number we follow the same logic as in the last chapter. We start from the limit $m \to \infty$ and track the gap-closings at the Dirac points at K and K'. The low energy expansion at these two points read

$$H_K = \frac{3}{2}(k_y\sigma_x - k_x\sigma_y) + \left(m - 3\sqrt{3}t\sin(\varphi)\right)\sigma_z, \tag{4.16}$$

$$H_{K'} = -\frac{3}{2}(k_y\sigma_x + k_x\sigma_y) + \left(m + 3\sqrt{3}t\sin(\varphi)\right)\sigma_z. \tag{4.17}$$

Note that the gap-closings at K and K' happen at different values of m (for $\varphi \neq 0, \pi$). Moreover, the two Dirac points give rise to a change in σ_{xy} of opposite sign has $\det(A)$ as a different sign. We can now construct the phase diagram

- $m > 3\sqrt{2}t\sin(\varphi)$: $\sigma_{xy} = 0$
- $-3\sqrt{2}t\sin(\varphi) < m \geq 3\sqrt{2}t\sin(\varphi)$ for $\varphi > 0$: At $m = 3\sqrt{2}t\sin(\varphi)$ the gap closes at K and we have a $\Delta\sigma_{xy} = -\frac{e^2}{h}$. The gap at K' stays open.
- $m \leq -3\sqrt{2}t\sin(\varphi)$ for $\varphi > 0$: The gap at K' closes at $m - 3\sqrt{2}t\sin(\varphi)$ and hence the Chern number changes back to 0.

For $\varphi < 0$ the signs of the Chern numbers are inverted. The resulting phase diagram is summarized in Fig. 4.10.

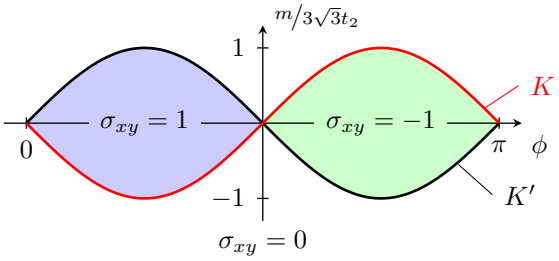

Figure 4.10: Phase diagram of the Haldane model.

The model of Haldane breaks time-reversal invariance $\mathcal{T}$. How can we build a model which is $\mathcal{T}$-symmetric? The easiest way is by doubling the degrees of freedom:

$$\mathcal{T}H\mathcal{T}^{-1} = H' \neq H \Rightarrow H_{\text{doubled}} = \begin{pmatrix} H & \\ & H' \end{pmatrix}.$$

We will see in the next chapter how Kane and Mele [2] took this step.

References

1. Haldane, F. D. M. "Model for a Quantum Hall Effect without Landau Levels". *Phys. Rev. Lett.* **61,** 2015 (1988).
2. Kane, C. L. & Mele, E. J. "Quantum Spin Hall Effect in Graphene". *Phys. Rev. Lett.* **95,** 226801 (2005).

Chapter 5

Topological insulators and superconductors

Learning goals

- We know the Kane Mele model.
- We can derive the topological index based on time reversal polarization.
- We understand the entries of the periodic table for topological insulators.
- We know what a $p_x + ip_y$ superconductor is.
- We are acquainted with the Kitaev wire.
- We know the Su-Schrieffer-Heeger model.

- M. König et al., Science **318**, 766 (2007)

In this chapter we try to understand what topological properties can arise for free fermion systems subject to some symmetry constraints. The exposition starts from a historical perspective with the first time-reversal symmetric topological insulator in two dimensions by Kane and Mele [1]. We then motivate on physical grounds how one can construct a topological index characterizing this new type of band insulator. Our derivation follows the historically motivated path covered in the book by Bernevig and Hughes [2]. The so derived topological index for two-dimensional systems readily generalizes to three dimensions. Once we established the presence of two- and three-dimensional topological insulators protected by time-reversal symmetry we take a somewhat more formal perspective and discuss the *periodic table for topological insulators* which catalogues all symmetry protected topological free fermion systems. We learn how to read and use the table and relate its entries to experimentally relevant response functions. Finally, we conclude this chapter by covering three archetypal models in different symmetry classes.

5.1 The Kane-Mele model

In the last chapter we have seen that we can construct lattice models where the Bloch bands have a non-vanishing Chern number despite the absence of a net magnetic field. Here we try to build a time-reversal invariant version based on Haldane's honeycomb model for a Chern insulator.
We start from the low energy version of graphene

$$H_0 = -i\hbar v_{\mathrm{F}} \left[\sigma_x \tau_z \partial_x + \sigma_y \partial_y\right], \tag{5.1}$$

where $\boldsymbol{\sigma}$ acts on the sub-lattice index and $\boldsymbol{\tau}$ on the valley (K, K') space.
Let us add spin $\mathbf{s}$ to the game. With this we arrive at an 8×8 problem. The question is what kind of terms can we add in order to open a "non-trivial" gap. We have seen that

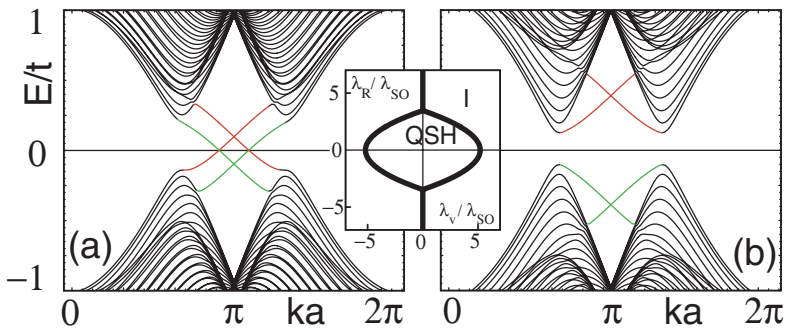

Figure 5.1: Edge spectrum of the Kane Mele model for two different values of λ_R. On the left, two edge states cross the gap (colors label the edge). On the right, no edge states cross the gap. The inset shows the phase diagram as a function of λ_v and λ_R. Figure take from Ref. [1] (Copyright (2005) by The American Physical Society).

$m\sigma_z + \tau_z\sigma_z 3\sqrt{3}t\sin(\varphi)$ does the job. However, this is not time-reversal symmetric for $\varphi \neq 0, \pi$ and m alone opens trivial gaps with $\mathcal{C} = 0$.
We construct a "non-trivial" time-reversal invariant gap step by step. First, in the sub-lattice space we need a σ_z term, otherwise we just move around the K and K' Dirac points in $\mathbf{k}$-space. Next, we need a spin dependent ($\mathbf{s}$) part to couple the two copies of the Haldane model. Let us try for the K point

$$\sigma_z \otimes s_z = \begin{pmatrix} \sigma_z & 0 \\ 0 & -\sigma_z \end{pmatrix}, \tag{5.2}$$

which gives us different gaps [with different "sign(m)"] for the two spins. How do we now add the valley degree of freedom ($\boldsymbol{\tau}$) in order to make it time-reversal invariant? The $\mathcal{T}$-operator acts in sub-lattice and spin space as

$$\mathcal{T} = \mathbb{1}_\sigma \otimes i s_y K = \begin{pmatrix} 0 & -\mathbb{1}_\sigma \\ \mathbb{1}_\sigma & 0 \end{pmatrix}. \tag{5.3}$$

Therefore, the term $\propto \sigma_z \otimes s_z$ transforms as

$$\begin{aligned} \mathcal{T}\sigma_z \otimes s_z \mathcal{T}^{-1} &= \begin{pmatrix} 0 & -\mathbb{1}_\sigma \\ \mathbb{1}_\sigma & 0 \end{pmatrix} \begin{pmatrix} \sigma_z & 0 \\ 0 & -\sigma_z \end{pmatrix} \begin{pmatrix} 0 & \mathbb{1}_\sigma \\ -\mathbb{1}_\sigma & 0 \end{pmatrix} \\ &= \begin{pmatrix} 0 & -\mathbb{1}_\sigma \\ \mathbb{1}_\sigma & 0 \end{pmatrix} \begin{pmatrix} 0 & \sigma_z \\ \sigma_z & 0 \end{pmatrix} = \begin{pmatrix} -\sigma_z & 0 \\ 0 & \sigma_z \end{pmatrix} = -\sigma_z \otimes s_z. \end{aligned} \tag{5.4}$$

Under time reversal, $K \to K'$. Hence, we need the gap opening term in K' to be $\mathcal{T}\sigma_z \otimes s_z \mathcal{T}^{-1} = -\sigma_z \otimes s_z$ to have $\mathcal{T}H(\mathbf{k})\mathcal{T}^{-1} = H(-\mathbf{k})$. From this we conclude that the full gap opening term should be of the form

$$H_{\mathrm{KM}} = \lambda_{\mathrm{SO}} \sigma_z \otimes \tau_z \otimes s_z. \tag{5.5}$$

We labelled the interaction with spin-orbit (λ_{SO}) to stress that H_{KM} couples spin (s_z) and orbital (τ_z) degrees of freedom. Moreover, H_{KM} is time-reversal invariant (TRI) by construction. Reverse engineering to a full lattice model we find

$$H_{\mathrm{KM}} = \sum_{\langle i,j\rangle,\alpha} c^\dagger_{i\alpha} c_{j\alpha} + i\lambda_{\mathrm{SO}} \sum_{\langle\langle i,j\rangle\rangle,\alpha\beta} \nu_{ij} c^\dagger_{i\alpha} s^z_{\alpha\beta} c_{j\beta} + \lambda_v \sum_{i\alpha} \epsilon_i c^\dagger_{i,\alpha} c_{i,\alpha}, \tag{5.6}$$

where ϵ_i and the sign strucutre of ν_{ij} are the same as in Haldane's '88 model [3]. The above model was the first TRI topological insulator proposed by Kane and Mele in 2005 [1]. As

it is TRI, the total Chern number cannot be non-zero. However, in the form (5.6), the spin projections $|\uparrow\rangle$, $|\downarrow\rangle$ are good eigenstates. Therefore, we can use the Chern number $\mathcal{C}_\sigma$ in each spin-sector to characterize the phases. Indeed

$$\nu = \frac{C_\uparrow - C_\downarrow}{2} \bmod 2 \quad \in \mathbb{Z}_2 \tag{5.7}$$

defines a good topological index as we will see below [4]. The addition of a Rashba term

$$H_R = \lambda_R \left[\sigma_x \tau_z s_x - \sigma_y s_x\right] \tag{5.8}$$

removes this conserved quantity. While H_R does not open a gap by itself (why?), it can influence the λ_{SO} induced gap, see Fig. 5.1. However, the above topological index ν is not well defined anymore. In the following section we aim at deriving a $\mathbb{Z}_2$ index which does not rely on spin-Chern numbers.

5.2 $\mathbb{Z}_2$ index

5.2.1 Charge polarization

We revisit Laughlin's pumping argument to make progess towards a $\mathbb{Z}_2$ index for TRI topological insulators. We consider a one dimensional system on a lattice (with lattice constant $a = 1$) with Bloch wave functions

$$|\psi_{n,k}\rangle = \frac{1}{\sqrt{L}} e^{ikx} |\varphi_{nk}(x)\rangle \qquad \text{with} \qquad |\varphi_{nk}(x)\rangle = |\varphi_{nk}(x+1)\rangle. \tag{5.9}$$

The corresponding Wannier functions are defined as

$$|W_{nR}(x)\rangle = \frac{1}{2\pi} \int_{-\pi}^{\pi} dk e^{ik(R-x))} |\varphi_{nk}(x)\rangle, \tag{5.10}$$

with $R = m \in \mathbb{Z}$ a lattice vector. Note that the Wannier functions are not gauge invariant as the relative phase between different $|\varphi_{nk}(x)\rangle$ is not a priori fixed. However, for a filled band, the Slater determinant is insensitive to a unitary transformation (which the transformation to Wannier states is) among the filled states. For a smooth gauge, the Wannier functions are exponentially localized around a well defined center [5].
The total charge polarization is now defined as

$$P = \sum_{n \text{ filled}} \int dx \, \langle W_{0n}(x)|x|W_{0n}(x)\rangle. \tag{5.11}$$

We try to write this polarization in a more familiar way

$$P = \sum_{n \text{ filled}} \frac{1}{(2\pi)^2} \frac{1}{L} \int_{-\pi}^{\pi} dk_1 \int_{-\pi}^{\pi} dk_2 e^{i(k_1-k_2)x} \langle \varphi_{nk_1}|i\partial_k|\varphi_{nk_2}\rangle \tag{5.12}$$

$$= \sum_{n \text{ filled}} \frac{i}{2\pi} \int_{-\pi}^{\pi} dk \, \langle \varphi_{nk}|i\partial_k|\varphi_{nk}\rangle = \frac{1}{2\pi} \int_{-\pi}^{\pi} dk \, \mathcal{A}_x(k), \tag{5.13}$$

with

$$\mathcal{A}_x(k) = \sum_{n \text{ filled}} i\langle \varphi_{nk}|\partial_k|\varphi_{nk}\rangle. \tag{5.14}$$

Two comments are in order:

1. If we re-gauge $|\varphi\rangle \to e^{i\vartheta(k)}|\varphi\rangle$ with a $\vartheta(k)$ that is winding by $2\pi m$ throughout the Brillouin zone, the corresponding polarization changes to

   $$P \to P + m.$$

   This is ok, as charge polarization is anyway only defined up to a lattice constant.

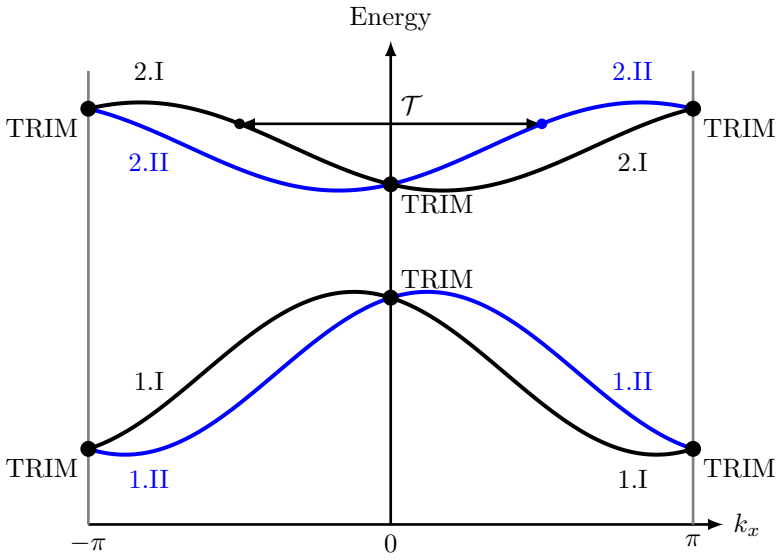

Figure 5.2: Energy levels for a time revesal invariant system.

2. P depends on the chosen gauge. But *changes in P by a smooth change in system parameters are gauge independent*. So let us imagine a tuning parameter k_y with

$$H(k_y) \to H(k_y')$$

which is slow in time. The change in charge polarization is given by

$$\Delta P = \frac{1}{2\pi}\left[\int_{-\pi}^{\pi} dk \mathcal{A}(k, k_y) - \int_{-\pi}^{\pi} dk\, \mathcal{A}(k, k_y')\right] \tag{5.15}$$

If we use Stokes' theorem we arrive at

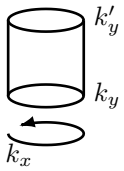

$$\Delta P = \int_{k_y}^{k_y'} dk_y \int_{-\pi}^{\pi} dk\, \mathcal{F}(k, k_y). \tag{5.16}$$

By chosing $k_y' = k_y + 2\pi$, we find for the change in charge polarization $\Delta P = \mathcal{C}$ where $\mathcal{C}$ is the Chern number. We known, however that $\mathcal{C} \sim \sigma_{xy}$ and hence is equal to zero for TRI systems.

Building on the above insight we try to refine the charge pumping of Laughlin to be able to characterize a TRI system.

5.2.2 Time reversal polarization

Let us now try to generalize the charge pumping approach to the TRI setup. For this it is beneficial to look at the structure of a generic energy diagram as shown in Fig 5.2. Under time-reversal, momenta k are mapped to $-k$. Moreover, there are special points in the Brillouin zone which are mapped onto themselves. This is true for all momenta which fulfill $k = -k + G$, where G is a reciprocal lattice vector. This is trivially true for $k = 0$, but also for special points

on the borders of the Brillouin zone. On such time reversal invariant momenta (TRIM's), the spectrum has to be doubly degenerate due to Kramer's theorem.
Owing to the symmetry between k and $-k$ we can constrain ourselves to only *half the Brillouin zone*. In this half, we label all bands by 1.I, 1.II, 2.I, 2.II, ... The arabic number simply label pairs of bands. Due to the double degeneracy at the TRIMs, we need an additional (roman number) to label the two (sub)-bands emerging form the TRIMs. One can also say that the roman index labels Kramers pairs

$$\mathcal{T}|\varphi_{n.\mathrm{I}}(k)\rangle = e^{i\chi_{n,k}}|\varphi_{n.\mathrm{II}}(-k)\rangle. \tag{5.17}$$

We now try to constuct the polarization for only one of the two labels $s = \mathrm{I}$ or II

$$P^s = \frac{1}{2\pi}\int_{-\pi}^{\pi} dk\, \mathcal{A}^s(k) \qquad \text{with} \qquad \mathcal{A}^s(k) = i\sum_{n \text{ filled}} \langle\varphi_{n.s}(k)|\partial_k|\varphi_{n.s}(k)\rangle. \tag{5.18}$$

It is clear that $P = P^{\mathrm{I}} + P^{\mathrm{II}}$ will vanish. However, the same must not hold for the *time reversal polarization*

$$P^{\mathcal{T}} = P^{\mathrm{I}} - P^{\mathrm{II}}. \tag{5.19}$$

The problem is, that we assigned the labels I and II. It is not a priori clear if this can be done in a gauge invariant fashion. In particular, the Slater determinant of a band insulator with $2n$ filled bands has a $SU(2n)$ symmetry, as basis changes of filled states do not affect the total wave function. With our procedure we explicitly broke this $SU(2n)$ symmetry. There is a way however, to formulate the same $\mathcal{T}$-polarization $P^{\mathcal{T}}$ in a way that does not rely on a specific labeling of the Kramers pairs. This can be achieved by the use of the so-called *sewing matrix* [2]

$$B_{mn}(k) = \langle\varphi_m(-k)|\mathcal{T}|\varphi_n(k)\rangle. \tag{5.20}$$

$B(k)$ has the following properties: (i) it is unitary, and (ii) it is anti-symmetric, i.e., $B^{\mathrm{T}}(k) = -B(k)$ only if k is a TRIM. Using this matrix one can show that

$$P^{\mathcal{T}} = \frac{1}{i\pi}\log\left[\frac{\sqrt{\det B(\pi)}}{\mathrm{Pf}\, B(\pi)}\frac{\mathrm{Pf}\, B(0)}{\sqrt{\det B(0)}}\right]. \tag{5.21}$$

This expression is manifestly invariant under $SU(2n)$ rotations within the filled bands. Moreover, it only depends on the two TRIMs $k = 0, \pi$, and it is defined modulo two.

The Pfaffian $\mathrm{Pf}\, B(k)$ of a $2n \times 2n$ anti-symmetric matrix matrix B is defined as

$$\mathrm{Pf}\, B = \frac{1}{2^n n!}\sum_{\sigma\in S_{2n}} \mathrm{sign}(\sigma)\prod_{i=1}^{n} b_{\sigma(2i-1),\sigma(1i)} \tag{5.22}$$

with the property

$$\mathrm{Pf}^2\, B = \det B. \tag{5.23}$$

Let us now see how we can describe changes in the time-reversal polarization under the influence of an additional parameter k_y. Written as in (5.21), it is only defined for $k_y = 0, \pi, 2\pi$, i.e, at TRIMs. In Fig. 5.3 we illustrate what we can expect from such a smooth change. We start at $k_y = 0$. If we now change k_y slowly, we know that due to TRI, we cannot build up a charge polarization. However, the Wannier centers of two Kramers pairs will evolve in opposite direction. At $k_y = \pi$, we can check how far these centers evolved away from each other. As $P^{\mathcal{T}}$ is well defined and equal to 0 or 1 we have two options: (i) Each Wannier center meets up with one coming from a neighboring site [Fig. 5.3(a)]. This gives rise to $P^{\mathcal{T}}(k_y = \pi) = 1$ and

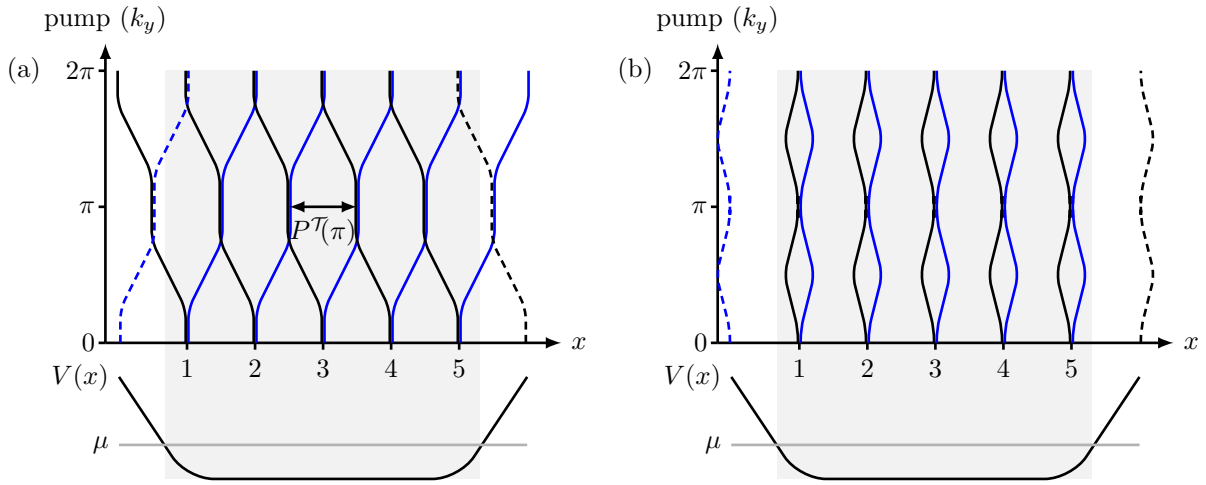

Figure 5.3: (a) Pumping of time reversal polarization in a topologically non-trivial state. (b) Pumping of time reversal polarization in a trivial state.

this effect is called *pair switching*. (ii) The centers fall back onto each other again [Fig. 5.3(b)], resulting in $P^{\mathcal{T}}(k_y = \pi) = 0$.

Let us further assume that we have a smooth confining potential $V(x)$ in x-direction. As in the case of the quantum Hall effect, we see how states can be pushed up-hill or pulled down-hill as a function of k_y. However, as opposed to the quantum Hall effect, we have here the situation that on each edge we have both a state coming down in energy as well as one climbing up! From that we conclude that if we have pair-switching, we expect two counter-propagating edge states on *both sides of the sample*.

We can now construct a topological index for the two-dimensional system: If the $\mathcal{T}$-polarization at $k_y = 0$ and $k_y = \pi$ differ by one, we expect an odd number of pairs of edge states. Hence, we define

$$\nu = \prod_{l=1}^{4} \frac{\sqrt{\det B(\mathbf{\Lambda}_l)}}{\mathrm{Pf}\, B(\mathbf{\Lambda}_l)} \in \mathbb{Z}_2 \qquad \text{with} \qquad \mathbf{\Lambda}_l \ : \ \text{TRIM}. \tag{5.24}$$

5.2.3 Three dimensional topological insulators

The above formulation immediately suggests a three-dimensional generalization of the $\mathbb{Z}_2$ index

$$\nu_s = \prod_{l=1}^{8} \frac{\sqrt{\det B(\mathbf{\Lambda}_l)}}{\mathrm{Pf}\, B(\mathbf{\Lambda}_l)} \in \mathbb{Z}_2 \qquad \text{with} \qquad \mathbf{\Lambda}_l \ : \ \text{TRIM}, \tag{5.25}$$

where now the product runs over all eight TRIMs of the three-dimensional Brillouin zone shown in Fig. 5.4. This index is called the *strong* topological index. Additionally, one can think of a three-dimensional system to be made out of planes of two-dimensional topological insulators. In Fig. 5.5 we show how one can attribute a *weak* topological index (ν_x, ν_y, ν_z) corresponding to the stacking directions.

According to our reasoning above, when we cut the system perpendicular to the direction defined by the weak index, we expect *two Dirac cones* on the resulting surface (why?). However, if we have a strong topological index, there is a single Dirac cone irrespective of the way we terminate the bulk system. To wrap up, we mention that one usually gathers the indices to

$$\boldsymbol{\nu} = (\nu_s; \nu_x, \nu_y, \nu_z). \tag{5.26}$$

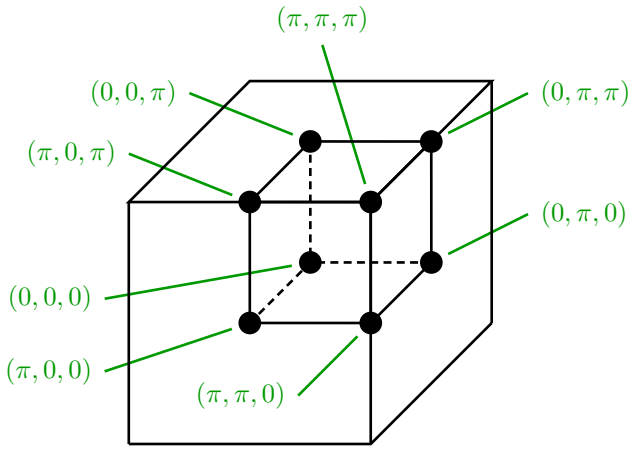

Figure 5.4: TRIMs of the three-dimensional Brillouin zone.

5.3 Complete classification

We now try to understand how one can put the above manipulations that lead to the $\mathbb{Z}_2$ index for TRI topological insulators into a bigger context. Let us review what (topological) classification schemes we already encountered. The first example was the characterization of a spin-1/2 in a magnetic field. There we discussed the geometric phase as a function of a smooth change in parameters of a Hamiltonian. The mathematical structure behind that was a fibre bundle. A fiber bundle is an object which locally looks like $M \times f$, where M is some base manifold and f the "fibre". For our case of the geometric phase, the base manifold was S^2 describing the parameter space of the ground state projector $|\psi_0\rangle\langle\psi_0|$. The fiber $f = U(1)$ was the phase of the ground state $|\psi_0\rangle$ that dropped out when we considered the projector. We have seen that one can classify such fibre bundles via a *Chern* number $\mathcal{C}$. For the example of a spin-1/2 in a magnetic field, the Chern number took the value $\mathcal{C} = -2\pi$. For the quantum Hall effect, we identified the fibre bundle with what looks locally like $\mathbb{T}^2 \times U(1)$ where $\mathbb{T}^2$ is the torus defined by the Aharonov Bohm fluxes through the openings of the (real space!) torus. We argued that also in this case the fibre bundle is characterized by the Chern number which can take any value in $2\pi\nu$ with $\nu \in \mathbb{Z}$ [6, 7].
We also considered special cases where the Aharonov-Bohm fluxes could be replaced by lattice momenta (k_x, k_y). Moreover, in the simple case of a two-band Chern insulator the Chern number was shown to be equivalent to the Skyrmion number which characterizes mappings $\mathbb{T}^2 \to S^2$ instead of fibre bundles. In general, we can hope to find the classification of mappings $\mathbb{T}^d \to M$, where $\mathbb{T}^d$ is the d-dimensional Brillouin zone and M is some target manifold.
Attempting a topological classification of free fermion systems really means to define equivalence classes of first quantized Hamiltonians. Not so surprisingly, such equivalence classes depend strongly on the presence of symmetries: If we allow for arbitrary deformations of Hamiltonians

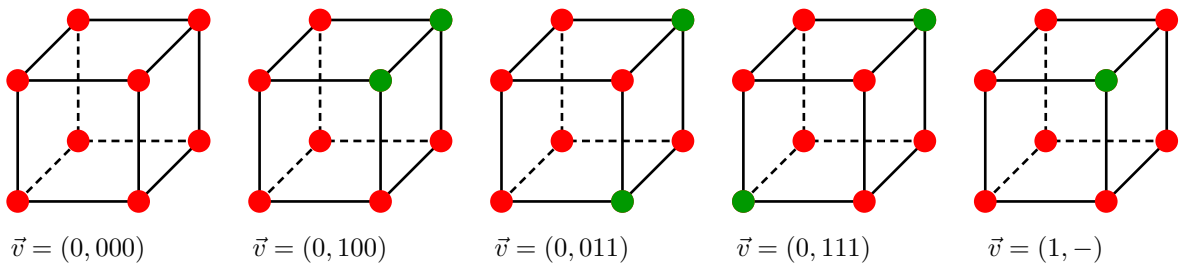

Figure 5.5: Stacking directions of 2D topological insulators.

(of course without the closing of the gap above the ground state!), we might be able to deform two Hamiltonians into each other that are distinct if we restrict the possible interpolation path by requiring symmetries.
A simple example of such a symmetry constraint is the following setup: Consider the restricted one-dimensional two-band system

$$H = \sum_i d_i(k)\sigma_i \qquad \text{with} \qquad \{H, \sigma_y\} = 0. \tag{5.27}$$

This symmetry requirement is identical with the demand that there is no y-component of the d-vector. In other words, the normalized d-vector lives on S^1. Thanks to this restriction, or symmetry, each Hamiltonian in this class defines a mapping

$$S^1 \to S^1 \tag{5.28}$$

which is characterized by the winding number $\mathcal{W}$. In the absence of the symmetry $\{H, \sigma_y\}$=0, the d-vector could point anywhere on S^2. Mappings

$$S^1 \to S^2 \tag{5.29}$$

are all trivial, however, as any closed one-dimensional path defined by the image of S^1 is smoothly contractible to a point. Hence, we cannot define a winding number in this case.
In the following we want to achieve three goals. First, we want to see how symmetries can influence the possible topological quantum numbers of band insulators. To this end we discuss three particular "symmetries" and see how they, together with the spatial dimension, give rise to a periodic table of topological insulators. The second goal will be to get the gist of what underlies the structure of the periodic table. The key ingredient will be the tool of dimensional reduction: We start with some topological quantum number (typically the Chern number) in some higher dimension. We then show how one can characterize families of lower-dimensional Hamiltonians obeying some symmetries using the higher dimensional topological number. Finally, our third goal is to be able to read the periodic table, find the right (hopefully simple) expression of the topological index and be able to calculate it. We will do so on three concrete examples in Sec. 5.4.

5.3.1 Anti-unitary symmetries

When we discuss symmetry constraints on possible equivalence relations between Hamiltonians we have to consider anti-unitary symmetries such as time reversal invariance with $\mathcal{T} i \mathcal{T}^{-1} = -i$. Unitary symmetries S that commute with the Hamiltonian $[H, S] = 0$ do not help us for the following reason: We simply go to combined eigenstates of both the symmetry S and the Hamiltonian. We want to assume that we only deal with such block-diagonal Hamiltonians from the outset. If we deal with anti-unitary symmetries, which do not have eigenstates, we cannot use this program of decomposing H into symmetric sub-blocks, however. The same holds for unitary symmetries S that anti-commute with the Hamiltonian, i.e., $\{H, S\} = 0$. We will see how such "symmetries" help us to classify topological insulators.
In the following we use a first quantized language where we write the single particle Hamiltonian as

$$H = \sum_{AB} \psi_A^\dagger \mathcal{H}_{AB} \psi_B, \tag{5.30}$$

where A, B run over all relevant quantum numbers. The object of interest is the matrix $\mathcal{H}_{AB}$. In case we deal with superconducting problems the corresponding matrix is constructed from the Nambu spinor

$$H = \sum_{AB} \begin{pmatrix} \psi_A^\dagger & \psi_{\bar{A}} \end{pmatrix} \mathcal{H}_{AB} \begin{pmatrix} \psi_B \\ \psi_{\bar{B}}^\dagger \end{pmatrix}. \tag{5.31}$$

Here A and $\bar{A}$ correspond to the paired quantum numbers: For example for an s-wave superconductor $A = (\mathbf{k}, \uparrow)$ and $\bar{A} = (-\mathbf{k}, \downarrow)$.

Time reversal

Let us now start with the anti-unitary time reversal symmetry

$$\mathcal{T}: \qquad U_{\mathcal{T}}^{\dagger}\mathcal{H}^{*}U_{\mathcal{T}}=\mathcal{H}, \qquad \text{with} \qquad U_{\mathcal{T}}^{\dagger}U_{\mathcal{T}}=\mathbb{1}, \tag{5.32}$$

for some unitary rotation $U_{\mathcal{T}}$. Using the second quantized language we find for these matrices

$$\mathcal{T}\psi_A\mathcal{T}^{-1}=\sum_B [U_{\mathcal{T}}]_{AB}\psi_B. \tag{5.33}$$

Applying this identity twice, and making use of the fact that $\mathcal{T}$ is anti-unitary, we find

$$\mathcal{T}^2\psi_A\mathcal{T}^{-2}=\sum_B [U_{\mathcal{T}}^{*}U_{\mathcal{T}}]_{AB}\psi_B=\pm\psi_A, \qquad \text{i.e.,} \qquad U_{\mathcal{T}}^{*}U_{\mathcal{T}}=\pm\mathbb{1}. \tag{5.34}$$

Here we used that $\mathcal{T}^2=-\mathbb{1}$ or $\mathcal{T}^2=\mathbb{1}$, depending on whether we deal with systems of half-integer spins or not. The last equation can also be written as

$$U_{\mathcal{T}}=\pm U_{\mathcal{T}}^{\mathrm{T}}. \tag{5.35}$$

Charge conjugation

The next (anti-) symmetry we consider is the charge-conjugation, or particle-hole symmetry

$$\mathcal{C}: \qquad U_{\mathcal{C}}^{\dagger}\mathcal{H}^{*}U_{\mathcal{C}}=-\mathcal{H} \qquad \text{with} \qquad U_{\mathcal{C}}^{\dagger}U_{\mathcal{C}}=\mathbb{1}. \tag{5.36}$$

Where again we find $U_{\mathcal{C}}$ via

$$\mathcal{C}\psi_A\mathcal{C}^{-1}=\sum_B [U_{\mathcal{C}}^{*}]_{AB}\psi_B^{\dagger}. \tag{5.37}$$

And also in this case we can either have

$$U_{\mathcal{C}}=\pm U_{\mathcal{C}}^{\mathrm{T}}, \tag{5.38}$$

depending on wether $\mathcal{C}^2=\pm\mathbb{1}$. As this particle hole symmetry is slightly less standard than the time reversal symmetry we give two concrete examples. First, the Hamiltonian of an s-wave superconductor can be written as

$$H=\sum_k \begin{pmatrix} c_{k\uparrow} & c_{k\downarrow} & c_{-k\uparrow}^{\dagger} & c_{-k,\downarrow}^{\dagger}\end{pmatrix}^{\dagger} \underbrace{\begin{pmatrix} \xi(k) & 0 & 0 & \Delta_s \\ 0 & \xi(k) & -\Delta_s & 0 \\ 0 & -\Delta_s^{*} & -\xi(k) & 0 \\ \Delta_s^{*} & 0 & 0 & -\xi(k)\end{pmatrix}}_{\mathcal{H}_s} \begin{pmatrix} c_{k\uparrow} \\ c_{k\downarrow} \\ c_{-k\uparrow}^{\dagger} \\ c_{-k,\downarrow}^{\dagger}\end{pmatrix}. \tag{5.39}$$

This Hamiltonian has the anti-symmetry

$$U_{\mathcal{C}}^{\dagger}\mathcal{H}_s^{*}U_{\mathcal{C}}=-\mathcal{H}_s \qquad \text{with} \qquad U_{\mathcal{C}}=i\sigma_y\otimes\mathbb{1} \qquad \text{and hence} \qquad U_{\mathcal{C}}=-U_{\mathcal{C}}^{\mathrm{T}}. \tag{5.40}$$

On the other hand, a triplet superconductor can be of the form

$$H=\sum_k \begin{pmatrix} c_{k\uparrow} & c_{k\downarrow} & c_{-k\uparrow}^{\dagger} & c_{-k,\downarrow}^{\dagger}\end{pmatrix}^{\dagger} \underbrace{\begin{pmatrix} \xi(k) & 0 & 0 & \Delta_t \\ 0 & \xi(k) & \Delta_t & 0 \\ 0 & \Delta_t^{*} & -\xi(k) & 0 \\ \Delta_t^{*} & 0 & 0 & -\xi(k)\end{pmatrix}}_{\mathcal{H}_t} \begin{pmatrix} c_{k\uparrow} \\ c_{k\downarrow} \\ c_{-k\uparrow}^{\dagger} \\ c_{-k,\downarrow}^{\dagger}\end{pmatrix}. \tag{5.41}$$

Now the Hamiltonian has the anti-symmetry

$$U_{\mathcal{C}}^{\dagger}\mathcal{H}_t^{*}U_{\mathcal{C}}=-\mathcal{H}_t \qquad \text{with} \qquad U_{\mathcal{C}}=\sigma_x\otimes\mathbb{1} \qquad \text{and hence} \qquad U_{\mathcal{C}}=U_{\mathcal{C}}^{\mathrm{T}}. \tag{5.42}$$

Note, that all Bogoliubov-de Gennes (BdG) Hamiltonians of mean-field superconductors have a $\mathcal{C}$-type symmetry built in by construction (via the Nambu formalism).

Chiral symmetry

One more option is for the Hamiltonian to posses the following anti-symmetry

$$\mathcal{S}: \qquad U_{\mathcal{S}}^{\dagger}\mathcal{H}U_{\mathcal{S}} = -\mathcal{H} \qquad \text{with} \qquad U_{\mathcal{S}}^{\dagger}U_{\mathcal{S}} = \mathbb{1}. \qquad \text{and} \qquad U_{\mathcal{S}}^{2} = \mathbb{1}. \tag{5.43}$$

This symmetry is called chiral or *sub-lattice* symmetry as it often occurs on bipartite lattice models. Note, that whenever the system has a chiral symmetry and either a particle-hole or time-reversal, it actually posses all three of them (show!).

5.3.2 The periodic table

Let us now classify all possible symmetry classes according to the above three "symmetries". For the time-reversal and particle-hole symmetry we have three options. Either there is no symmetry, one that squares to $\mathbb{1}$, or one that squares to $-\mathbb{1}$. We denote these cases with $0, 1, -1$. Together, there are $3 \times 3 = 9$ different options. Turning around the argument above that a $\mathcal{C}$ ($\mathcal{T}$) together with an $\mathcal{S}$ type symmetry implies a $\mathcal{T}$ ($\mathcal{C}$) symmetry we see that $\mathcal{S} = \mathcal{C} \circ \mathcal{T}$. Therefore, for all cases where either $\mathcal{T}$ or $\mathcal{C}$ are present the presence or absence of $\mathcal{S}$ is fixed. Only if both particle-hole and time-reversal symmetry are absent, $\mathcal{S}$ can be either present (1) or absent (0). This yields in total 10 different symmetry classes. In a series of papers Kitaev [8] and Ludwig and co-workers [9, 10] classified all possible topological indices given the symmetry class and the spatial dimension. We summarize their results in Tab. 5.1.

label	**symmetry**			**spatial dimension**							
	$\mathcal{T}$	$\mathcal{C}$	$\mathcal{S}$	$d=1$	$d=2$	$d=3$	$d=4$	$d=5$	$d=6$	$d=7$	$d=8$	...
the complex cases:												
A	0	0	0	0	$\mathbb{Z}$	0	$\mathbb{Z}$	0	$\mathbb{Z}$	0	$\mathbb{Z}$	...
AIII	0	0	1	$\mathbb{Z}$	0	$\mathbb{Z}$	0	$\mathbb{Z}$	0	$\mathbb{Z}$	0	...
the real cases:												
AI	1	0	0	0	0	0	$2\mathbb{Z}$	0	$\mathbb{Z}_2$	$\mathbb{Z}_2$	$\mathbb{Z}$	...
BDI	1	1	1	$\mathbb{Z}$	0	0	0	$2\mathbb{Z}$	0	$\mathbb{Z}_2$	$\mathbb{Z}_2$	...
D	0	1	0	$\mathbb{Z}_2$	$\mathbb{Z}$	0	0	0	$2\mathbb{Z}$	0	$\mathbb{Z}_2$	...
DIII	-1	1	1	$\mathbb{Z}_2$	$\mathbb{Z}_2$	$\mathbb{Z}$	0	0	0	$2\mathbb{Z}$	0	...
AII	-1	0	0	0	$\mathbb{Z}_2$	$\mathbb{Z}_2$	$\mathbb{Z}$	0	0	0	$2\mathbb{Z}$	...
CII	-1	-1	1	$2\mathbb{Z}$	0	$\mathbb{Z}_2$	$\mathbb{Z}_2$	$\mathbb{Z}$	0	0	0	...
C	0	-1	0	0	$2\mathbb{Z}$	0	$\mathbb{Z}_2$	$\mathbb{Z}_2$	$\mathbb{Z}$	0	0	...
CI	1	-1	1	0	0	$2\mathbb{Z}$	0	$\mathbb{Z}_2$	$\mathbb{Z}_2$	$\mathbb{Z}$	0	...

Table 5.1: Periodic table of topological insulators and superconductors. $\mathbb{Z}_2$ and $\mathbb{Z}$ denote binary and integer topological indices, respectively. $2\mathbb{Z}$ denotes an even integer. The symmetries $\mathcal{T}$, $\mathcal{C}$ and $\mathcal{S} = \mathcal{T} \circ \mathcal{C}$ are explained in the text. A zero denotes the absence of the symmetry and for $\mathcal{T}$ and $\mathcal{C}$, the ± 1 indicates if these symmetries square to $\pm\mathbb{1}$.

One observes an obvious 8-fold symmetry in the direction of the spatial dimension. The explanation of this repetition lies beyond the scope of this course. However, as dimensional reduction plays a key role in the derivation of Tab. 5.1, we present on such step for the case of symmetry class D, going from $d = 2 \to 1$. Before we do so, it is worth mentioning, that from a applicative point of view, our standard job will be to:

1. Identify the symmetries and with that the class A, AI, AII, AIII, BDI, etc.

2. Check in Tab. 5.1 if for the given symmetry class and spatial dimension there can be a topologically non-trivial state.

3. Go to the paper by Ryu et al. [9].

4. Find the explicit formula for the respective index.

5. Compute it.

5.3.3 Dimensional reduction

This section is following the derivation in Ref. [11].

Our goal is to take the step of dimensional reduction to relate the $\mathbb{Z}$ index of symmetry class D in three dimensions to the $\mathbb{Z}_2$ index of the same symmetry class in one spatial dimension. in this section. We consider one dimensional lattice systems where the Hamiltonian matrix fulfills

$$U_{\mathcal{C}}^{\dagger}\mathcal{H}^{*}(-k)U_{\mathcal{C}} = \mathcal{H}(k) \qquad \text{with} \qquad U_{\mathcal{C}} = U_{\mathcal{C}}^{\mathrm{T}}. \tag{5.44}$$

We now try to establish an equivalence relation between two such Hamiltonians $\mathcal{H}_1(k)$ and $\mathcal{H}_2(k)$. To borrow the Chern number from one dimension higher, we construct a path, or interpolation $\mathcal{H}(k,\vartheta)$, with $\vartheta \in [0,\pi]$ connecting the two Hamiltonians

$$\mathcal{H}(k,0) = \mathcal{H}_1(k) \qquad \text{and} \qquad \mathcal{H}(k,\pi) = \mathcal{H}_2(k). \tag{5.45}$$

In general, the Hamiltonian for an arbitrary $\vartheta \in [0,\pi]$ will not posses the symmetry (5.44). We correct for this by explicitly constructing the cyclic interpolation for $\vartheta \in [\pi, 2\pi]$

$$\mathcal{H}(k,\vartheta) = -U_{\mathcal{C}}^{\dagger}\mathcal{H}^{*}(-k, 2\pi-\vartheta)U_{\mathcal{C}}. \tag{5.46}$$

Interpreted as a two-dimensional problem, $H(k,\vartheta)$ is now manifestly particle-hole symmetric. By requiring for the whole interpolation the system to be gapped we can define the Chern number of this cyclic interpolation[1]

$$\mathcal{C}_{\mathcal{H}} = \oint d\vartheta \frac{\partial P(\vartheta)}{\partial \vartheta}, \tag{5.49}$$

[1] To see that these formula indeed corresponds to our known result we first state that (we drop the label and sum over n for simplicity)

$$\begin{aligned}\mathcal{F}_{\vartheta k} &= \partial_\vartheta i\langle\varphi_k|\partial_k\varphi_k\rangle - \partial_k i\langle\varphi_k|\partial_\vartheta\varphi_k\rangle = i\langle\partial_\vartheta\varphi_k|\partial_k\varphi_k\rangle + i\langle\varphi_k|\partial_\vartheta\partial_k\varphi_k\rangle - i\langle\partial_k\varphi_k|\partial_\vartheta\varphi_k\rangle - i\langle\varphi_k|\partial_k\partial_\vartheta\varphi_k\rangle \\ &= i\langle\partial_\vartheta\varphi_k|\partial_k\varphi_k\rangle - i\langle\partial_k\varphi_k|\partial_\vartheta\varphi_k\rangle.\end{aligned}$$

We now write

$$\begin{aligned}\oint d\vartheta \frac{\partial P(\vartheta)}{\partial\vartheta} &= \oint d\vartheta \frac{\partial}{\partial\vartheta}\oint \frac{dk}{2\pi} i\langle\varphi_k|\partial_k\varphi_k\rangle = \oint d\vartheta \oint \frac{dk}{2\pi}\left(i\langle\partial_\vartheta\varphi_k|\partial_k\varphi_k\rangle + i\langle\varphi_k|\partial_\vartheta\partial_k\varphi_k\rangle\right) \\ &\overset{\text{P.I.}}{=} \oint d\vartheta \oint \frac{dk}{2\pi}\left(i\langle\partial_\vartheta\varphi_k|\partial_k\varphi_k\rangle - i\langle\partial_k\varphi_k|\partial_\vartheta\varphi_k\rangle\right) + \oint d\vartheta \underbrace{i\langle\varphi_{k=2\pi}|\partial_\vartheta\varphi_{k=2\pi}\rangle}_{\mathcal{A}_\vartheta(k=2\pi)} + \oint d\vartheta \underbrace{i\langle\varphi_{k=0}|\partial_\vartheta\varphi_{k=0}\rangle}_{\mathcal{A}_\vartheta(k=0)}.\end{aligned}$$

From the discussion of fiber bundles we know that we cannot necessarily choose a smooth gauge such that $\boldsymbol{\mathcal{A}}$ is a single-valued function over the whole torus. However, we can always choose a gauge where $\mathcal{A}_\vartheta$ is single valued (akin the Landau gauge for the electro-magnetic gauge potential). For such a gauge the integrals

$$\oint d\vartheta \mathcal{A}_\vartheta(k) = 0 \tag{5.47}$$

for both $k = 0$ and $k = 2\pi$. With this we established

$$\oint d\vartheta \frac{\partial P(\vartheta)}{\partial\vartheta} = \oint d\vartheta \oint \frac{dk}{2\pi}\left(i\langle\partial_\vartheta\varphi_k|\partial_k\varphi_k\rangle - i\langle\partial_k\varphi_k|\partial_\vartheta\varphi_k\rangle\right) = \frac{1}{2\pi}\oint d\vartheta\oint dk\,\mathcal{F}_{\vartheta k} = \mathcal{C}, \tag{5.48}$$

as we tried to prove.

where as before we defined the charge polarization as a function of the pumping parameter ϑ

$$P(\vartheta) = \oint \frac{dk}{2\pi} \sum_{n\,\text{filled}} i\langle\varphi_{nk}|\partial_k\varphi_{nk}\rangle \tag{5.50}$$

To make further progress in establishing an equivalence relation between one dimensional Hamiltonians of class D we note that owing to the particle-hole symmetry, eigenstates of different locations in the Brillouin zone are related to each other. Without showing the full algebraic manipulations [11], we state that

$$P(\vartheta) = -P(2\pi - \vartheta). \tag{5.51}$$

An immediate consequence is

$$\int_0^\pi d\vartheta P(\vartheta) = \int_\pi^{2\pi} d\vartheta P(\vartheta). \tag{5.52}$$

We remind ourselves that these two equations rely crucially on the presence of the particle-hole symmetry. Consider now another particle-hole symmetric interpolation $\mathcal{H}'(k,\vartheta)$ between $\mathcal{H}_1(k)$ and $\mathcal{H}_2(k)$. We denote the corresponding polarization with $P'(\vartheta)$. The relative Chern number of the two interpolations is then given by

$$\mathcal{C}_\mathcal{H} - \mathcal{C}_{\mathcal{H}'} = \oint d\vartheta \left(\frac{\partial P(\vartheta)}{\partial\vartheta} - \frac{\partial P'(\vartheta)}{\partial\vartheta} \right). \tag{5.53}$$

One can define two yet different interpolations $\mathcal{G}_1(k,\vartheta)$ and $\mathcal{G}_2(k,\vartheta)$ (not particle-hole symmetric!) via

$$\mathcal{G}_1(k,\vartheta) = \begin{cases} \mathcal{H}(k,\vartheta) & \vartheta \in [0,\pi] \\ \mathcal{H}'(k,2\pi-\vartheta) & \vartheta \in [\pi,2\pi] \end{cases}, \tag{5.54}$$

and

$$\mathcal{G}_2(k,\vartheta) = \begin{cases} \mathcal{H}'(k,2\pi-\vartheta) & \vartheta \in [0,\pi] \\ \mathcal{H}(k,\vartheta) & \vartheta \in [\pi,2\pi] \end{cases}. \tag{5.55}$$

These interpolations are shown in Fig. 5.6. We see that $\mathcal{G}_1$ is obtained by reconnecting $\mathcal{H}$ and $\mathcal{H}'$ such that it always runs in the upper half-space and vice-versa for $\mathcal{G}_2$. It is straightforward to see that

$$\mathcal{C}_{\mathcal{G}_1} = \int_0^\pi d\vartheta \left(\frac{\partial P(\vartheta)}{\partial\vartheta} - \frac{\partial P'(\vartheta)}{\partial\vartheta} \right), \tag{5.56}$$

and

$$\mathcal{C}_{\mathcal{G}_2} = \int_\pi^{2\pi} d\vartheta \left(\frac{\partial P(\vartheta)}{\partial\vartheta} - \frac{\partial P'(\vartheta)}{\partial\vartheta} \right). \tag{5.57}$$

From this it is easy to see that $\mathcal{C}_\mathcal{H} - \mathcal{C}_{\mathcal{H}'} = \mathcal{C}_{\mathcal{G}_1} + \mathcal{C}_{\mathcal{G}_2}$. Moreover, if we use the symmetry (5.52) we see that $\mathcal{C}_{\mathcal{G}_1} = \mathcal{C}_{\mathcal{G}_2}$ and hence

$$\mathcal{C}_\mathcal{H} - \mathcal{C}_{\mathcal{H}'} = 2\nu \qquad \text{with} \qquad \nu \in \mathbb{Z}. \tag{5.58}$$

How can we understand this result? Remember that each interpolation gives rise to a two-dimensional band-structure. The Chern number of this band-structure, $\mathcal{C}_\mathcal{H}$ can only change if when going from $\mathcal{H} \to \mathcal{H}'$ we close a gap. However, due to the particle-hole symmetry, such gap closings always occur in two points in the Brillouin zone, see Fig. 5.6. Therefore, for all possible interpolations between our original one dimensional problems $\mathcal{H}_1(k)$ and $\mathcal{H}_2(k)$ the parity of the Chern number is conserved. We can thus write the *relative Chern parity*

$$N[\mathcal{H}_1(k), \mathcal{H}_2(k)] = (-1)^{\mathcal{C}_{\mathcal{H}(k,\vartheta)}}. \tag{5.59}$$

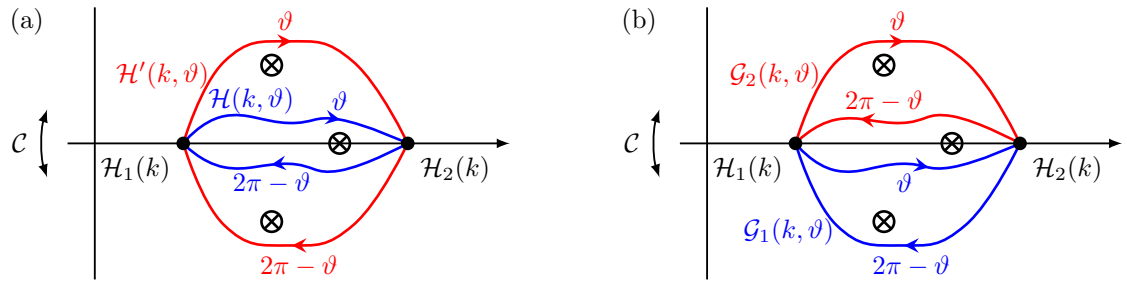

Figure 5.6: (a) Interpolation between two particle-hole symmetric one dimensional Hamiltonians $\mathcal{H}_{1/2}(k)$. Along the horizontal axis we move between different one-dimensional Hamiltonians. Along the vertical axis, the particle-hole symmetry operation on the one-dimensional Hamiltonians corresponds to a mirroring around the horizontal axis. Hence, we see that the blue (red) interpolation paths are constructed such that the interpolation, interpreted as a two-dimensional Hamiltonian, is manifestly symmetric under $\mathcal{C}$. The crosses correspond to gap closings in $\mathcal{H}(k,\vartheta)$ and hence the interpolations are not allowed to touch them in order for $\mathcal{H}(k,\vartheta)$ to have a well defined Chern number. Due to symmetry constraints, all gap closings away from the particle-hole symmetric line appear in pairs. Consequently, we might change the Chern number by deforming the interpolation, but always by two. Hence, independently of how $\mathcal{H}_1(k)$ and $\mathcal{H}_2(k)$ are connected, the Chern number parity is independent of the interpolation and hence can be used as a $\mathbb{Z}_2$ index. (b) Different interpolation paths to make the arguments in (a) formal.

It is easy to prove that this relative Chern parity has the property

$$N[\mathcal{H}_1(k),\mathcal{H}_2(k)]N[\mathcal{H}_2(k),\mathcal{H}_3(k)] = N[\mathcal{H}_1(k),\mathcal{H}_3(k)] \tag{5.60}$$

and consequently defines an equivalence relation. Equivalence classes are given by Hamiltonians in symmetry class D which have the same relative Chern parity. We can moreover define an absolute $\mathbb{Z}_2$ index by choosing a naturally "trivial" Hamiltonian $\mathcal{H}_0$ and then define

$$\mathcal{H}(k) \in \text{D} \quad \text{trivial} \quad \Leftrightarrow \quad N[\mathcal{H}(k),\mathcal{H}_0] = 1, \tag{5.61}$$

$$\mathcal{H}(k) \in \text{D} \quad \text{non-trivial:} \quad \Leftrightarrow \quad N[\mathcal{H}(k),\mathcal{H}_0] = -1. \tag{5.62}$$

While the above developments might appear somewhat formal, they have a direct physical consequence. Imagine a one dimensional system $\mathcal{H}_{\text{nt}}$ which is non-trivial according to (5.62). The two dimensional system given by the interpolation between $\mathcal{H}_0$ and $\mathcal{H}_{\text{nt}}$ therefore has an odd Chern number and correspondingly an odd number of surface modes traversing the gap on a each side of a finite cylinder. Let us imagine ϑ to be the momentum along the edge of the cylinder. Due to the particle hole symmetry between ϑ and $2\pi-\vartheta$, zero levels always appear in pairs at ϑ and $2\pi-\vartheta$. As we need an odd number of them, there has to be one either at $\vartheta = 0$ or π. As $\vartheta = 0$ corresponds to the trivial atomic Hamiltonian $\mathcal{H}_0$, there are no end states at $\vartheta = 0$. In other words, a non-trivial $\mathbb{Z}_2$ index in class D guarantees the existence of zero energy end states for a one dimensional system with an end.

This concludes our discussion of the structure of the periodic table 5.1. We have seen on one concrete example how a Chern number of a higher-dimensional member of a symmetry class can give rise to a $\mathbb{Z}_2$ index in one dimension lower. We refer the interested reader to the publications by Ryu et al. [9] and Kitaev [8] for further details. Instead of pursuing the study of what lies behind the periodic table further, we move to the discussion of three prototypical models of topological free fermion systems. One important void owing to this strategy is that we did not discuss topological field theories that describe the electro-magnetic response of topological insulators. For this we need a bit more technical tools which we will develop before we discuss the fractional quantum Hall effect. Once we are acquainted with these tools we will come back to this issue.

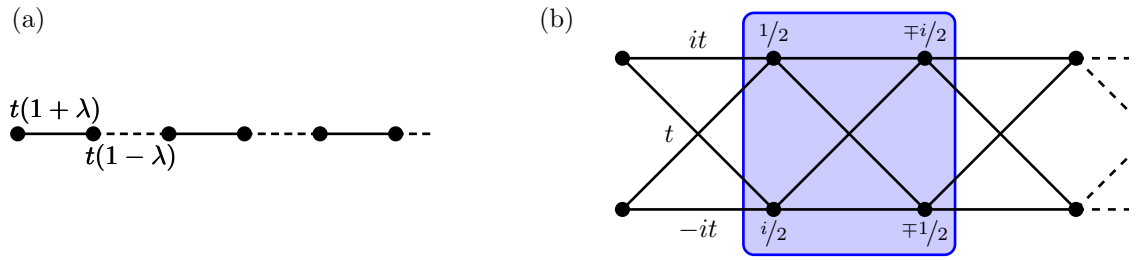

Figure 5.7: (a) The Su-Schrieffer-Heeger model. (b) Localized eigenstate in the flat band Creutz model.

5.4 Examples of topological free fermion systems

5.4.1 Su-Schrieffer-Heeger and Creutz model

In this section we discuss a simple one dimensional hopping model originally introduced by Su, Schrieffer and Heeger (SSH) to describe certain aspects of polyacetylene [12]. Consider the following tight binding model

$$H = -t\sum_i [(-1)^i\lambda + 1]c_i^\dagger c_{i+1} + \text{H.c.} \qquad \Rightarrow \qquad \mathcal{H}(k) = -t\sum_i d_i(k)\sigma_i, \tag{5.63}$$

with

$$d_x(k) = 2\cos(k), \qquad d_y(k) = 2\lambda\sin(k), \qquad d_z(k) = 0. \tag{5.64}$$

If we rotate the d-vector, the structure of the problem does not change. However, we will see that the physical interpretation of the model can be quite different and is then known as the Creutz ladder [13], cf. Fig. 5.7. We rotate by $\pi/2$ around the x-axis to obtain

$$d_x(k) = 2\cos(k), \qquad d_y(k) = 0, \qquad d_z(k) = 2\lambda\sin(k). \tag{5.65}$$

As the d-vector does not contain a y-component, we immediately conclude that $\{\mathcal{H}, \sigma_y\} = 0$ with $\sigma_y^2 = \mathbb{1}$, i.e., we have a chiral symmetry. Moreover, the Hamiltonian has the property

$$\mathcal{H}^*(k) = \mathcal{H}(k) = -\sigma_z\mathcal{H}(-k)\sigma_z \tag{5.66}$$

which we identify as a particle hole symmetry with $U_\mathcal{C} = \sigma_z$. Hence, we also have a time reversal symmetry with $U_\mathcal{T} = U_\mathcal{C}^{-1}U_\mathcal{S} = \sigma_z\sigma_y = -i\sigma_x$. We see that both $U_{\mathcal{C}/\mathcal{T}} = U_{\mathcal{C}/\mathcal{T}}^\mathrm{T}$ and hence both $\mathcal{T}$ and $\mathcal{C}$ square to one, which puts us in symmetry class BDI. Consulting Tab. 5.1, we expect a $\mathbb{Z}$ quantum number. Note, however, that we can break either (and hence both) particle-hole or time-reversal symmetry and we end up in class AIII, which is again described by a $\mathbb{Z}$ topological index. We therefore consult the Ryu paper [9] for class AIII. From Ref. [9] we learn that we should consider the projector onto the ground state $|v_-(k)\rangle$

$$P(k) = |v_-(k)\rangle\langle v_-(k)| = \frac{1}{2}\left[\mathbb{1} - \bar{Q}(k)\right] = \left[\frac{1}{2}\mathbb{1} - \frac{1}{2}\mathbf{d}(k)\boldsymbol{\sigma}\right]. \tag{5.67}$$

Due to the chiral symmetry, the $\bar{Q}$-matrix can be brought in off-diagonal form in the eigen-basis of the $\mathcal{S}$-symmetry, i.e.,

$$\begin{aligned} Q(k) = \frac{1}{2}\begin{pmatrix} -i & 1 \\ i & 1 \end{pmatrix}\bar{Q}(k)\begin{pmatrix} i & -i \\ 1 & 1 \end{pmatrix} &= \begin{pmatrix} 0 & q(k) \\ q^*(k) & 0 \end{pmatrix} \\ &= \begin{pmatrix} 0 & -\lambda\sin(k) - i\cos(k) \\ -\lambda\sin(k) + i\cos(k) & 0 \end{pmatrix}. \end{aligned} \tag{5.68}$$

The winding number density is now given by [9]

$$w(k) = iq^{-1}(k)\partial_k q(k) = \frac{i\lambda\cos(k)+\sin(k)}{i\cos(k)+\lambda\sin(k)} = \begin{cases} 1 & \lambda = 1, \\ -1 & \lambda = -1. \end{cases} \tag{5.69}$$

As the gap is closing only at $\lambda = 0$, the two special values $\lambda = \pm 1$ suffice for the calculation of the total winding number in the two distinct phases

$$\mathcal{W} = \int_{-\pi}^{\pi} \frac{dk}{2\pi} w(k) = \begin{cases} 1 & \lambda > 0, \\ -1 & \lambda < 0. \end{cases} \tag{5.70}$$

What does this winding number signify? From expression (5.67), it is clear that it corresponds to the winding of the d-vector throughout the Brillouin zone. However, we know, that the spinor-wave function of a spin-1/2 only returns to itself after a rotation by 4π. To investigate this further, let us specialize to $\lambda = 1$ for simplicity. In this case, the dispersion reduces to

$$|\mathbf{d}(k)| = \pm 2, \tag{5.71}$$

i.e., we deal with two completely flat bands. In the case of the SSH model, this is somewhat trivial, as we cut the chain into a set to independent dimers. For the Creutz ladder, this indicates a rather delicate interference effect, see Fig. 5.7! The ground state wave function can be explicitly written as

$$|v_-(k)\rangle = \begin{pmatrix} \cos[(\pi-2k)/4] \\ -\sin[(\pi-2k)/4] \end{pmatrix} \qquad \text{with} \qquad |v_-(-\pi)\rangle = -|v_-(\pi)\rangle. \tag{5.72}$$

Hence, we see that indeed the winding number $\mathcal{W}$ is responsible for a phase jump of π at the Brillouin zone-boundary. We try to see what this means for the Wannier functions

$$W_{\alpha,-}(l) = \int_{-\pi}^{\pi} \frac{dk}{2\pi}\, v_{\alpha,-}(k) e^{ikl}, \tag{5.73}$$

where α is the sub-lattice index label. Let us see what we can deduce from the presence of non-trivial winding number

$$\begin{aligned} W_{\alpha,-}(l) &= \int_{-\pi}^{\pi} \frac{dk}{2\pi}\, v_{\alpha,-}(k) e^{ikl} = \frac{1}{2\pi i l}\langle v_{\alpha,-}(k) e^{ikl}\rangle\Big|_{k=-\pi,\pi} - \frac{1}{il}\int_{-\pi}^{\pi}\frac{dk}{2\pi}\, v'_{\alpha,-}(k)e^{ikl} \\ &= \frac{(-1)^l \Delta v_{\alpha,-}}{2\pi i l} + \frac{1}{2\pi l^2}\langle v'_{\alpha,-}(k)e^{ikl}\rangle\Big|_{k=-\pi,\pi} - \frac{1}{l^2}\int_{-\pi}^{\pi}\frac{dk}{2\pi}\, v''_{\alpha,-}(k)e^{ikl} = \\ &= \frac{(-1)^l}{2\pi}\left[\frac{\Delta v_{\alpha,-}}{il} + \frac{\Delta v'_{\alpha,-}}{l^2} - \frac{\Delta v''_{\alpha,-}}{il^3} + \mathcal{O}(1/l^4)\right]. \end{aligned} \tag{5.74}$$

We make the following two observations. (i) If $\mathcal{W} = 0$, all the discontinuities $\Delta v^{(n)}_{\alpha,-} \equiv 0$. This was to be expected as in this case we know that the Wannier functions are exponentially localized [14] and hence have an essential singularity at $1/l \to 0$. (ii) If $\mathcal{W} = \pm 1$, $v_{\alpha,-}(k)$ is a 4π-periodic function and generically has non-zero $\Delta v_{\alpha,-}(k)$ and therefore

$$w_{\alpha\nu}(l) \overset{l\to\infty}{\propto} \frac{1}{l}. \tag{5.75}$$

(iii) For an even winding number, there is no such discontinuity. For our problem of the Creutz ladder we deduce from the above considerations that the large-l behavior is given by

$$W_{\alpha,-}(l) \sim \frac{-i}{\sqrt{2\pi l}}. \tag{5.76}$$

This result is in accordance with the full expression

$$W_{\alpha,-}(l) = \frac{\sqrt{2}(-1)^l(-1 \pm 2il)}{\pi\,(4l^2-1)}. \tag{5.77}$$

Instead of site-centered, we can use bond centered Wannier functions for the lower band

$$W^{\text{bond}}_{\alpha,-}(l) = \int_{-\pi}^{\pi} \frac{dk}{2\pi}\, v_{\alpha,-}(k) e^{ik(l+1/2)} = \begin{cases} \frac{1+i}{2\sqrt{2}}\delta_{l,-1} + \frac{1-i}{2\sqrt{2}}\delta_{l,0} & \alpha = 1, \\ -\frac{1-i}{2\sqrt{2}}\delta_{l,-1} - \frac{1+i}{2\sqrt{2}}\delta_{l,0} & \alpha = 2. \end{cases} \tag{5.78}$$

These states are not only exponentially but strictly localized to one bond! How can we reconcile this with the above result that Wannier functions have an $1/l$-tail? To see this, we make the following observation: In the form we wrote the eigenstates $|v_-(k)\rangle$ we made a certain gauge choice. We are free to choose a different one. Led by the above observation that the bond centered Wannier function are localized, we make an explicitly gauge transformation

$$|v_-(k)\rangle \longrightarrow |\tilde{v}_-(k)\rangle = e^{ik/2}|v_-(k)\rangle = \begin{pmatrix} e^{ik/2}\cos[(\pi-2k)/4] \\ -e^{ik/2}\sin[(\pi-2k)/4] \end{pmatrix}, \tag{5.79}$$

with the property

$$|\tilde{v}_-(-\pi)\rangle = |\tilde{v}_-(\pi)\rangle. \tag{5.80}$$

Using this gauge, it becomes clear that there are no non-vanishing terms in the $1/l$ expansion of the Wannier function. This is a very deep truth: If there is no obstruction to a smooth gauge for the Bloch wave functions, Wannier functions can be localized (at least) exponentially. Also the opposite statement is true: If there is an obstruction to a smooth gauge, we cannot localize the Wannier functions. As we know that the Chern number exactly signals such an impossibility to choose a smooth gauge. From this we deduce that in a Chern insulator the Wannier functions can never be localized!

5.4.2 Kitaev wire

In this section we discuss Kitaev's toy model for a spinless p-wave superconducting chain described by

$$H = -\mu \sum_{i=1}^{N} c_i^\dagger c_i - \sum_{i=1}^{N-1} \left(t c_i^\dagger c_{i+1} + e^{i\varphi}\Delta c_i c_{i+1} + \text{H.c.} \right). \tag{5.81}$$

Here, N is the number of sites, μ the chemical potential, and t and Δ the hopping and pairing amplitude, respectively. If we write the same Hamiltonian in momentum space we find

$$H = \frac{1}{2}\sum_k \begin{pmatrix} c_k & c_{-k}^\dagger \end{pmatrix}^\dagger \underbrace{\begin{pmatrix} -t\cos(k) - \mu & e^{i\varphi}\Delta i \sin(k) \\ -e^{-i\varphi}\Delta i \sin(k) & t\cos(k) + \mu \end{pmatrix}}_{\mathcal{H}_k} \begin{pmatrix} c_k \\ c_{-k}^\dagger \end{pmatrix} \qquad \text{with} \qquad \mathcal{H}_k = \sum_i d_i(k)\sigma_i,$$

where the d-vector is given by

$$d_x(k) = \sin(\varphi)\Delta\sin(k), \tag{5.82}$$

$$d_y(k) = \cos(\varphi)\Delta\sin(k), \tag{5.83}$$

$$d_z(k) = -t\cos(k) - \mu. \tag{5.84}$$

As we are dealing with a BdG problem, the particle hole symmetry is built in with a $U_{\mathcal{C}} = \sigma_x$. $U_{\mathcal{C}} = U_{\mathcal{C}}^{\mathrm{T}}$ as expected for a triplet superconductor. It is a bit more involved to determine if there is also an $\mathcal{S}$ symmetry (and consequently also time reversal). A little exercise shows that

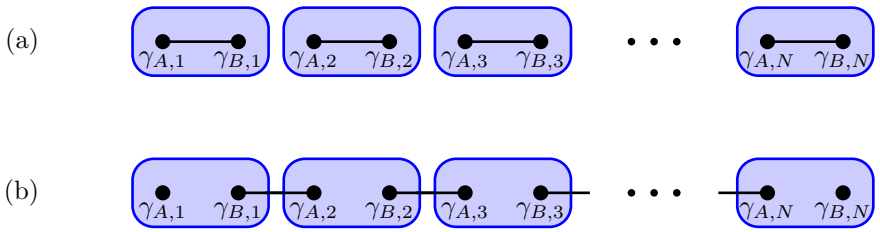

Figure 5.8: (a) Eigenstates for the Kitaev wire for $\mu < 0$ and $t = \Delta = 0$. (b) The same for $\mu > 0$, and $\Delta = t \neq 0$.

for $\varphi = 0$, $\sigma_x \mathcal{H}(k) \sigma_x = -\mathcal{H}(k)$. Hence, we only need to transform away the phase φ of the superconducting order parameter. This can be done via

$$r(\varphi) = \cos(\varphi/2)\mathbb{1} + i \sin(\varphi/2)\sigma_z. \tag{5.85}$$

With this find an $\mathcal{S}$-symmetry with $U_{\mathcal{S}} = r(\varphi)\sigma_x$. As a by-product, the time-reversal symmetry is established for a unitary $U_{\mathcal{T}} = U_{\mathcal{C}}^{-1} U_{\mathcal{S}} = \sigma_x r(\varphi) \sigma_x = r(-\varphi)$. A quick look at Tab. 5.1 tells us that we are in symmetry class BDI characterized by a $\mathbb{Z}$ index. Owing to the rotation $r(\varphi)$, which does not depend on k, it is clear that we can use the winding number of chiral systems to obtain this index. However, we want to anticipate a potential breaking of time reversal invariance. In this case we deal with a class D-problem for which we established the relative Chern parity as a good topological index. Recall that the relative Chern parity is obtained by assuming $\mathcal{H}(k)$ to be the $k_y = \pi$ cut of a two-dimensional Hamiltonian. As a reference we took for $k_y = 0$ a trivial reference state. Owing to the fact that we deal with a two-band system we obtain the Chern number from the Skyrmion number (4.9). However, we know that along $k_y = 0$ the d-vector can be chosen to point constantly in positive z-direction. Moreover, the particle-hole symmetry forces

$$d_x(0) = d_y(0) = d_x(\pi) = d_y(\pi) = 0. \tag{5.86}$$

Hence, in order for the Chern number of the interpolation path to be odd, we need (show!)

$$\frac{d_z(0)}{|d_z(0)|} \frac{d_z(\pi)}{|d_z(\pi)|} = s_0 s_\pi = \nu < 0. \tag{5.87}$$

For the present case, this means we require

$$\nu = -(t - \mu)(t + \mu) < 0 \quad \Rightarrow \quad |\mu| < t. \tag{5.88}$$

Let us see what this index means for a finite system with edges. To this end it is convenient to introduce two *real fermions* per site

$$c_i = \frac{e^{i\varphi}}{2} (\gamma_{iA} + i\gamma_{iB}) \qquad \text{with the properties} \qquad \gamma_{i\alpha}^\dagger = \gamma_{i\alpha} \quad \text{and} \quad \{\gamma_{i\alpha}, \gamma_{j\beta}\} = 2\delta_{\alpha\beta}\delta_{ij}. \tag{5.89}$$

In these new real, or *Majorana*, fermions the Hamiltonian reads

$$H = -\frac{\mu}{2} \sum_{i=1}^{N} (1 + i\gamma_{iA}\gamma_{iB}) - \frac{i}{4} \sum_{i=1}^{N-1} \left[(\Delta + t)\gamma_{iB}\gamma_{i+1A} + (\Delta - t)\gamma_{iA}\gamma_{i+1B} \right]. \tag{5.90}$$

Let us consider two special points in the phase diagram. For the topologically trivial region we choose $\mu < 0$ and $\Delta = t = 0$. In this case the Hamiltonian is trivial and it is clear that in order

to write in terms of complex fermions again, we just revert procedure (5.89), cf. Fig 5.8. For the topologically non-trivial case we choose $\mu = 0$ and $\Delta = t \neq 0$. The Hamiltonian now reduces to

$$H = -\frac{i}{2} t \sum_{i=1}^{N-1} \gamma_{iB} \gamma_{i+1A}. \tag{5.91}$$

We make two observations: (i) The Majorana operators γ_{1A} and γ_{NB} do not appear in the Hamiltonian. (ii) We can go back to a fermionic representation by "paring" Majorana fermions over bonds

$$d_i = \frac{1}{2} \left(\gamma_{i+1A} + i \gamma_{iB} \right). \tag{5.92}$$

Written in these fermions the Hamiltonian is again strikingly simple

$$H = t \sum_{i=1}^{N-1} \left(d_i^\dagger d_i + \frac{1}{2} \right). \tag{5.93}$$

Clearly, the d_i-fermions are the quasi-particle excitations above the superconducting ground state. However, owing to the fact that γ_{1A} and γ_{NB} did not appear in the Hamiltonian, we can form another fermion, see Fig 5.8

$$f = \frac{1}{2} \left(\gamma_{1A} + i \gamma_{NB} \right). \tag{5.94}$$

This f-fermion formed out of the Majorana modes at the two edges does not appear in the Hamiltonian. Therefore, the ground state is doubly degenerate: If $f|0\rangle = 0$ is a ground state, also $|1\rangle = f^\dagger |0\rangle$ is.

5.4.3 Two dimensional $p_x + ip_y$ superconductor

The two-dimensional generalization of a spin-less fermion system that realizes unpaired Majorana fermions is a $p_x + ip_y$ superconductor.[2] In a continuum model such a superconductor is described by the Hamiltonian [16]

$$H = \int d\mathbf{r} \left\{ \psi^\dagger \left(-\frac{\nabla^2}{2m} - \mu \right) \psi + \frac{\Delta}{2} \left[e^{i\varphi} \psi \left(\partial_x + i \partial_y \right) \psi + \text{H.c} \right] \right\}. \tag{5.95}$$

Here, ψ creates a spinless fermion with mass m and φ is the phase of the superconducting order parameter $\Delta \in \mathbb{R}$. We consider a system with periodic boundary conditions in both x- and y-directions (a torus). Introducing the notation $\boldsymbol{\psi}_{\mathbf{k}}^\dagger = [\psi_{\mathbf{k}}^\dagger, \psi_{-\mathbf{k}}]$ the above Hamiltonian can be written as

$$H = \frac{1}{2} \int \frac{d\mathbf{k}}{(2\pi)^2} \boldsymbol{\psi}_{\mathbf{k}}^\dagger \mathcal{H}(\mathbf{k}) \boldsymbol{\psi}_{\mathbf{k}} \qquad \text{with} \qquad \mathcal{H}(\mathbf{k}) = \sum_i d_i(\mathbf{k}) \sigma_i. \tag{5.96}$$

The d-vector looks like

$$d_x(\mathbf{k}) = -\Delta (k_x \sin(\varphi) + k_y \cos(\varphi)), \tag{5.97}$$

$$d_y(\mathbf{k}) = \Delta (k_x \cos(\varphi) - k_y \sin(\varphi)), \tag{5.98}$$

$$d_z(\mathbf{k}) = \frac{k^2}{2m} - \mu. \tag{5.99}$$

This Hamiltonian is again particle hole symmetric with $U_{\mathcal{C}} = \sigma_x$ as it describes a triplet superconductor. However, due to the $k_x + ik_y$ nature of the pairing, time reversal symmetry is broken,

[2] So far we have discussed only lattice models. The same can be done for a two-dimensional $p_x + ip_y$ superconductor. However, the main features we want to touch upon are also accessible in a (simpler) continuum model. The interested reader is referred the publication by Asahi and Nagaosa [15] for a lattice version.

which puts us in class D. Hence, we have to calculate the Chern number. The bulk excitation spectrum $\pm d(\mathbf{k})$ is gapped for all values of $\mathbf{k}$ and $\mu \neq 0$. To see if $\mu = 0$ corresponds to a topological phase transition we study the evolution of the d-vector as a function of $\mathbf{k}$. Remember that we had to regularize the Dirac fermion problem in Sec. 4. One can do so by putting the system on a lattice [15]. Alternatively, we note that for $k \to \infty$ the director $\hat{d}(\mathbf{k})$ tends to a unique vector which does not depend on the direction of $\mathbf{k}$. At this point we can cut off the momentum integral as there is no further contribution to the Skyrmion density $\epsilon_{\alpha\beta\gamma}\hat{d}_\alpha \partial_{k_x}\hat{d}_\beta \partial_{k_y}\hat{d}_\gamma$.[3]
Let us start with the case $\mu < 0$. Note that for momenta with fixed k, d_x and d_y always sweep out a circle on the unit sphere at height d_z. At k=0 we start at the north pole and slowly slide down towards the equator before we move back to the north pole at $k \to \infty$. Therefore, the d-vector does not wrap around S^2 and the Chern number is zero. For $\mu > 0$ the d-vector starts at the south-pole for $k = 0$ and smoothly moves up to the north-pole at $k \to \infty$. Hence, the Chern number is non-zero, concretely $\mathcal{C} = -1$.

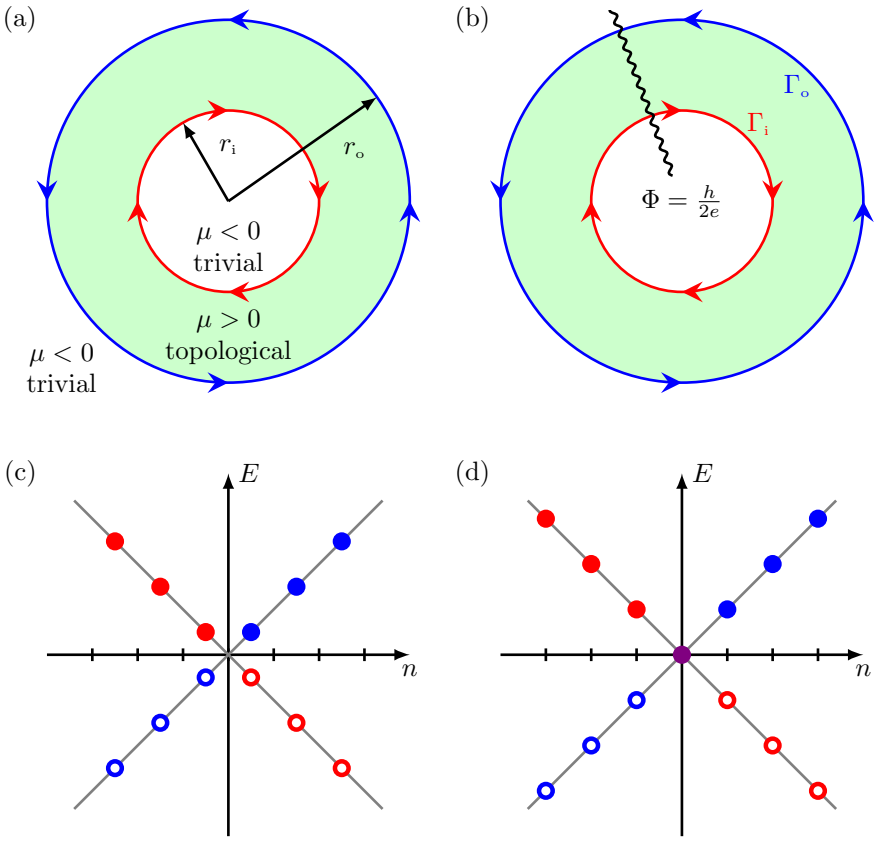

Figure 5.9: (a) Geometry for the chiral Majorana edge modes. (b) Toy model for a vortex in a $p_x + ip_y$ superconductor. (c) Edge spectrum for (a). (d) Spectrum for (b).

As for the Kitaev chain we would like to investigate the physical consequences of this Chern number. We know that at an interface between a topologically trivial and non-trivial region (where the Chern number changes by one) we expect one chiral edge channel. Following the very nice review by Alicea [16], we consider an Corbino disk by assuming the the chemical potential $\mu(r)$ smoothly goes from positive inside the annulus to negative outside, see Fig. 5.9(a). If we are interested in the low-energy modes in the vicinity of the edge and if $\mu(r)$ varies slowly enough,

[3] This tendency towards a direction independent $\hat{d}(\mathbf{k})$ for large k was not present in the Dirac problem, which resulted in a half-quantized "Chern" number.

we can neglect the ∇^2-term in the Hamiltonian and write in polar coordinates[4] (r, ϑ)

$$H_{\text{edge}} = \int d\mathbf{r} \left\{ -\mu(r)\psi^\dagger\psi + \left[\frac{\Delta}{2} e^{i\varphi} e^{i\vartheta} \psi \left(\partial_r + \frac{i\partial_\vartheta}{r} \right) \psi + \text{H.c} \right] \right\} \tag{5.105}$$

Note that the factor $e^{i\vartheta}$ above means that the pairing couples states with different angular momentum. To simplify this problem with change to new variables[5]

$$\psi \to \psi' = e^{-i\vartheta/2}\psi. \tag{5.106}$$

It is important to note that in the new variables ψ', we need to look for solutions with anti-periodic boundary conditions when encircling the annulus. In the new variables $\boldsymbol{\psi}'^\dagger = [\psi'^\dagger, \psi']$ the Hamiltonian is written as $H = \frac{1}{2}\int d\mathbf{r}\, \boldsymbol{\psi}'^\dagger \mathcal{H}(r,\vartheta)\boldsymbol{\psi}$, with

$$\mathcal{H}(r,\vartheta) = \begin{pmatrix} -\mu(r) & \Delta e^{-i\varphi}(-\partial_r + i\partial_\vartheta/r) \\ \Delta e^{i\varphi}(\partial_r + i\partial_\vartheta/r) & \mu(r) \end{pmatrix}. \tag{5.107}$$

To solve for $\mathcal{H}(r,\vartheta)\chi(r,\vartheta) = E\chi(r,\vartheta)$ we make the Ansatz

$$\chi(r,\vartheta) = e^{i(n+1/2)\vartheta} \begin{pmatrix} e^{-\varphi/2}[f(r) + ig(r)] \\ e^{i\varphi/2}[f(r) - ig(r)] \end{pmatrix}, \qquad \text{with} \qquad n \in \mathbb{Z}. \tag{5.108}$$

The prefactor $e^{i(n+1/2)\vartheta}$ accounts for the anti-periodic boundary conditions. From the eigenvalue equation we obtain

$$[E - (n+1/2)\Delta/r]g(r) = -i[\mu(r) - \Delta\partial_r]f(r) \tag{5.109}$$

$$[E + (n+1/2)\Delta/r]f(r) = \quad i[\mu(r) + \Delta\partial_r]f(r) \tag{5.110}$$

If $\chi(\vartheta, r)$ is well localized around the inner (r_{i}) or the outer (r_{o}) radius of the Corbino disk, we can replace $1/r \to 1/r_{\text{i/o}}$. Therefore the above equations have a solution for the outer edge with $f(r) \equiv 0$

$$E_{\text{o}} = \frac{(n+1/2)\Delta}{r_{\text{o}}}, \tag{5.111}$$

$$\chi^n_{\text{o}}(r,\vartheta) = e^{i(n+1/2)\vartheta} e^{\frac{1}{\Delta}\int_{r_{\text{o}}}^{r} dr'\,\mu(r')} \begin{pmatrix} ie^{i\varphi/2} \\ -ie^{-i\varphi/2} \end{pmatrix}. \tag{5.112}$$

[4] We use

$$x = r\cos(\vartheta) \qquad r = \sqrt{x^2+y^2}, \tag{5.100}$$

$$y = r\sin(\vartheta) \qquad \cos(\vartheta) = \frac{x}{\sqrt{x^2+y^2}} \qquad \sin(\vartheta) = \frac{y}{\sqrt{x^2+y^2}}. \tag{5.101}$$

Therefore

$$\frac{\partial}{\partial x} = \frac{\partial\vartheta}{\partial x}\frac{\partial}{\partial\vartheta} + \frac{\partial r}{\partial x}\frac{\partial}{\partial r} = -\frac{\sin(\vartheta)}{r}\frac{\partial}{\partial\vartheta} + \cos(\vartheta)\frac{\partial}{\partial r}, \tag{5.102}$$

$$\frac{\partial}{\partial y} = \frac{\partial\vartheta}{\partial y}\frac{\partial}{\partial\vartheta} + \frac{\partial r}{\partial y}\frac{\partial}{\partial r} = \quad \frac{\cos(\vartheta)}{r}\frac{\partial}{\partial\vartheta} + \sin(\vartheta)\frac{\partial}{\partial r}. \tag{5.103}$$

The pairing term now reads

$$\partial_x + i\partial_y = [\cos(\vartheta) + i\sin(\vartheta)]\partial_r + [-\sin(\vartheta) + i\cos(\vartheta)]\frac{\partial_\vartheta}{r} = e^{i\vartheta}\left[\partial_r + \frac{i\partial_\vartheta}{r}\right]. \tag{5.104}$$

[5] Remember that this is what we usually do to gauge aways a vector potential for the problem of a particle on a ring. Correspondingly, this transformation induces a term $i\partial_\vartheta \to i\partial_\vartheta + 1/2$. However, this constant terms vanishes in the pairing due to the Pauli principle.

And for the inner edge with $g(r) \equiv 0$

$$E_{\rm i} = -\frac{(n+1/2)\Delta}{r_{\rm i}}, \tag{5.113}$$

$$\chi^n_{\rm i}(r,\vartheta) = e^{i(n+1/2)\vartheta} e^{-\frac{1}{\Delta}\int_{r_{\rm i}}^{r} dr'\,\mu(r')} \begin{pmatrix} e^{i\varphi/2} \\ e^{-i\varphi/2} \end{pmatrix}. \tag{5.114}$$

These solutions have a few remarkable features. First, there is always a finite energy gap of $\frac{\Delta}{2r_{\rm i/o}}$, see Fig. 5.9. Second, the excitations are chiral with opposite chirality on the inner and outer edge. This looks a bit like the quantum Hall effect. However, here, the edge excitations are not regular complex fermions but are chiral Majorana modes. To see this we consider

$$\boldsymbol{\psi}'(r,\vartheta) = \sum_n \left[\chi^n_{\rm i}(r,\vartheta)\Gamma^n_{\rm in} + \chi^n_{\rm o}(r,\vartheta)\Gamma^n_{\rm o}\right]. \tag{5.115}$$

Since the upper and lower components of $\boldsymbol{\psi}'(r,\vartheta)$ are related by Hermitian conjugation, the above equations imply that

$$\Gamma^n_{\rm i/o} = [\Gamma^{-n}_{\rm i/o}]^\dagger. \tag{5.116}$$

This means that the operators

$$\Gamma_{\rm i/o}(\vartheta) = \sum_n e^{in\vartheta}\Gamma^n_{\rm i/o} = \Gamma^\dagger_{\rm i/o}(\vartheta). \tag{5.117}$$

are actually Majorana fermions.
In order to complete this section we show that vortices in a $p_x + ip_y$ superconductor carry a Majorana *zero mode*. The simplest model for a vortex is to take the annulus of before and thread a flux $h/2e$ through the inner hole. Such a flux quantum gives rise to a phase winding of the order parameter Δ, i.e., $\Delta \to \Delta(\vartheta) = e^{-i\vartheta}\Delta$. We immediately observe that this swallows the $e^{i\vartheta}$ in (5.105). This in turn, allows us to write the same solutions for ψ instead of ψ', which obey *periodic* instead of anti-periodic boundary conditions. Consequently, we have to shift the pre-factor $e^{i(n+1/2)\vartheta} \to e^{in\vartheta}$ in $\chi(r,\vartheta)$. Hence the energies for the states on the inner edge read now, cf. Fig. 5.9

$$E_{\rm i/o} = \frac{n\Delta}{r_{\rm i/o}} \qquad \text{with} \qquad n \in \mathbb{Z}. \tag{5.118}$$

In particular the $n = 0$ solution is a *zero energy Majorana mode*.[6] To understand the implications of this zero energy Majorana mode we refer to the seminal paper by Ivanov [17].

References

1. Kane, C. L. & Mele, E. J. "Quantum Spin Hall Effect in Graphene". *Phys. Rev. Lett.* **95,** 226801 (2005).
2. Bernevig, B. A. & Hughes, T. L. *Topological insulators and superconductors* (Princeton University Press, 2013).
3. Haldane, F. D. M. "Model for a Quantum Hall Effect without Landau Levels". *Phys. Rev. Lett.* **61,** 2015 (1988).
4. Sheng, D. N., Weng, Z. Y., Scheng, L. & Haldane, F. D. M. "Quantum Spin-Hall Effect and Topologically Invariant Chern Numbers". *Phys. Rev. Lett.* **97,** 036808 (2006).
5. Kohn, W. "Analytic properties of bloch waves and wannier functions". *Phys. Rev.* **115,** 809 (1959).

[6] The Majorana property follows from $-n = n$ for $n = 0$, in Eq. (5.116)

6. Nakahara, M. *Geometry, Topology and Physics* (Taylor and Francis, New York and London, 2003).

7. Bohm, A., Mostafazadeh, A., Koizumi, H., Niu, Q. & Zwanziger, J. *The Geometric Phase in Quantum Systems* (Springer-Verlag, Heidelberg, 2003).

8. Kitaev, A. "Periodic table for topological insulators and superconductors". *AIP Conf. Proc.* **1134,** 22 (2009).

9. Ryu, S., Schnyder, A. P., Furusaki, A. & Ludwig, A. W. W. "Topological insulators and superconductors: tenfold way and dimensional hierarchy". *New J. Phys.* **12,** 065010 (2010).

10. Schnyder, A. P., Ryu, S., Furusaki, A. & Ludwig, A. W. W. "Classification of topological insulators and superconductors in three spatial dimensions". *Phys. Rev. B* **78,** 195125 (2008).

11. Qi, X.-L., Hughes, T. L. & Zhang, S.-C. "Topological field theory of time-reversal invariant insulators". *Phys. Rev. B* **78,** 195424 (2008).

12. Su, W. P., Schrieffer, J. R. & Heeger, A. J. "Solitons in Polyacetylene". *Phys. Rev. Lett.* **42,** 1698 (1979).

13. Creutz, M. "End States, Ladder Compounds, and Domain-Wall Fermions". *Phys. Rev. Lett.* **83,** 2636 (1999).

14. Kohn, W. "Construction of Wannier Functions and Applications to Energy Bands". *Phys. Rev. B* **7,** 4388 (1973).

15. Asahi, D. & Nagaosa, N. "Topological indices, defects, and Majorana fermions in chiral superconductors". *Phys. Rev. B* **86,** 100504(R) (2012).

16. Alicea, J. "New directions in the pursuit of Majorana fermions in solid state systems". *Rep. Prog. Phys.* **75,** 076501 (2012).

17. Ivanov, D. A. "Non-Abelian Statistics of Half-Quantum Vortices in p-Wave Superconductors". *Phys. Rev. Lett.* **86,** 268 (2001).

Chapter 6

Significant others

Learning goals

- We know the basic phenomenology of the quantum Hall effect (QHE)
- We know the structure of the lowest Landau level (LLL)
- We understand the role of disorder for the QHE.

- K. von Klitzing, G. Dorda, and M. Pepper, Phys. Rev. Lett. **45**, 494 (1980)

6.1 Introduction

Up to now we were dealing with topological effects in electronic systems. We started with the quantum Hall effect and have seen that many more variants of electronic systems can have topological band structures. In the present chapter we want to see how the ideas of topological band theory found applications in other, seemingly unrelated, fields such as photonic or mechanical systems.

This chapter is also somewhat unusual as we follow a different approach in how the topic is being taught. We will see that among the systems in which topological bands can show up are (i) coupled ring resonators, (ii) evanescently coupled optical wave guides, (iii) periodically driven systems (electronic or photonic), and (iv) idealized mechanical systems. In the lecture we provide a few necessary ingredients to understand the core aspects of these physical systems. These prerequisites should then allow you to understand the original research papers we list at the end of this chapter covering the topics (i) – (iv).

6.2 Photonic systems

6.2.1 Coupled ring resonators

This section follows closely Ref. [1]. One can create "tight-binding" models for optical systems by weakly coupling high-Q resonators. Similar to the tight-binding approach for electronic band structures one assumes the electromagnetic field to be well described by the mode of a single high-Q cavity $\mathbf{E}_\Omega(\mathbf{r},t)$ with frequency Ω. When several cavities are weakly coupled, for example by evanescent waves, the electric field will largely be described by the local cavity fields $\mathbf{E}_\Omega(\mathbf{r},t)$ plus a small correction due to their coupling. In other words, the local cavities play the roles of the atomic orbitals and the evanescent coupling corresponds to the tunneling matrix element between these orbitals.
We assume a one dimensional chain of coupled cavities separated by a length a in $\hat{\mathbf{e}}_x$ direction for simplicity. Let us write for the electric field of the full problem

$$\mathbf{E}_k(\mathbf{r},t) = e^{i\omega_k t}\sum_{n\in\mathbb{Z}} e^{-ikna}\,\mathbf{E}_\Omega(\mathbf{r}-na\hat{\mathbf{e}}_x). \tag{6.1}$$

We readily recognize $\mathbf{E}_\Omega(\mathbf{r})$ as the Wannier function and $\mathbf{E}_k(\mathbf{r},t)$ as the corresponding Bloch "wave"-function. Recall that in the absence of source terms the Maxwell equations read

$$\nabla\wedge\mathbf{E} = -\frac{\partial\mathbf{B}}{\partial t}, \tag{6.2}$$

$$\nabla\wedge\mathbf{B} = \mu_0\epsilon(\mathbf{r})\frac{\partial\mathbf{E}}{\partial t}, \tag{6.3}$$

where μ_0 is the vacuum permeability and $\epsilon(\mathbf{r})$ the dielectric constant of the coupled resonators. The above equations can be combined to

$$\nabla\wedge[\nabla\wedge\mathbf{E}_k(\mathbf{r})] = \mu_0\epsilon(\mathbf{r})\omega_k^2\mathbf{E}_k(\mathbf{r}). \tag{6.4}$$

We assume $\mathbf{E}_\Omega(\mathbf{r})$ to be real and normalized to

$$\int d\mathbf{r}\,\epsilon(\mathbf{r})\mathbf{E}_\Omega(\mathbf{r})\cdot\mathbf{E}_\Omega(\mathbf{r}) = 1. \tag{6.5}$$

$\mathbf{E}_\Omega(\mathbf{r},t)$ satisfies the same equation with $\epsilon(\mathbf{r})$ replaced by $\epsilon_0(\mathbf{r})$, the dielectric constant of a single resonator. If we insert (6.1) into (6.4) we obtain

$$\omega_k^2 = \Omega^2\frac{1+\sum_{n\neq0}\exp(-ikna)\beta_n}{1+\Delta\alpha\sum_{n\neq0}\exp(-ikna)\alpha_n}, \tag{6.6}$$

where

$$\alpha_n = \int d\mathbf{r}\,\epsilon(\mathbf{r})\mathbf{E}_\Omega(\mathbf{r})\cdot\mathbf{E}_\Omega(\mathbf{r}-na\hat{\mathbf{e}}_x), \tag{6.7}$$

$$\beta_n = \int d\mathbf{r}\,\epsilon_0(\mathbf{r}-na\hat{\mathbf{e}}_x)\mathbf{E}_\Omega(\mathbf{r})\cdot\mathbf{E}_\Omega(\mathbf{r}-na\hat{\mathbf{e}}_x), \tag{6.8}$$

$$\Delta\alpha = \int d\mathbf{r}\,[\epsilon_0(\mathbf{r})-\epsilon(\mathbf{r})]\mathbf{E}_\Omega(\mathbf{r})\cdot\mathbf{E}_\Omega(\mathbf{r}). \tag{6.9}$$

For the case of weakly coupled resonators we can assume that $\alpha_n = \beta_n = 0$ for $n\neq 1,-1$. Moreover, symmetry requires $\alpha_1 = \alpha_{-1}$ and $\beta_1 = \beta_{-1}$. Putting these observations together we find

$$\omega_k = \Omega\left[1-\frac{\Delta}{2}+\kappa_1\cos(ka)\right], \tag{6.10}$$

where

$$\kappa_1 = \beta_1 - \alpha_1 = \int d\mathbf{r}\,[\epsilon_0(\mathbf{r} - a\hat{\mathbf{e}}_x) - \epsilon(\mathbf{r} - a\hat{\mathbf{e}}_x)]\mathbf{E}_\Omega(\mathbf{r}) \cdot \mathbf{E}_\Omega(\mathbf{r} - na\hat{\mathbf{e}}_x). \tag{6.11}$$

From these considerations one can clearly see that the system of coupled resonators is described exactly like a tight-binding hopping model for electrons.
In the papers by Hafezi et al. [2, 3] there is a small twist on the setup presented here. The "hopping" is not merely through evanescent coupling, but via the help of another wave-guide, or cavity, of variable length. Read the papers [2] and [3] and try to understand how their setup connects to what we learned in the last chapter.

6.2.2 Paraxial wave equation

Let us assume the wave equation describing the evolution of the electric field $\mathbf{E}(\mathbf{r}, t) = e^{i\omega t}\mathbf{E}(\mathbf{r})$

$$\nabla^2\mathbf{E}(\mathbf{r}) = -\omega^2\mu_0\epsilon(\mathbf{r})\mathbf{E}(\mathbf{r}). \tag{6.12}$$

We are now making the assumption that the electro-magnetic wave propagate mainly in z-direction and can be written as

$$\mathbf{E}(\mathbf{r}) = E_0(\mathbf{r})e^{ik_0 z}\hat{\mathbf{e}}_x, \tag{6.13}$$

where $E_0(\mathbf{r})$ is a slowly varying envelope that fulfills

$$|\partial_z^2 E_0(\mathbf{r})| \ll |k_0\partial_z E_0(\mathbf{r})|. \tag{6.14}$$

Hence, we can write (6.12) as

$$i\partial_z E_0(x, y, z) = -\frac{1}{2k_0}\left[\partial_x^2 + \partial_y^2 + \omega^2\mu_0\epsilon(x, y, z)\right] E_0(x, y, z). \tag{6.15}$$

Imagine now a periodic collection of parallel wave guides running along the z-direction. In other words, $\epsilon(x, y, z) = \epsilon(x, y)$ with $\epsilon(x+na, y+mb) = \epsilon(x, y)$ for some $a, b \in \mathbb{R}$ and $n, m \in \mathbb{Z}$. Hence, we can think of the z-direction as the time axis. The transverse dynamics is then equivalent to the one governed by the single particle Schrödinger equation in the periodic potential $\epsilon(x, y)$.
These considerations are a first step in understanding the "Photonic Floquet topological insulator" presented in Ref. [4]. Before we can embark on this paper, however, we need a few more prerequisites.

6.2.3 Floquet theory

A system which is topologically trivial might be rendered non-trivial by the application of a periodic perturbation. In order for us to apply our toolbox for the classification of topological insulators we need to have a time-independent problem at hand. Owing to the periodic nature of the perturbation, we can use the time-domain analog to Bloch theory: Floquet theory [5]. The basic observation is that solutions of the Schrödinger equation of a Hamiltonian of the form $H(t) = H(t + T)$ can be written as

$$\psi(t) = e^{i\epsilon_\alpha t}\Phi_\alpha(t) \qquad \text{with} \qquad \Phi_\alpha(t) = \Phi_\alpha(t + T). \tag{6.16}$$

Clearly we observe that ϵ_α, called the quasi-energy, is the counterpart to the quasi-momentum in Bloch theory. Moreover, if we are only interested in the "stroboscopic" evolution to times $t = nT$, with $n \in \mathbb{Z}$, the wave-function changes by

$$\psi(T) = e^{i\epsilon_\alpha T}\Phi_\alpha(0). \tag{6.17}$$

It is easy to show that $\Phi_\alpha(t)$ are the solutions to

$$[H(t) - i\hbar\partial_t]\Phi_\alpha(t) = \mathcal{H}_F(t)\Phi_\alpha(t) = \epsilon_\alpha\Phi_\alpha(t). \tag{6.18}$$

$\mathcal{H}_F$ is called the Floquet operator. Furthermore, we can write for the evolution operator

$$K(T) = \mathcal{T} \exp\left[-\frac{i}{\hbar}\int_0^T dt\, H(t)\right] = \exp\left[\frac{i}{\hbar} H_F\right], \tag{6.19}$$

where $\mathcal{T}$ is time time-ordering operator. The Floquet Hamiltonian H_F is time-independent, has the eigenvalues ϵ_α, and governs the topological properties at long times.[1] The standard task in Floquet theory is to find the effective time-independent H_F corresponding to the time-dependent Floquet operator $\mathcal{H}_F$.
A complete coverage of Floquet theory is well beyond the scope of this lecture. However, there are two limiting cases where we can understand what has to be done.

The resonant case

First, in the limit where the drive frequency ω is (near) resonant with a level spacing of the Hamiltonian we can apply the rotating wave approximation (RWA). Let us consider a simple example

$$H(t) = \frac{\hbar\omega_0}{2}\sigma_z + \lambda\cos(\omega t)\sigma_x. \tag{6.20}$$

We can go to a rotating frame by

$$U = P_+ + P_- e^{i\omega t} = \begin{pmatrix} 1 & 0 \\ 0 & 0 \end{pmatrix} + \begin{pmatrix} 0 & 0 \\ 0 & 1 \end{pmatrix} e^{i\omega t}. \tag{6.21}$$

We now transform

$$U^\dagger \mathcal{H}_F U = \underbrace{\begin{pmatrix} \frac{\hbar\omega_0}{2} & \frac{\lambda}{2} + \frac{\lambda}{2}e^{i2\omega t} \\ \frac{\lambda}{2} + \frac{\lambda}{2}e^{-i2\omega t} & \hbar\omega - \frac{\hbar\omega_0}{2} \end{pmatrix}}_{H_F} - i\hbar\partial_t. \tag{6.22}$$

If $\omega \approx \omega_0$ and $\lambda \ll \hbar\omega_0$, the two states are approximately degenerate and we can neglect the term $\propto \exp(2i\omega t)$ as it quickly averages to zero. Hence, we found a time-independent Hamiltonian H_F. This approximation is relevant for a resonant drive as discussed in Ref. [6].

The off-resonant case

In the second limit, where ω is much larger than any frequency in the Hamiltonian we can find H_F in a series in $1/\omega$. To this end, we expand the time-ordered product in (6.19)

$$H_F^0 = \frac{1}{T}\int_0^T dt H(t), \qquad H_F^1 = -\frac{i}{2T}\int_0^T dt \int_0^t dt' \,[H(t), H(t')]. \tag{6.23}$$

We now write $H(t)$ as a Fourier-series ($\omega = 2\pi/T$)

$$H(t) = \sum_{n\in Z} H_n e^{i\omega n t}, \tag{6.24}$$

which leads to

$$H_F^0 = H_0, \tag{6.25}$$

$$H_F^1 = \frac{1}{\omega}\sum_{n=1}^{\infty}\frac{1}{n}\left([H_n, H_{-n}] - [H_n, H_0] + [H_{-n}, H_0]\right). \tag{6.26}$$

Applying this procedure to graphene in a circularly polarized electric field, one can understand both Refs. [4] and [7].

[1] Here, we gallantly overlooked how this procedure depends on the initial time t (which we set to zero) and the phase of the periodic driving.

6.3 Publications

Study the following papers in groups of two to three students and explain them in two weeks in a short presentation:

- Quantum spin Hall effect in silicon photonics [2, 3].
- Floquet topological insulators in semi-conductors [6].
- Photonic topological insulator in coupled wave-guides [4].
- Quantum spin Hall effect for phonons [8].

References

1. Yariv, A., Xu, Y., Lee, R. K. & Schere, A. "Coupled-resonator optical waveguide: a proposal and analysis". *Optics Lett.* **24,** 711 (1999).
2. Hafezi, M., Demler, E. A., Lukin, M. D. & Taylor, J. M. "Robust optical delay lines with topological protection". *Nature Phys.* **7,** 907 (2011).
3. Hafezi, M., Mittal, S., Fan, J., Migdall, A. & Taylor, J. M. "Imaging topological edge states in silicon photonics". *Nature Photon.* **7,** 1001 (2013).
4. Rechtsman, M. C. *et al.* "Photonic Floquet topological insulators". *Nature* **496,** 196 (2013).
5. Floquet, G. "Sur les équations différentielles linéaires à coefficients périodiques". *Ann. l'Écol. Norm. Sup.* **12,** 47 (1883).
6. Lindner, N. H., Refael, G. & Galitski, V. "Floquet topological insulator in semiconductor quantum wells". *Nature Phys.* **7,** 490 (2011).
7. Jotzu, G. *et al.* "Experimental realisation of the topological Haldane model". *Nature* **515,** 237 (2014).
8. Süsstrunk, R. & Huber, S. D. "Observation of phononic helical edge states in a mechanical 'topological insulator'". *arXiv:1503.06808.* <`http://arxiv.org/abs/1503.06808`> (2015).

Chapter 7

The fractional quantum Hall effect I

Learning goals

- We are acquainted with the basic phenomenology of the fractional quantum Hall effect.
- We know the Laughlin wave function.
- We can explain the mutual statistic of Laughlin quasi-particles

- D.C. Tsui, H.L. Stormer, and A.C. Gossard, Phys. Rev. Lett. **48**, 1559 (1982)

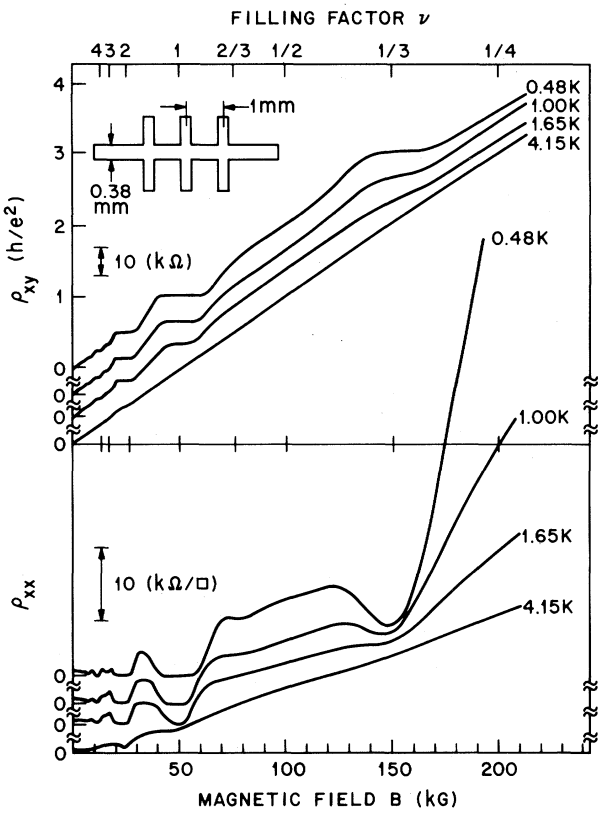

Figure 7.1: Measurements of the longitudinal and transverse resistance in a semiconductor heterostructure. At low temperatures a Hall plateau develops at a filling fraction $\nu = 1/3$ together with a dip in the transverse conductance. Figure take from Ref. [1] (Copyright (1982) by The American Physical Society).

We have seen that the Hall conductance in a large magnetic field is quantized to multiples of the quantum of conductance e^2/h. We could explain this quantization via a mapping of the linear

response expression for the Hall conductance to the calculation of the Chern number of ground state wave function. The seminal experiment of Tsui et al. showed, however, that in a very clean sample, the Hall conductance develops a fractional plateau at one third of a quantum of conductance, see Fig. 7.1. In this chapter we try to understand how this can come about and how it is compatible with our derivation of the integer-quantized Hall conductance. So far we have only dealt with free fermion systems where the ground state was a Slater determinant of single particle states. Let us start from such a ground state and see how we might understand the fractional quantum Hall effect via a wave function inspired by such a Slater determinant.

7.1 Many particle wave functions

We have seen in the exercise class that in the symmetric gauge, where $\mathbf{A} = -\frac{1}{2}\mathbf{r} \wedge \mathbf{B}$, the lowest Landau level wave function can be written as

$$\psi_m(z) \propto z^m e^{-\frac{1}{4}|z|^2}, \qquad z = \frac{1}{l}(x + iy), \qquad l = \sqrt{\frac{\hbar}{eB}}. \tag{7.1}$$

We have also seen that the m'th wave function is peaked on a ring that encircles m flux quanta. A direct consequence of (7.1) is that any function

$$\psi(z) = f(z)e^{-\frac{1}{4}|z|^2} \tag{7.2}$$

with an analytic $f(z)$ is in the lowest Landau level. Let us make use of that to address the many-body problem at fractional filling. At fractional fillings, these is no single-particle gap as the next electron can also be accommodated in the same, degenerate, Landau level. Hence, we need interactions to open up a gap. Let us assume a rotational invariant interaction, e.g., $V(r) = e^2/\epsilon r$. Moreover, we start with the two-particle problem. Requiring relative angular momentum m and total angular momentum M, the only *analytic* wave function is

$$\psi_{m,M}(z_1, z_2) = (z_1 - z_2)^m (z_1 + z_2)^M e^{-\frac{1}{4}\left(|z_1|^2 + |z_2|^2\right)}. \tag{7.3}$$

Given the azimuthal part (angular momentum), no radial problem had to be solved! The requirement to be in the lowest Landau level fixes the radial part. ⇒ All we need to know about $V(r)$ are the Haldane pseudo-potentials[1]

$$v_m = \langle Mm|V|Mm\rangle. \tag{7.4}$$

7.1.1 The quantum Hall droplet

Let us now construct the many-body state for the two-particle state centered around $z = 0$. For $\nu = 1$ we construct the Slater determinant with the orbits $m = 0, 1$

$$\psi(z_1, z_2) = f(z_1, z_2)e^{-\frac{1}{4}\sum_{j=1}^{2}|z_j|^2} \qquad \text{with} \qquad f(z_1, z_2) = \begin{vmatrix} 1 & 1 \\ z_1 & z_2 \end{vmatrix} = -(z_1 - z_2). \tag{7.5}$$

The generalization to N particles with $m = 0, \ldots, N-1$ will fill a circle of radius $\sqrt{2N}$ and f is given by the Vandermonde determinant

$$f = -\prod_{i<j}(z_i - z_j). \tag{7.6}$$

[1] If we neglect Landau level mixing!

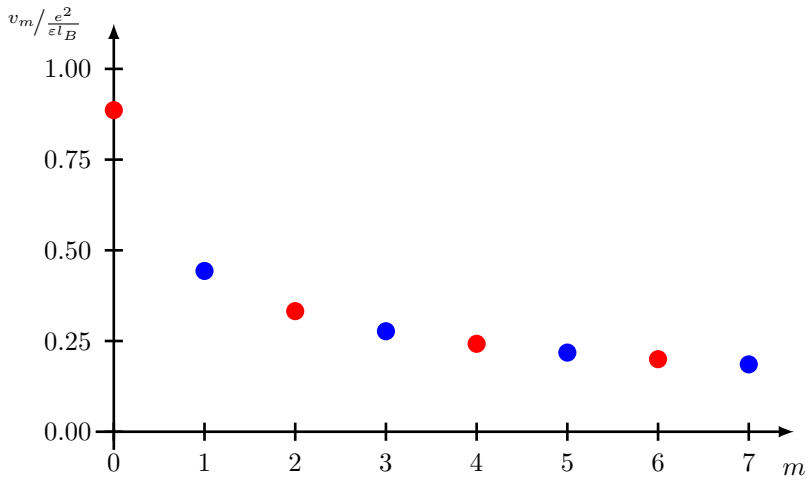

Figure 7.2: Haldane pseudo potentials for the Coulomb interaction in the lowest Landau level as a function of relative angular momentum m. The even relative angular momenta (red) are irrelevant for a fermionic system. In the following we approximate the full Coulomb potential with the first pseudo potential by setting $v_{m>1} \equiv 0$

Therefore, the many-body wave function of a filled lowest Landau level is given by

$$\psi(\{z_i\}) = \prod_{i<j}(z_i - z_j)e^{-\frac{1}{4}\sum_{j=1}^{N}|z_j|^2}. \tag{7.7}$$

Building on this form of the ground state wave function R. Laughlin made the visionary step [2] of proposing the following wave function for the one third filled Landau level[2]

$$\psi_{\mathrm{L}}(\{z_i\}) = \prod_{i<j}(z_i - z_j)^3 e^{-\frac{1}{4}\sum_{j=1}^{N}|z_j|^2}. \tag{7.8}$$

Before we embark on a detailed analysis of this wave function, let us make a few simple comments: (i) No pair of particles has a relative angular momentum $m < 3! \Rightarrow$ if we only keep the smallest non-trivial Haldane pseudo potential v_1, ψ_{L} is an exact ground state wave function in the lowest Landau level. (ii) if $g(\{z_i\})$ is a symmetric (under exchange $i \leftrightarrow j$) polynomial, then $\psi = g\psi_{\mathrm{L}}$ is also in the lowest Landau level. In particular

$$\psi_{\{w_s\}}(\{z_i\}) = \prod_{s=1}^{n}\prod_{j=1}^{N}(z_j - w_s)\psi_{\mathrm{L}}(\{z_i\}) \tag{7.9}$$

is a wave function of N particles depending on the n (two dimensional) parameters $w_n = x_n + iy_n$ and is in the lowest Landau level. We will study this generalization if the Laughlin wave-function in the following. Keep in mind that the ground-state shall be described by $\psi_{\mathrm{L}}(\{z_i\})$ and we will argue that $\psi_{\{w_s\}}(\{z_i\})$ corresponds to an excited state with quasi-holes at the positions w_s.

7.2 The plasma analogy

In order to better understand the Laughlin wave function we make use of a very helpful analogy called the "plasma analogy" [3]. We write the probability distribution in the form

$$|\psi_{\{w_s\}}(\{z_i\})|^2 = \exp\left[-6E_{\{w_s\}}(\{z_i\})\right] = e^{-\beta E}, \quad Z = \int d\mathbf{z}e^{-\beta E}, \tag{7.10}$$

[2]It is maybe interesting to state here the *full* abstract of this paper: *This Letter presents variational ground-state and excited-state wave functions which describe the condensation of a two-dimensional electron gas into a new state of matter.* Keep its length in mind when you write your Nobel paper...

with

$$E_{\{w_s\}}(\{z_i\}) = -\frac{1}{3}\sum_{sj}\log|z_j - w_s| - \sum_{i<j}\log|z_i - z_j| + \sum_j \frac{|z_j|^2}{12}. \tag{7.11}$$

We will argue in the following that $|\psi_{\{w_s\}}(\{z_i\})|^2$ is given by the Boltzmann weight if a *fake* classical plasma at inverse temperature $\beta = 6$. Note that this is just a way of interpreting a quantum mechanical wave function. There is no plasma involved. Moreover, when we speak of "charges" in the following, we mean the fake charges of our plasma analogy. When we are interested in real, electronic charges, we will calculate (electron) densities with the help of the plasma analogy. From these real electron densities we will infer the actual real charge.
Let us remind ourselves of two-dimensional electrodynamics. From Gauss' law we find

$$\int d\mathbf{s}\,\mathbf{E} = 2\pi Q \quad \Rightarrow \quad \mathbf{E}(\mathbf{r}) = \frac{Q\hat{\mathbf{r}}}{r} \quad \Rightarrow \quad \phi(\mathbf{r}) = -Q\log(r/r_0) \tag{7.12}$$

and the two dimensional Poisson equation is given by

$$\nabla\cdot\mathbf{E} = -\nabla^2\phi = 2\pi Q\delta(\mathbf{r}). \tag{7.13}$$

We can now interpret the terms in $E_{\{w_s\}}(\{z_i\})$:

1. $-\log|z_i - z_j|$: electrostatic repulsion between two unit charges (fake charges...).
2. $-\frac{1}{3}\log|z_i - w_s|$: interaction of a unit charge at z_i with a charge $1/3$ at w_s.
3. $-\nabla^2|z|^2/12 = -1/3l^2 = 2\pi\rho_{\rm b}$ with $\rho_{\rm b} = -\frac{1}{3}\frac{1}{2\pi l^2}$. Hence, $\sum_j |z_j|^2/12$ is a background potential to keep the plasma (in the absence of w_s) charge neutral (Jellium).

With these interpretations we are in the position to analyze the properties of $\psi_{\{w_s\}}(\{z_i\})$:

1. $\log r$ – interactions make density variations extremely costly. Therefore the ground state, i.e., $\psi_{\rm L}(\{z_i\})$ has uniform density:

$$\Rightarrow \rho = \frac{1}{3}\frac{1}{2\pi l^2} \Rightarrow \nu = \frac{1}{3}. \tag{7.14}$$

   This we could also have inferred from the fact that the largest monomial z_j^M appearing in $\psi_{\{w_s\}}(\{z_i\})$ has $M = 3N$. Hence, the radius of the droplet would be $\propto\sqrt{3N}$ and hence the area three times larger than for the $\nu = 1$ case.

2. Each w_s corresponds to a charge $1/3$. Therefore, it will be screened by the z-Plasma with a compensating charge $-1/3$. $\Rightarrow$ each w_s corresponds to a *quasi-hole with* $e^* = -\frac{e}{3}$.

3. The plasma analogy also allows us to find to normalization of the wave function $\psi_{\{w_s\}}(\{z_i\})$:

$$\psi_{\{w_s\}}(\{z_i\}) = C\prod_{s<p}|w_s - w_p|^{1/3}\prod_{sj}(z_j - w_s)\prod_{i<j}(z_i - z_j)^3 e^{-\sum_j\frac{|z_j|^2}{4}}e^{-\sum_s\frac{|w_s|^2}{12}}. \tag{7.15}$$

   For this normalization we find a new plasma energy

$$E = -\frac{1}{9}\sum_{s<p}\log|w_s - w_p| - \frac{1}{3}\sum_{sj}\log|z_j - w_s| - \sum_{i<j}\log|z_j - z_i| + \sum_j\frac{|z_j|^2}{12} + \sum_s\frac{|w_s|^2}{36}. \tag{7.16}$$

   We see that all "forces" between w_s, z_j are mediated by two-dimensional Coulomb electrodynamics $\Rightarrow$ all forces on w_s are screened $\Rightarrow$

$$F_{w_s} = \frac{\partial\log Z}{\partial w_s} \approx 0 \qquad \text{for} \qquad |w_s - w_p| \gg 1. \tag{7.17}$$

   Hence $Z = \int d\mathbf{z}\,|\psi|^2 = \text{const}$, and we can normalize it with an appropriate C.

Before we calculate the charge of a quasi particle in another way that highlights the relation to their mutual statistics, σ_{xy}, and eventually the ground-state degeneracy on the torus, we want to convince ourselves that ψ_{L} is describing a ground state with a gapped excitation spectrum above it: If we want to make an *electronic* excitation we have to change the relative angular momentum by one. Therefore, we will have to pay the cost v_1 corresponding to the first Haldane pseudo potential! How did ψ_{L} manage to be such a good candidate wave function? One argument is due to Halperin [3]:
Fix all z_j expect for z_i. Take z_i around the whole droplet. ψ_{L} needs to pick up an Aharonov-Bohm phase $2\pi N/\nu = 2\pi N3$. ψ_{L} must also have N zeros (whenever $z_i \to z_j$) due to the Pauli principle. $\Rightarrow$ $2N$ zeros could be somewhere else, not bound to any special particle configuration (like to the coincidence of two particles as above) to pick up the proper Aharonov-Bohm phase. However, the *Laughlin wave function does not "waste" any zeros but uses them all to avoid interactions.*

7.3 Mutual statistics

We want to move the quasi-particle described by the location w_s around and see what Aharonov-Bohm and statistical phase they pick up. For this we calculate the Berry phase

$$\phi = \oint \mathcal{A}_\mu du^\mu \qquad \text{with} \qquad \mathcal{A}_\mu = i \left\langle \psi \middle| \partial_{u^\mu} \psi \right\rangle . \tag{7.18}$$

Our "slow" parameters u^μ are the x and y coordinates of the positions w_s of the quasi-holes. There is a problem with the above formula, however: At $w_s \to w_p$, the normalized $\psi_{\{w_s\}}(\{z_i\})$ is not differentiable. In order to make it differentiable we apply a gauge transformation

$$\tilde{\psi}_{\{w_s\}}(\{z_i\}) = e^{\frac{i}{3}\sum_{s<p}\arg(w_s - w_p)} \psi_{\{w_s\}}(\{z_i\}). \tag{7.19}$$

For fixed positions $\{w_s\}$ it is clear that this amounts to a simple global phase change. However, through

$$e^{\frac{i}{3}\sum_{s<p}\arg(w_s - w_p)} = \prod_{s<p} \frac{(w_s - w_p)^{1/3}}{|w_s - w_p|^{1/3}} \tag{7.20}$$

it cures the problem with differentiability for $w_s \to w_p$ and we can use (7.18) to calculate Berry phases. Note, however, that we made $\tilde{\psi}_{\{w_s\}}(\{z_i\})$ multivalued. The requirement of global integrability necessitated this step: a phenomena we saw already in the calculation of the Chern number.
The calculation of the Berry curvature is now straight forward. We use $w_s = x_s + iy_s$ and $\bar{w}_s = x_s - iy_s$ as our coordinates. Let us start with

$$\begin{aligned} A_{\bar{w}_s} &= i \left\langle \psi \middle| \partial_{\bar{w}_s} \psi \right\rangle & (7.21)\\ &= i|C|^2 \int d\mathbf{z} \int d\bar{\mathbf{z}} \prod_{a<b} \prod_{cd} \prod_{e<f} (\bar{w}_a - \bar{w}_b)^{1/3} (\bar{w}_c - \bar{z}_d)(\bar{z}_e - \bar{z}_f)^3 e^{-\frac{\sum_g z_g \bar{z}_g}{4}} e^{-\frac{\sum_h w_h \bar{w}_h}{12}} \\ &\quad \times \partial_{\bar{w}_s} \prod_{i<j} \prod_{kl} \prod_{m<n} (w_i - w_j)^{1/3} (w_k - z_l)(z_m - z_n)^3 e^{-\frac{\sum_o z_o \bar{z}_o}{4}} e^{-\frac{\sum_p w_p \bar{w}_p}{12}} & (7.22)\\ &= -i\frac{w_s}{12}. & (7.23) \end{aligned}$$

For A_{w_s} we use the fact that our wave function is normalized

$$0 = \partial_{w_s}\langle\psi|\psi\rangle = \langle\partial_{w_s}\psi|\psi\rangle + \langle\psi|\partial_{w_s}\psi\rangle \qquad \Rightarrow A_{w_s} = \langle\psi|\partial_{w_s}\psi\rangle = -\langle\partial_{w_s}\psi|\psi\rangle. \tag{7.24}$$

The last term, however, is now easy to calculate as $\langle\psi|$ depends on w_s only through the exponential factor. Hence the calculation of A_{w_s} is analogous to the one of $A_{\bar{w}_s}$ and we find

$$A_{w_s} = i\frac{\bar{w}_s}{12}. \tag{7.25}$$

The Berry curvature is then given by

$$F_{w_s\bar{w}_s} = \partial_{w_s} A_{\bar{w}_s} - \partial_{\bar{w}_s} A_{w_s} = -\frac{i}{6}. \tag{7.26}$$

From this we can calculate the Berry phase for bringing the coordinate w_s around an area A

$$\varphi_A = -i \oiint_A dw_s d\bar{w}_s \, F_{w_s\bar{w}_s} = -\frac{1}{6} \oiint_A dxdy \frac{2}{l^2} = -\frac{\Phi_A}{3}, \tag{7.27}$$

where Φ_A is the magnetic flux through the area A. This confirms again the finding that each w_s in the wave-function $\psi_{\{w_s\}}(\{z_i\})$ describes a quasi-particle of charge

$$e^* = -\frac{e}{3}. \tag{7.28}$$

Note, that hand in hand with the appearance of a fractional charge e^*, we also picked up a non-trivial mutual statistics: If we move w_s once around w_p, we go back to the same wave-function up to a phase factor $\exp(2\pi i/3)$. This readily leads to a mutual statistical phase of $\exp(\pi i/3)$. Therefore our $e/3$ quasi-particles are neither bosons nor fermions but anyons with a statistical angle of $\pi/3$.

Figure 7.3: Mutual statistics.

To elucidate the connection between σ_{xy}, $e^* = -e/3$ and $\exp(i\pi/3)$ further we go through a Gedankenexperiment in analogy to Laughlin's pumping argument for the integer quantum Hall effect, cf. Fig 7.4. Let us consider a disk displaying the 1/3 fractional quantum Hall effect. We insert a flux quantum through a thin solenoid in the center. The induced current in radial direction is then given by

$$J_{\hat{\mathbf{r}}} = \sigma_{xy} E_{\hat{\boldsymbol{\varphi}}} = -\sigma_{xy} \frac{\partial \varphi}{\partial t}. \tag{7.29}$$

Therefore the charge accumulated on the center of the disk is given by

$$Q_{\text{center}} = \int dt \, J_{\hat{\mathbf{r}}} = -\frac{1}{3}\frac{e^2}{h} \int dt \, \frac{\partial \varphi}{\partial t} = -\frac{e}{3}. \tag{7.30}$$

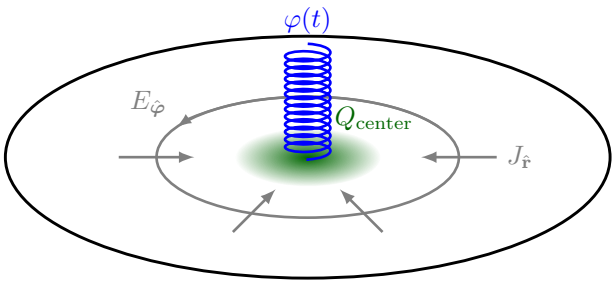

Figure 7.4: Pumping argument. Inserting a flux quantum h/e leads to an accumulation of charge $-e/3$. In the limit of an infinitely small solenoid we can gauge h/e away and we end up with a stable excitation in the form of a quasi-hole carrying one third of an electronic charge.

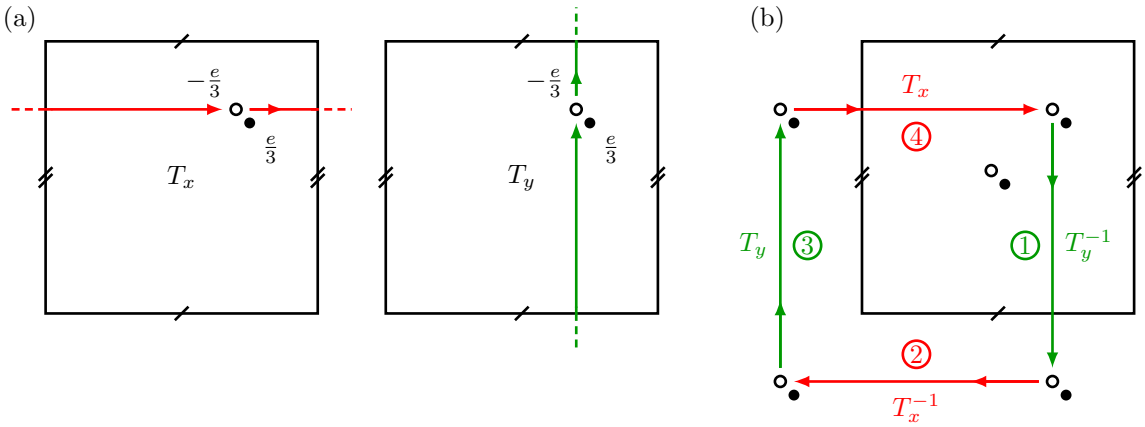

Figure 7.5: Illustration of the actions of (a) $T_{x(y)}$ and (b) $T_xT_yT_x^{-1}T_y^{-1}$ (see text).

After we inserted a full flux quantum h/e through the solenoid, we can gauge the phase away and we arrive at the same Hamiltonian. However, we do not necessarily reach the same state but we might end up in another *eigenstate* of the Hamiltonian. The accumulated charge $-e/3$ in the center must therefore be a *stable* quasi-hole after the system underwent spectral flow!
Let us bring a test quasi-hole around the solenoid: Either we think of $\exp(2\pi/3)$ as a statistical flux after we gauged away the h/e. Equivalently we can think of the additional flux of the solenoid spread over a finite area. We can then not gauge the flux away and hence we did not induce a stable quasi-hole. In contrary, the test particle accumulated a $\exp(2\pi/3)$ Aharonov-Bohm phase. This links the properties

$$\sigma_{xy} = \frac{1}{3}\frac{e^2}{h} \quad \Leftrightarrow \quad e^* = -\frac{e}{3} \quad \Leftrightarrow \quad e^{i\pi/3} - \text{anyons.} \tag{7.31}$$

7.4 Ground state degeneracy on the torus

During the discussion of the integer quantum Hall effect we found that the Hall conductivity has to be an integer multiple of e^2/h. How can we reconcile this with the fractionally quantized plateau at $\nu = 1/3$ in Fig. 7.1? The key issue was the assumption of a unique ground state on the torus with a finite gap to the first excited state. We are now proving that this is not the case of a state described by Laughlin's wave function for the $\nu = 1/3$ plateau.
Consider an operator T_x (T_y) that creates a quasi-particle – quasi-hole pair, moves the quasi-hole around the torus in x (y) direction an annihilates the two again, cf. Fig. 7.5(a). We consider now the action of $T_xT_yT_x^{-1}T_y^{-1}$. T_x shall create the pair in the middle of the chart in Fig. 7.5(b), T_y close to a corner. Moreover, the T_y movements we perform on a given chart, for the T_x movements we move the chart in the opposite direction. From this we see that one quasi-hole encircles the other! $\Rightarrow$ $T_xT_y = \exp(2\pi i/3)T_yT_x$. In addition we have the following property $T_x^3 = T_y^3 = \mathbb{1}$ as moving a full electron around the torus has to be harmless as this is what we demand for the boundary conditions.[3] The fact that $[T_x, T_y] \neq 0$ means they act on a space which is more than one-dimensional. However, they act on the ground-state manifold of the fractional quantum Hall effect on the torus. *This requires that there are several ground state sectors for the $\nu = 1/3$ state.* One can show that

$$T_x = \begin{pmatrix} 0 & 1 & 0 \\ 0 & 0 & 1 \\ 1 & 0 & 0 \end{pmatrix} \qquad T_y = \begin{pmatrix} 1 & 0 & 0 \\ 0 & e^{2\pi i/3} & 0 \\ 0 & 0 & e^{4\pi i/3} \end{pmatrix} \tag{7.32}$$

[3] Remember the gluing phase in chapter 3.

are the unique irreducible representation of the algebra defined by the above conditions. We conclude that the $\nu = 1/3$ state is threefold degenerate on the torus.
We conclude this chapter by stating that X.-G. Wen generalized the observation that ground-state degeneracy on the torus and fractional statistics are deeply linked a give rise to a new classification scheme of intrinsically topologically states (as opposed to non-interaction topological states such as the integer quantum Hall effect or more generally topological insulators) [4].

References

1. Tsui, D. C., Stormer, H. L. & Gossard, A. C. "Two-Dimensional Magnetotransport in the Extreme Quantum Limit". *Phys. Rev. Lett.* **48,** 1559 (1982).
2. Laughlin, R. B. "Anomalous Quantum Hall Effect: An Incompressible Quantum Fluid with Fractionally Charged Excitations". *Phys. Rev. Lett.* **50,** 1395 (1983).
3. Halperin, B. I. "Theory of quantized Hall conductance". *Helv. Phys. Acta* **56,** 75 (1983).
4. Wen, X.-G. "Topological orders and edge excitations in fractional quantum Hall states". *Adv. in Phys.* **44,** 405 (1995).

Chapter 8

Composite fermions

Learning goals

- We know what a coherent state path integral is.
- We know the concept of a composite fermion.
- We know how to get from composite fermions to a Chern-Simons theory.

- Willett, R. et al., Phys. Rev. Lett. **59**, 1776 (1987)

8.1 Path integrals

8.1.1 Why do we need a path integral

In this section we try to argue why we need a path integral representation of the partition sum

$$Z = \int D[\bar{\phi}\phi] e^{-S[\bar{\phi},\phi]}. \tag{8.1}$$

First of all, we trade non-commuting bosonic *operators* with an integral over all "field" configurations, i.e.,

$$[.,.] \to D[\bar{\phi},\phi]. \tag{8.2}$$

Moreover, we replace complicated anti-commutations for fermions we a simple tool called Grassmann numbers. Before we are going to explain what we exactly mean with expression (8.1), we list a few nice properties that we will gain from a path integral formalism.

1. We can use Gaussian integrals

$$\int D[\bar{\phi}\phi] e^{-\bar{\phi}^{\mathrm{T}} A\phi} = \frac{1}{\det A}. \tag{8.3}$$

2. We can complete the square

$$\int D[\bar{\phi}\phi] e^{-\bar{\phi}^{\mathrm{T}} A\phi + \vartheta^{\mathrm{T}}\bar{\phi} + \bar{\vartheta}^{\mathrm{T}}\phi} = \int D[\bar{\phi}\phi] e^{-(\bar{\phi}-A^{-1}\bar{\vartheta})^{\mathrm{T}} A(\phi - A^{-1}\vartheta) + \bar{\vartheta}^{\mathrm{T}} A^{-1}\vartheta} = \frac{e^{\bar{\vartheta}^{\mathrm{T}} A^{-1}\vartheta}}{\det A}. \tag{8.4}$$

   This completing of the square in turn has three important applications:

   (a) Greens functions (or more generally, two-point correlators) in a quadratic theory can be calculated by coupling sources ϑ

$$\langle \bar{\phi}_i \phi_j \rangle = \frac{\int D[\bar{\phi}\phi] \bar{\phi}_i \phi_j e^{-S[\bar{\phi},\phi]}}{\int D[\bar{\phi}\phi] e^{-S[\bar{\phi},\phi]}} = \frac{\delta^2}{\delta\vartheta_i \delta\bar{\vartheta}_j}\bigg|_{\vartheta=\bar{\vartheta}=0} e^{\bar{\vartheta}^{\mathrm{T}} A^{-1}\vartheta} = [A^{-1}]_{ij}. \tag{8.5}$$

(b) "Integrating out" linearly coupled quadratic degrees of freedom

$$\int D[\bar{\phi}\phi]D[\bar{\vartheta}\vartheta]e^{-S[\bar{\phi},\phi]+\phi^{\mathrm{T}}\bar{\vartheta}+\bar{\phi}^{\mathrm{T}}\vartheta-\bar{\vartheta}^{\mathrm{T}}B\vartheta} = \int D[\bar{\phi}\phi]e^{-S[\bar{\phi},\phi]+\bar{\phi}^{\mathrm{T}}B^{-1}\phi} = \int D[\bar{\phi}\phi]e^{-S_{\mathrm{eff}}[\bar{\phi},\phi]}. \quad (8.6)$$

(c) Or the reverse of it, called *Hubbard Stratonovich transformation*

$$\int D[\bar{\phi}\phi]e^{-\bar{\phi}^{\mathrm{T}}A\phi+\bar{\phi}^{\mathrm{T}}\phi\bar{\phi}^{\mathrm{T}}\phi} = \int D[\bar{\phi}\phi]D[\vartheta]e^{-(\bar{\vartheta}-\bar{\phi}^{\mathrm{T}}\phi)(\vartheta-\bar{\phi}^{\mathrm{T}}\phi)-\phi^{\mathrm{T}}A\phi+\bar{\phi}^{\mathrm{T}}\phi\bar{\phi}^{\mathrm{T}}\phi} \quad (8.7)$$

$$= \int D[\bar{\phi}\phi]D[\vartheta]e^{-\bar{\vartheta}\vartheta+2\vartheta\bar{\phi}^{\mathrm{T}}\phi-\bar{\phi}^{\mathrm{T}}\phi\bar{\phi}^{\mathrm{T}}\phi-\bar{\phi}^{\mathrm{T}}A\phi+\bar{\phi}^{\mathrm{T}}\phi\bar{\phi}^{\mathrm{T}}\phi} \quad (8.8)$$

$$= \int D[\bar{\phi}\phi]D[\vartheta]e^{-\bar{\vartheta}\vartheta-\bar{\phi}^{\mathrm{T}}(A+2\vartheta)\phi} \quad (8.9)$$

$$= \int D[\vartheta]e^{-\bar{\vartheta}\vartheta-\mathrm{tr}\log[A+2\vartheta]}. \quad (8.10)$$

This is still not a quadratic theory, but the logarithm can be expanded step by step to get an effective theory.

3. We can do mean-field calculations

$$\frac{\delta S[\bar{\phi},\phi]}{\delta\bar{\phi}} = 0 \qquad \Rightarrow \qquad \phi_{\mathrm{MF}}. \quad (8.11)$$

After all these expected profits, let us start introducing such a path integral representation of the partition sum.

8.1.2 Coherent state path integral

Given a quantum mechanical problem defined by a Hamiltonian H, we want to express the partition sum

$$Z = \mathrm{tr}e^{-\beta H} = \sum_n \langle m|e^{-\beta H}|m\rangle, \quad (8.12)$$

as a path integral. For this we use coherent states

$$|\phi\rangle = e^{\eta\sum_i \phi_i c_i^\dagger}|\mathrm{vac}\rangle \quad \Rightarrow c_i|\phi\rangle = \phi_i|\phi\rangle, \quad (8.13)$$

and we used $\eta = \pm 1$ for bosons (fermions), respectively. Remember that they are not orthogonal

$$\langle\phi|\vartheta\rangle = e^{\bar{\phi}^{\mathrm{T}}\vartheta}. \quad (8.14)$$

For bosons, $\phi_i \in \mathbb{C}$. For fermions we need to take care of anti-commutations. This can be achieved by requiring ϕ_i to be Grassmann numbers.
Grassmann numbers are defined by

$$\phi_i\phi_j = -\phi_j\phi_i; \quad \partial_{\phi_i}\phi_j = 0; \quad \int d\phi_i = 0; \quad \int d\phi_i\phi_i = 1. \quad (8.15)$$

From this follows immediately

$$\int d\bar{\phi}_i d\phi_i\, e^{-\bar{\phi}_i a\phi_i} = \int d\bar{\phi}_i d\phi_i\,[1-\phi_i\phi_i a] = a. \quad (8.16)$$

Which immediately leads to

$$\int d(\bar{\phi}\phi)\, e^{-\bar{\phi}^{\mathrm{T}}A\phi} = \prod_n \int d\bar{\phi}_n d\phi_n\, e^{-\sum_{rs}\bar{\phi}_r A_{rs}\phi_s} = \det A. \quad (8.17)$$

Note that this is similar to the bosonic case, however $[\det A]^{-1}$ is replaced with $\det A$.
With the help of the coherent states $|\phi\rangle$ we can now write a complicated but tremendously useful resolution of the unity

$$\mathbb{1} = \int d(\bar{\phi}\phi)\, e^{-\bar{\phi}^{\mathrm{T}}\phi} |\phi\rangle\langle\phi|. \tag{8.18}$$

To proof this identity, we have to show that c_i and $c_i^\dagger$ commute with the right-hand side:

$$c_i \int d(\bar{\phi}\phi)\, e^{-\bar{\phi}^{\mathrm{T}}\phi} |\phi\rangle\langle\phi| = \int d(\bar{\phi}\phi)\, e^{-\bar{\phi}^{\mathrm{T}}\phi} c_i |\phi\rangle\langle\phi| = \int d(\bar{\phi}\phi)\, e^{-\bar{\phi}^{\mathrm{T}}\phi} \phi_i |\phi\rangle\langle\phi| \tag{8.19}$$

$$= -\int d(\bar{\phi}\phi)\, [\partial_{\bar{\phi}_i} e^{-\bar{\phi}^{\mathrm{T}}\phi}] |\phi\rangle\langle\phi| \tag{8.20}$$

$$\overset{\text{P.I.}}{=} \int d(\bar{\phi}\phi)\, e^{-\bar{\phi}^{\mathrm{T}}\phi} [\underbrace{(\partial_{\bar{\phi}_i}|\phi\rangle)}_{=0}\langle\phi| + |\phi\rangle(\partial_{\bar{\phi}_i}\langle\phi|)] \tag{8.21}$$

$$= \int d(\bar{\phi}\phi)\, e^{-\bar{\phi}^{\mathrm{T}}\phi} |\phi\rangle\langle\phi| c_i. \tag{8.22}$$

In the last line we used

$$c_i^\dagger |\phi\rangle = \partial_{\phi_i} |\phi\rangle \qquad \Rightarrow \qquad \partial_{\phi_i}\langle\phi| = \langle\phi_i| a_i. \tag{8.23}$$

With this we showed that c_i indeed commutes with the alleged unity. For $c_i^\dagger$ one starts from the other end end and goes through the same manipulations (show!). As all operators in the Fock space can be written as products (and sums) of the creation and annihilation operators, we have shown that indeed

$$\int d(\bar{\phi}\phi)\, e^{-\bar{\phi}^{\mathrm{T}}\phi} |\phi\rangle\langle\phi| \propto \mathbb{1}. \tag{8.24}$$

Let us check for the proportionality factor

$$\langle \mathrm{vac}|\mathbb{1}|\mathrm{vac}\rangle = 1 = \int d(\bar{\phi}\phi)\, e^{-\bar{\phi}^{\mathrm{T}}\phi} \langle \mathrm{vac}|\phi\rangle\langle\phi|\mathrm{vac}\rangle. \tag{8.25}$$

Let us now rewrite the trace in the partition sum

$$Z = \sum_n \langle n|e^{-\beta H}|n\rangle = \int d(\bar{\phi}\phi) \sum_n \langle n|\phi\rangle\langle\phi|e^{-\beta H}|n\rangle e^{-\bar{\phi}^{\mathrm{T}}\phi} \tag{8.26}$$

$$= \int d(\bar{\phi}\phi)\, e^{-\bar{\phi}^{\mathrm{T}}\phi} \sum_n \langle \eta\phi|n\rangle\langle n|e^{-\beta H}|\phi\rangle = \int d(\bar{\phi}\phi)\, e^{-\bar{\phi}^{\mathrm{T}}\phi} \langle \eta\phi|e^{-\beta H}|\phi\rangle. \tag{8.27}$$

Now we need to fix an important property. In order for our path integral approach to go through, we need to normal order our Hamiltonian. This means, we arrange all operators in H such that all $c_i^\dagger$ stand to the left of all c_i. As the fields ϕ_i are just complex numbers (for bosons, at least), this will be the last time we can take care of the operator nature of second quantized quantum mechanics. We write for the normal ordered Hamiltonian explicitly

$$Z = \int d(\bar{\phi}\phi)\, e^{-\bar{\phi}^{\mathrm{T}}\phi} \langle \eta\phi|e^{-\beta H(c^\dagger, c)}|\phi\rangle. \tag{8.28}$$

Next, we re-write

$$\beta H(c^\dagger, c) = \frac{\beta}{N} \sum_{i=1}^{N} H(c^\dagger, c) \tag{8.29}$$

and we insert a unity in between all resulting factors

$$Z = \int_{\phi^1 = \eta\phi^N,\, \bar{\phi}^1 = \eta\bar{\phi}^N} \prod_{i=1}^{N} d(\bar{\phi}^i\phi^i) e^{\frac{\beta}{N}\sum_{i=1}^{N} \frac{(\bar{\phi}^i - \bar{\phi}^{i+1})\phi^i}{\beta/N} + H(\bar{\phi}^i, \phi^i)}. \tag{8.30}$$

Note that the superscript i labels the i'th insertion of the unity. One often calls β the "imaginary time" in relation to the real time propagator $\exp(itH)$. Within this interpretation, i corresponds to the i'th time slice. If we now take the limit $N \to \infty$, we are taking a continuum limit in imaginary time where

$$\phi^i \to \phi(\tau) \qquad \text{and} \qquad \frac{\beta}{N}\sum_i \to \int_0^\beta d\tau. \tag{8.31}$$

We can now write down our sought path integral

$$Z = \int D[\bar{\phi}\phi] e^{-S[\bar{\phi},\phi]}, \tag{8.32}$$

$$S[\bar{\phi},\phi] = \int_0^\beta d\tau\, \bar{\phi}^{\mathrm{T}}\partial_\tau \phi + H(\bar{\phi},\phi), \tag{8.33}$$

$$D[\bar{\phi},\phi] = \lim_{N\to\infty}\prod_{i=1}^N d(\bar{\phi}^i\phi^i); \quad \bar{\phi}(0) = \eta\bar{\phi}(\beta), \;\; \phi(0) = \eta\phi(\beta). \tag{8.34}$$

8.1.3 Kubo formula

We already got acquainted with the Kubo formula in Chap. 3. We want to revisit here in the language of our newly introduced coherent state path integral. Imagine a "force" $F(\mathbf{r},\omega)$ coupled to the "coordinate"

$$\hat{X} = \sum_{\alpha\beta} c_\alpha^\dagger X_{\alpha\beta} c_\beta. \tag{8.35}$$

We then ask for the linear response coefficient

$$X(\mathbf{r},\omega) = \int dr' \chi(\mathbf{r}-\mathbf{r}',\omega) F(\mathbf{r}',\omega). \tag{8.36}$$

In path integral formalism the expetation value on the right hand side is expressed as

$$X(\tau) = \sum_{\alpha\beta} \langle \bar{\phi}_\alpha(\tau) X_{\alpha\beta}\phi_\beta(\tau)\rangle_F, \tag{8.37}$$

where the subscript F indicates that we have to evaluate this expression in the presence of the force F

$$\delta S_F = \int_0^\beta d\tau\, F(\tau)\bar{\phi}_\alpha(\tau) X_{\alpha\beta}\phi_\beta(\tau). \tag{8.38}$$

To generate the expectation value (8.37) we can add another ficticious force F' to the action

$$\delta S_{F'} = \int_0^\beta d\tau\, F'(\tau)\bar{\phi}_\alpha(\tau) X'_{\alpha\beta}\phi_\beta(\tau). \tag{8.39}$$

With this addition, one can write

$$X(\tau) = -\frac{\delta}{\delta F'(\tau)}\Big|_{F'=0} \log(Z[F,F']). \tag{8.40}$$

For the sake of linear response, we imagine F to be small. Therefore, we can apply a Taylor expansion

$$X(\tau) = \int d\tau' \left[\frac{\delta^2}{\delta F'(\tau)\delta F(\tau')}\bigg|_{F=F'=0} \log(Z[F,F'])\right] F(\tau') \tag{8.41}$$

With this expression we can immediately indentify the linear response coeffiecient. If we assume at $X(\tau) = 0$ in the absence of the for

$$\chi(\tau,\tau') = -\frac{1}{Z}\frac{\delta^2}{\delta F'(\tau)\delta F(\tau')}\bigg|_{F=F'=0} Z[F,F']. \tag{8.42}$$

Electromagnetic response

We consider a system subject to an electromagnetic field $A^\mu = (i\varphi, \mathbf{A})$. The system might react via a redistribution of charge ρ or via an onset of a current $\mathbf{j}$. We write $j_\mu = (i\rho, \mathbf{j})$ and look for

$$j_\mu(x) = \int_{t'<t} dx' K_{\mu\nu}(x - x') A^\nu(x'), \tag{8.43}$$

where x describes the four-coordinate $(it, \mathbf{x})$. We remember that we coupled the A^μ-field as $j_\mu A^\mu$ to the Hamiltonian. Therefore,

$$j_\mu = \frac{\delta S}{\delta A^\mu} \qquad \Rightarrow \qquad F = F' = A^\mu. \tag{8.44}$$

With this we find

$$K_{\mu\nu}(x - x') = -\frac{1}{Z} \frac{\delta^2}{\delta A^\mu(x) \delta A^\nu(x')} Z[A^\mu]. \tag{8.45}$$

Effective theories

If we have a system of charged particles, $H(c^\dagger, c)$, and we are intersted in its electro-magnetic response, all we need to know is $K_{\mu\nu}$. In a path integral language, we say we *integrate out the fermions* to obtain an *effective action* in terms of th A^μ-field alone. The peculiar structure of $K_{\mu\nu}$ will fully describe our system in terms of its electro-mangetic system

$$S_{\text{eff}}[A^\mu] = \int_0^\beta d\tau \int dx dx' \, A^\mu(x) K_{\mu\nu}(x - x') A^\nu(x'). \tag{8.46}$$

8.2 Composite fermions

8.2.1 From a wave functions to a field theory

In the last chapter we got to know the Laughlin wave function for filling fractions $\nu = \frac{1}{2p+1}$ with $p \in \mathbb{N}$

$$\psi(\{z_i\}) = \prod_{i<j} (z_i - z_j)^{\frac{1}{\nu}} e^{-\frac{1}{4}\sum_i |z_i|^2}. \tag{8.47}$$

These wave functions are manifestly in the lowest Landau level and in addition to the $(z_i - z_j)^1$ term needed for the Pauli principle three are two (for $\nu = 1/3$) more zeros attached to the conincidence of two particles. This observation is identical to attaching $1/\nu - 1$ fluxes of 2π to each particle[1]

In the last chapter, we only considered the Laughlin wave function and analyzed its properties. Here, we follow a more ambitious goal. Building on the insight gain throught the Laughlin wave function, we want to construct an effective theory for the fractional quantum Hall effect including the Hamiltonian! However, we want to assume that the important players are not electrons, but the "bound states of electrons with statistical fluxes" that were at the heart of the Laughlin wave function. In other words, we want to go from an electron wave function (theory), to one of *composite fermions* by

$$\psi(\{\mathbf{x}_i\}) \mapsto \psi(\{\mathbf{x}_i\}) e^{2is\sum_{i<j} \arg(\mathbf{x}_i - \mathbf{x}_j)} \quad \text{with} \quad s \in \mathbb{Z}. \tag{8.49}$$

[1] Up to the fact that a pure flux attachement would require a factor

$$e^{-2i\sum_{i<j} \arg(z_i - z_j)} = \prod_{i<j} \frac{(z_i - z_j)^2}{|z_i - z_j|^2}. \tag{8.48}$$

The absence of the factor $1/|z_i - z_j|^2$ in the Laughlin wave function can be seen as the effect of the projection to the lowest Landau level.

This amounts to attaching $2s$ phase vortices to each electron[2]

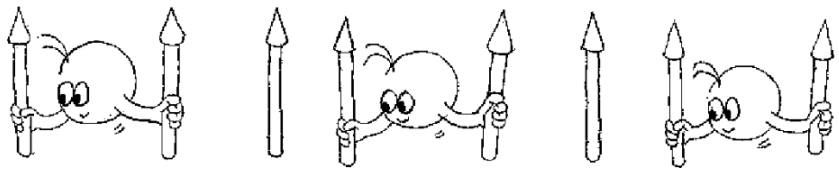

Our task is now to find a many-body theory formulated in terms of this new degrees of freedom. In a second quantized version, Eq (8.49) looks like

$$c^\dagger(\mathbf{x}) \quad \mapsto \quad c^\dagger(\mathbf{x}) \exp\left[-2is\int d\mathbf{x}' \arg(\mathbf{x}-\mathbf{x}')\rho(\mathbf{x}')\right]. \tag{8.50}$$

Substituted into the Hamiltonian this leads to

$$H \quad \mapsto \quad \int d\mathbf{x}\, c^\dagger(\mathbf{x}) \left[\frac{1}{2m}\left(-\partial_{\mathbf{x}} + \hat{\mathbf{A}}(\mathbf{x})\right)^2 + V(\mathbf{x})\right] c(\mathbf{x}) + H_{\rm int}[\rho], \tag{8.51}$$

where

$$\hat{\mathbf{A}}(\mathbf{x}) = \mathbf{A}_{\rm ext}(\mathbf{x}) + \hat{\mathbf{a}}(\mathbf{x}) \quad \text{with} \quad \hat{\mathbf{a}}(\mathbf{x}) = -2s\int d\mathbf{x}' \, \frac{(x_1-x_1')\hat{\mathbf{x}}_1 + (x_2-x_2')\hat{\mathbf{x}}_2}{|\mathbf{x}-\mathbf{x}'|^2}\rho(\mathbf{x}'). \tag{8.52}$$

This is very annoying! The kinetic energy operator became highly non-local and depends on six! operators. Let us fix this. We can relocate the condition (8.52) to another place in the action. Two observations are needed for this:

(i) Eq. (8.52) us only giving rise to the transversal part of $\mathbf{A}$: $\hat{\mathbf{a}} = \hat{\mathbf{a}}_\perp$ as $\sum_i \partial_i \hat{a}_i = 0$.

(ii) $b = \epsilon^{ij}\partial_i a_{\perp,j}$ fulfills $b = -4\pi s\rho(\mathbf{x})$.

Using these two observations we can write

$$Z = \int D[\bar\psi\psi]D[a_\perp]D[\phi] e^{iS_{\rm CF}[\bar\psi,\psi,a_\perp,\phi] + i\frac{\Theta}{2}S'_{\rm CS}[a_\perp,\phi]}, \tag{8.53}$$

where $\Theta = 1/2\pi s$. Furthermore,

$$S_{\rm CF}[\bar\psi,\psi,a_\perp,\phi] = \int d\mathbf{x}\int dt\,\bar\psi\left[i\partial_t + \mu - \phi + \frac{1}{2m}\left(-i\partial_{\mathbf{x}} + \hat{\mathbf{A}}\right)^2 - V\right]\psi + S_{\rm int}[\bar\psi,\psi]. \tag{8.54}$$

$$S'_{\rm CS}[a_\perp,\phi] = -\int d\mathbf{x}\int dt\,\phi\,\underbrace{\epsilon_{ij}\partial_i a_{\perp,j}}_{b}. \tag{8.55}$$

$\hat{\mathbf{A}}$ is still given by $\mathbf{A}_{\rm ext} + \hat{\mathbf{a}}$, but the constraint (8.52) is replaced by teh functional δ-fucntion

$$\int D[\phi] e^{i\int d\mathbf{x}\int dt\,\phi\left(\frac{b}{4\pi s}+\rho\right)}. \tag{8.56}$$

With this we are almost done. We see that $a_\perp = (\phi, \mathbf{a}_\perp)$ enters Z like a gauge field. However, $S'_{\rm CS}$ is not gauge invariant. Hence, we propose to use

$$S_{\rm CS}[a] = -\int dx^\mu \epsilon_{\mu\nu\sigma} a^\mu \partial_\nu a^\sigma. \tag{8.57}$$

with $x^\mu = (x^0, x^1, x^2)$; $\partial_\mu = (-\partial_0, \partial_1, \partial_2)$ wich is gauge invariant. The old $S'_{\rm CS}$ is nothing but $S_{\rm CS}$ evaluated in the Coulomb gauge $\partial_\mu a^\mu = 0$. Therefore, our full effective theory is now given by

$$Z = \int D[\bar\psi\psi]D[a]\exp\left\{iS_{\rm CF}[\bar\psi,\psi,a] + i\frac{\Theta}{4}S_{\rm CS}[a]\right\}, \tag{8.58}$$

with

$$S_{\rm CF}[\bar\psi,\psi,a] = \int d\mathbf{x}\int dt\,\bar\psi\left[i\partial_t + \mu - \phi + \frac{1}{2m}\left(-i\partial_{\mathbf{x}} + \mathbf{A}_{\rm ext} - \mathbf{a}\right)^2 - V\right]\psi + S_{\rm int}[\bar\psi,\psi]. \tag{8.59}$$

[2]Cartoon due Kwon Park.

8.2.2 Analyzing the composite fermion Chern-Simons theory

Before we emabark on the analysis of the above effective theory, let us make a hand-waving mean-field analysis. We see that for $s = 1$, each electron binds two flux quanta. If we *assume* the density to be homogeneous (recall the plasma analogy for the Laughlin wave function), and if we neglect fluctutations, then the electrons see *on average* a flux corresponding to $\mathbf{A}_{\rm ext} - \langle \mathbf{a} \rangle$. In other words, the composite fermions see a smaller $\mathbf{B}$-field! Several scenarios are possbile

(i) $\mathbf{A}_{\rm ext} = \langle \mathbf{a} \rangle \;\Rightarrow$ no magnetic field. This happens at $\nu = 1/2$. The fact that the the composite fermion prediction at $\nu = 1/2$ looks like a Fermi liquid is one of the great successes of the composite fermion construction [1].

(ii) Maybe, for some filling fraction ν, the effective $\mathbf{B}$-field corrsponding to $\mathbf{A}_{\rm ext} - \langle \mathbf{a} \rangle$ leads to an effective new filling fraction $\nu^* \in \mathbb{Z}$, i.e., the fractional quantum Hall effect for electrons would be mapped to an integer quantum Hall effect for composite fermions.

We are now trying to analyze the composite-fermion Chern-Simons (CF-CS) theory in mean-field. The only term which gives a real headache is the interaction term $S_{\rm int}[\bar\psi, \psi]$. We re-write it using a Hubbard-Stratnovich transformation

$$e^{iS_{\rm int}} = \int D[\sigma] \exp\left\{ \frac{i}{2} \int dx^3 dx'^3 \, \sigma(x) [V^{-1}](x,x') \delta(x_0 - x_0') \sigma(x') + i \int dx^3 (\rho(x) - \rho_0) \sigma(x) \right\}. \tag{8.60}$$

For the interpretation of the σ-field it helps to note that when completing the square, it appears as next to $\bar\psi\psi$, hence it describes a (rescaled) density field.[3] Now ψ and $\bar\psi$ (and $\rho = \bar\psi\psi$) only appear quadratically (linearly) in the action and we can integrate out $\bar\psi, \psi$. With this we obtain an effective theory

$$S_{\rm eff}[\sigma, a] = \underbrace{-i \,\mathrm{tr}\log\left[i\partial_0 + \mu - a_0 - \sigma + \frac{1}{2m}(-i\nabla + A)^2 \right]}_{S_\psi[a,A]} \tag{8.61}$$

$$- \rho_0 \int dx^3 \, \sigma(x) + \frac{1}{2} \int dx^3 dx'^3 \, \sigma(x) [V^{-1}](x,x') \delta(x_0 - x_0') \sigma(x') \tag{8.62}$$

$$+ \frac{\Theta}{4} S_{\rm CS}[a], \tag{8.63}$$

where $A = A_{\rm ext} + a$. The first line arises from integrating out the fermions ψ. On this effective theory we want to apply a mean-field, or saddle-point, approximation. As there are no ψ-fields present anymore, it can be difficult to interpret the different terms in the theory. To provide remedy to this problem, we note that the local density of fermions is given by taking the derivative of the original fermionic action with respect to $a_0(x)$. This property obviously survives the elimination of the ψ field. Therefore, we can get an "effective" expression for the density by

$$\frac{\delta S_\psi}{\delta a_0} = \rho[a, \sigma]. \tag{8.64}$$

Therefore,

$$\rho[a,\sigma] = \left[i\partial_0 + \mu - a_0 - \sigma + \frac{1}{2m}(-i\nabla + A)^2 \right]^{-1} (x,x). \tag{8.65}$$

Next, let us write down the saddle-point (Euler-Lagrange) equations. We start with

$$\left. \frac{\delta S_{\rm eff}}{\delta a_o} \right|_{\bar\sigma, \bar a} = 0 : \qquad \rho[\bar a, \bar\sigma] = \frac{1}{4\pi s} \bar b. \tag{8.66}$$

[3] We also say that we decouple the action in the density-density channel.

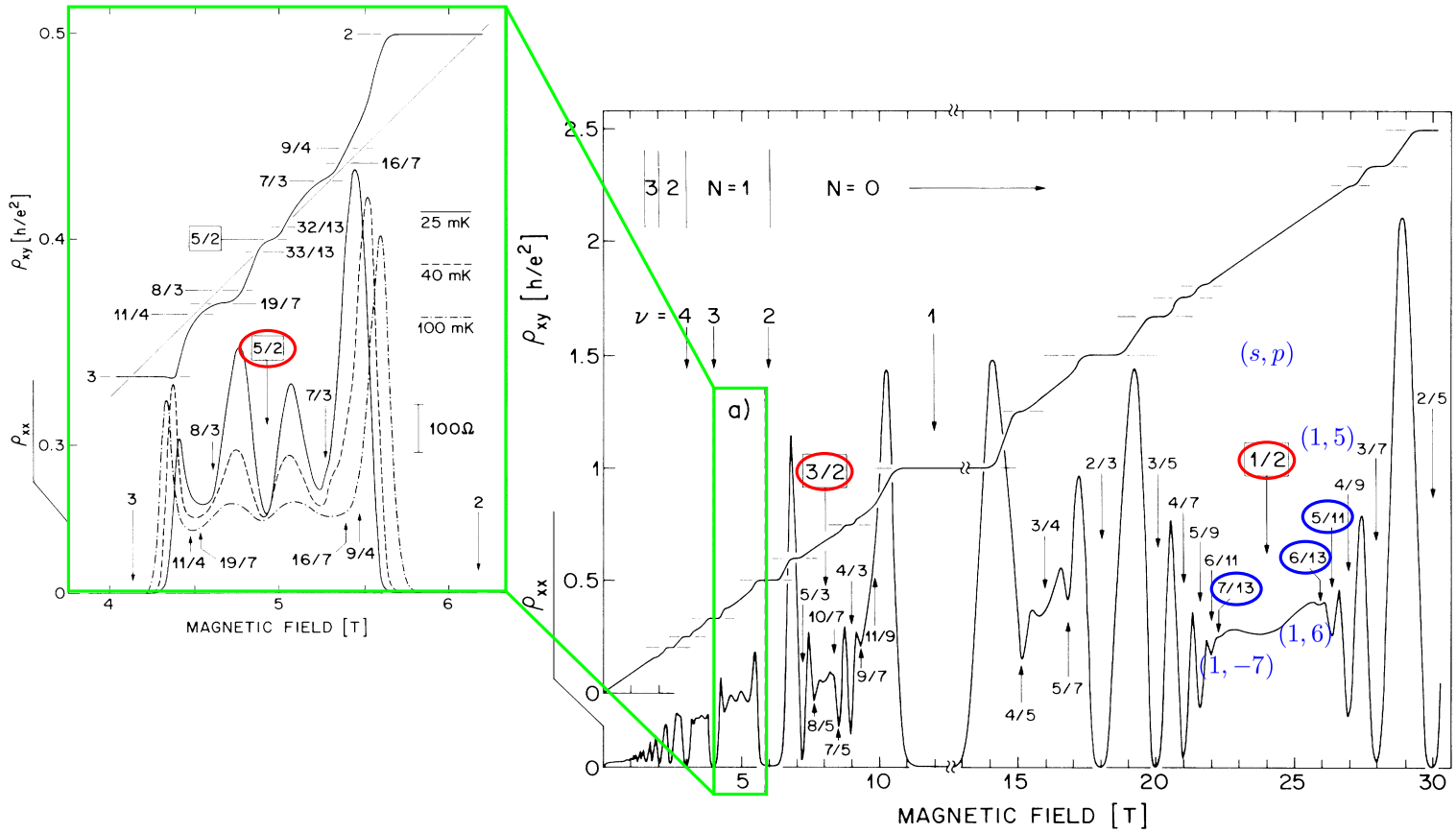

Figure 8.1: Overview of diagonal resistivity ρ_{xx} and Hall resistance ρ_{xy}. The blue numbers denote the fractions which are well explained by an integer quantum Hall plateau of composite fermions. The inset shows the details around $\nu = 5/2$. Figure adapted from Ref. [2] (Copyright (1987) by The American Physical Society).

This is nothing but the expected relation between the $\bar{b}$ field and the density.[4]
Next, we also need to minimize the action with respect to the field σ

$$\frac{\delta S_{\text{eff}}}{\delta \sigma}\Big|_{\bar{\sigma},\bar{a}} = 0 \qquad \Rightarrow \qquad \rho(x) - \rho_0 = -\int dx'^3 [V^{-1}](x,x')\sigma(x')\delta(x_0 - x_0'), \tag{8.67}$$

or

$$\sigma(x) = -\int dx'^3 V(x-x')[\rho(x') - \rho_0]\big|_{x_0'=x_0}. \tag{8.68}$$

Here we recognize that deviations of $\rho(x)$ from its mean value give rise to an "interaction potential" $\sigma(x)$. We can solve the mean-field equations by

$$\rho[\bar{a},0] = \rho_0 \tag{8.69}$$

$$\bar{\sigma} = \bar{a} = 0 \tag{8.70}$$

$$\bar{b} = 4\pi s\rho_0 \quad \Rightarrow \mathbf{a} = 2s\nu \mathbf{A}_{\text{ext}}. \tag{8.71}$$

When can we expect this mean-field calculation to be reliable? Certainly, if the resulting ground-state is gapped, we can hope that fluctuations around the mean-field solutions will not do too much harm. One way to ensure a gapped mean-field solution is by asking for the effective $A - A_{\text{ext}} - a$ to give rise to a *filled effective Landau level*. Therefore we ask

$$\nu_{\text{eff}} = p \quad \text{or} \quad \Phi_{\text{eff}} = \frac{2\pi N}{p} \quad \text{with} \quad \Phi_{\text{eff}} = (B_{\text{ext}} - \bar{b})L^2. \tag{8.72}$$

Inserting $b = 4\pi s N/L^2$ we immediately obtain

$$\nu = \frac{2\pi N}{B_{\text{ext}}L^2} = \frac{2\pi N}{\frac{2\pi N}{p} + 4\pi s N} \qquad \Rightarrow \qquad \nu = \frac{p}{1+2sp}. \tag{8.73}$$

We can summarize the mean-field discussion with the following list and Fig. 8.1

(i) We can explain many fractions which are symmetrically distributed around $1/2s$ by an integer quantum Hall effect for composite fermions. Note, however, that the gap is entirely due to interactions!

(ii) For $\nu = p/2s$, CF-CS predicts a Fermi-liquid theory in $B_{\text{eff}} = 0$

  (a) This seems to describe $\nu = 1/2$ well [1].

  (b) For $3/2 = 1/2+1$ and $5/2 = 1/2+2$ one could have expected the same Fermi-liquid as they are nothing but the $1/2$ plateaus in higher (real) Landau levels. This is however not the case. One can imagine that in these cases, residual interactions beyond the mean-field descriptions lead to an instability of the Fermi surface.

8.2.3 Fluctuations around the mean-field solution

We want to take a step beyond the mean-field considerations. For this, let us expand $S[a,A]$ to second order in a.[5]
We could take the CF-CS action and expand to leading order around $\bar{a}$. However, we can do a much simpler thing. Let us just say that

$$S^{(2)}[a,A] = \frac{1}{2}\int dx^3 dx'^3\, (A+a)^\mu(x) K_{\mu\nu}(x-x')(A+a)^\nu(x') + \frac{\Theta}{4} S_{\text{CS}}[a]. \tag{8.74}$$

Without actually calculating $K_{\mu\nu}$, we try to constrain it from general considerations

[4] Check that the minimization of the action with respect to a_1 and a_2 only provides the continuity equation of the density and does not give any further constraints in the mean-field value of a.

[5] Why not in σ?

- $K_{\mu\nu}$ has to be gauge invariant.
- $K_{\mu\nu}(q)$ can be expanded in q.
- Via the Kubo formula (8.46), we know that $K_{\mu\nu}$ encodes the electromagnetic response.

We know that $\sigma_{11} = 0$ due to the gap for composite fermions. The transverse response, σ_{12}, however, can be non-zero. Recall, that

$$\sigma_{12} = -i \lim_{\mathbf{q}\to 0} \frac{1}{\omega} K_{12}(\omega, \mathbf{q}). \tag{8.75}$$

From this we conclude that we have

$$K_{\mu\nu} = -i\sigma_{12}^{(0)} \epsilon_{\mu\sigma\nu} q_\sigma. \tag{8.76}$$

Here $\sigma_{12}^{(0)}$ denotes the composite fermion mean-field value for the transverse response. Inserted into the expression for $S^{(2)}[a, A]$ we find

$$S^{(2)}[a, A] = \frac{\sigma_{12}^{(0)}}{2} S_{\text{CS}}[a + A] + \frac{\Theta}{4} S_{\text{CS}}[a]. \tag{8.77}$$

This effective action is clearly (i) gauge invariant, (ii) the lowest order expansion in q, and (iii) provides $K_{\mu\nu}$ that reproduces the electromagnetic of the effective theory. Actually, we would expect that

$$\frac{\delta^2 Z}{\delta A_\mu \delta A_\nu} \tag{8.78}$$

provides us with the desired response function. However, this is only true after we integrated out the fluctuations in a! What we need in the following is the formula valid for quadratic actions (Show!)

$$\int D[a]\, e^{c_1 S[a+b] + c_2 S[b]} = e^{\frac{1}{\frac{1}{c_1} + \frac{1}{c_2}} S[b]}. \tag{8.79}$$

Using this formula we obtain after integrating over the field a

$$S_{\text{eff}}[A] = \frac{1}{\frac{1}{\sigma_{12}^0} + \frac{2}{\Theta}} S_{\text{CS}}[A]. \tag{8.80}$$

And hence,

$$\sigma_{12} = \frac{e^2}{h} \frac{p}{1 + 2sp} \qquad s, p \in \mathbb{Z}. \tag{8.81}$$

References

1. Halperin, B. I., Lee, P. A. & Read, N. "Theory of the half-filled Landau level". *Phys. Rev. B* **47,** 7312 (1993).
2. Willett, R. *et al.* "Observation of an even-denominator quantum number in the fractional quantum Hall effect". *Phys. Rev. Lett.* **59,** 1776 (1987).